CLIMATIC CHANGES IN TEMPERATURE AND SALINITY IN THE SUBTROPICAL NORTH ATLANTIC

by

Alicia María Lavín Montero

Licenciada en Ciencias Físicas
Universidad de Cantabria (Spain)
(1977)

Submitted to the Department of Earth, Atmospheric and Planetary Science in partial fulfillment of the requirements for the degree of

Master of Science
in Physical Oceanography

at the

MASSACHUSETTS INSTITUTE OF TECHNOLOGY

May 1993

Signature of Author .....
Earth, Atmospheric and Planetary Science
Massachusetts Institute of Technology
May 19, 1993

Certified by .....
Carl Wunsch
Cecil and Ida Green Professor of Physical Oceanography
Thesis Supervisor

Accepted by .....
Thomas H. Jordan
Department Head,
Massachusetts Institute of Technology

CLIMATIC CHANGES IN TEMPERATURE AND SALINITY IN THE SUBTROPICAL NORTH ATLANTIC

by
Alicia María Lavín Montero

Submitted in partial fulfillment of the requirements for the degree of
Master of Science in Physical Oceanography at the
Massachusetts Institute of Technology
May 19, 1993

Abstract

Three sets of hydrographic data are used to examine the changes in temperature and salinity in the subtropical North Atlantic. Transatlantic hydrographic sections at 24.5°N were obtained in October 1957, in August 1981, and finally in July-August 1992.

A general warming was found over the upper 3000 m of the North Atlantic at 24.5°N, over the entire 35-year period. There is high variability over time over most of the upper 1000 m. In the layer between 1000 m and 3000 m, a significant warming of 0.1±0.02 °C has been observed. The rate of warming is 0.03°C/decade and is nearly steady in the two periods. Significant cooling is found in water deeper than 3000 m in both the North American (-0.027±0.016 °C) and the Canary Basins (-0.013±0.005 °C). There are some indications that the θ/S relationship at 24.5 °N has changed over time. The nonuniform change of the depth of isotherms, due to the diverse pattern of warming or cooling, results in a change in the volume of water masses. Expansion in the North American Basin occurs in the transition zone between Antarctic Bottom Water and lower North Atlantic Deep Water, with a rate of 9 km^2/year. In the Canary Basin the expansion is larger and has mostly taken place in the last 11 years. Contraction occurs in the North Atlantic Deep Water, and expansion in the thermocline water.

Finally, using a simple heat calculation, we find that there is no significant difference between the heat flux estimated from the three surveys performed in 1957, 1981, and 1992 at 24.5°N .

Thesis Supervisor: Carl Wunsch,
Cecil and Ida Green Professor of Physical Oceanography
Department of Earth, Atmospheric and Planetary Sciences
Massachusetts Institute of Technology

Acknowledgments

I would first like to thank my thesis advisor, Carl Wunsch, for his guidance and patience during the research. To Harry Bryden for his continuous support and advice during the cruise and after it, he was always ready to help me. To Bob Millard, he had to work hard to finish the cruise calibrations on time to be used for the thesis, and he generously spared his time for me. To T. Joyce and M. McCartney for their helpful comments about the results. To Charmaine King for her assistance in data and computer matters. To Alison MacDonald, Gwyneth Hutfford, Jim Gunson and many others fellow students and post-docs that have help me with the thesis and the subjects.

To Rafael Robles, Director, and Alvaro Fernández, Subdirector of the Instituto Español de Oceanografía (IEO), Ministerio de Agricultura, Pesca y Alimentación, my employer, Orestes Cendrero, Director of Centro Oceanográfico de Santander (IEO), F. F. Castillejo and J.R. Pascual for allowing me to come to MIT and supporting me during this period of study.

To Gregorio Parrilla (IEO), chief scientist of the Hespérides cruise, and all the participants of the cruise. Gregorio gave me complete freedom to work the data, and worked hard, with M. Jesus Garcia in the final calibration of the cruise data.

To Miguel Losada, Professor of Ocean Engineering, University of Cantabria.

To the Fundación Marcelino Botín (Santander, Spain) that funded me to stay at MIT, without it I couldn't have obtained this Master Degree.

To my husband Mac for his support in many difficult moments during this period and his Fulbright grant that allowed us to spend this time of study at M.I.T.

This research was mainly supported by the Fundación Marcelino Botín (Santander, Spain), the Instituto Español de Oceanografía, NSF OCE-9114465 and NSF OCE-9205942 also contributed

Contents

Introduction

As scientific understanding of the causal mechanisms for environmental changes improves there is an accompanying public awareness of the susceptibility of the present environment to significant regional and global change. Understanding the basic mechanisms of climate is a key to early detection of change in the earth's climate system.

Since the ocean-atmosphere system is driven by the sun's radiation, it is important to know what the response of the system is to the known radiative input. The ocean carries a significant fraction of the meridional heat flux that makes the middle latitudes of the earth habitable. Vonder Haar and Oort (1973) found that in the region of maximum net northward energy transport by the ocean-atmosphere system (30-35°N) the ocean transports 47% of the required energy. At 20°N, where the ocean transport reaches a maximum, they estimate that the ocean accounts for 74% of the total meridional heat transport. So the ocean is critical in the redistribution of solar energy.

The Atlantic Ocean is the most saline of all the world oceans. It has significant exchange of water masses, heat and salt with several marginal seas, regions in which important transformations of water masses take place. A complex thermohaline-driven circulation moves water masses both northward and southward along its western boundary regions. The Atlantic Ocean has been well surveyed in the twentieth century with various large scale surveys such as International Geophysical Year (IGY), Geochemical Ocean Sections Studies (GEOSECS), Long Lines (LL), South

Atlantic Ventilation Experiment (SAVE) and the World Ocean Circulation Experiment (WOCE). The Atlantic is the source of North Atlantic Deep Water (NADW), and in it can be found several other important water masses: Mediterranean Water, Antarctic Intermediate Water (AAIW) and Antarctic Bottom Water (AABW).

The 24.5°N transatlantic section is an archetypic transoceanic hydrographic section. It is rich in water masses and crosses the North Atlantic in the middle of the subtropical gyre. It provides a census of major intermediate, deep and bottom water masses whose sources are in the Antarctic and far northern Atlantic as well as estimates of the thermohaline circulation of these water masses and of the wind-driven circulation in the upper water column. Furthermore, the 24.5°N section crosses the northward flowing Gulf Stream through the Florida Straits and the southward wind-driven Sverdrup flow in mid-ocean at essentially the latitude of maximum wind stress curl.

The 24.5°N section was measured in 1957 (IGY data) (Fuglister, 1960), and 1981 (Roemmich and Wunsch, 1984). Although hydrography is a traditional method for obtaining the geostrophic flow throughout the water column, the quantity and quality of the measurements have been dramatically increased since the use of electronic instrumentation such as CTD (Brown, 1974). This new technique has been used in the later periods of sampling.

From analyses of the 1957 section, Hall and Bryden (1982) determined that the Antarctic Intermediate water flows northward across 24°N between 600 and 1100 m depth, North Atlantic deep water flows southward between 1200 and 4500 m, and Antarctic bottom water flows northward below 4500 m depth. They found a vertical meridional cell with a net northward flow across 24°N of 18 x 10^6 m^3/s of warmer water in the upper 1000 m of the water column and a southward return as intermediate and deep water between 1000 and 4500 m depths. Roemmich and Wunsch (1985) reported a similar pattern of water masses and meridional flow on the 1981 section.

The 24.5°N section was one of the sections repeated during WOCE (section A-5, WOCE Implementation Plan) which Gregorio Parrilla from the Instituto Español de Oceanografía (IEO), proposed to the Spanish government. For this proposal, Parrilla had the important support of Harry Bryden and Robert Millard from Woods Hole Oceanographic Institution. Parrilla obtained the approval of his proposal with the help of two favorable conditions. First in 1992 Spain was celebrating the Quincentennial of one important episode in its modern history The Discovery of America. In 1492 Columbus and his Spanish sailors left Palos de Moguer (Golfo de Cádiz) for the Islas Canarias. After that, they sailed westward approximately at 24°N reaching San Salvador (Bahamas Islands) on October 12, 1492. The second favorable circumstance was the building of a new oceanographic ship for the Spanish Antarctic Program.

The cruise was carried out in July-August of 1992 with the participation of scientists from the Instituto Español de Oceanografía, Woods Hole Oceanographic Institution, and other Spanish and American institutions such as Instituto de Investigaciones Marinas, Centro de Estudios Avanzados de Blanes, Ciencias del Mar de la Universidad de Las Palmas, Universidad de La Coruña, Programa de Clima Marítimo del MOPT, Ainco-Inter Ocean, Lamont Doherty Geological Observatory, and RSMAS University of Miami.

The objective of this research is to quantify the response of the ocean to the warmer atmospheric conditions of the last decade and compare the conditions with previous surveys. Roemmich and Wunsch (1984) reported warming between 700 and 3000 m, and weak cooling above and below those depths. We have done the same calculation for the two periods of comparison 1957-1981 and 1981-1992. The procedure was as follows. First, the comparison was made using two methods based on cubic splines and objective mapping, and the differences between the cruises and the zonal average of the differences were calculated. Next, the area occupied by the different water masses in the three cruises was calculated, and these areas are related

to the strength of their possible sources. The changes in the temperature/salinity relationship are examined.

Second, we discuss the transport of heat. Using a simple heat calculation, we have tried to see whether the heat transport across 24°N has changed in time from one cruise to other.

Chapter 1

Description of the Data

1.1 Introduction

The objective of this research is to investigate the climatic variations of temperature, salinity, and heat fluxes over the subtropical Atlantic Ocean from the surface to 6000 m depth during the last 35 years. The data used includes three oceanographic cruises on which zonal hydrographic sections at latitude 24.5°N were carried out: the first one in October 1957, by the British R.R.S. *Discovery II* of the National Institute of Oceanography (Chief Scientist L.V. Worthington, Woods Hole Oceanographic Institution) during the International Geophysical Year (Fuglister 1960); the second one in August 1981, by the R.V. *Atlantis II* of the Woods Hole Oceanographic Institution (Chief Scientist D. Roemmich, at that time Woods Hole Oceanographic Institution) (Roemmich and Wunsch, 1985); the last one in July-August of 1992 by the Spanish B.I.O. *Hespérides* of the Armada Española, (Chief Scientist Gregorio Parrilla, Instituto Español de Oceanografía).

The section chosen is situated in the central part of the subtropical gyre. The transect was done always downwind, westward from Africa to America. It began at the African continental shelf, which is quite flat, with depths increase slowly, reaching

4000 m around 20°W, and 5500 m around 25°W. The bottom of the Canary Basin is situated between 30°and 35°W, west of this longitude the beginning of the Mid-Atlantic Ridge becomes apparent. The Mid-Atlantic Ridge extends until 53°W, is centered at about 45°W, with the shallowest parts reaching 3000 m. West of the ridge, the bottom is smooth in the North American Basin with depths between 5500 and 6500 m. The western boundary is quite steep from 5000 m to the Bermuda Bank. The extent of both basins is 3000 Km, but the North American basin is deeper on average than the African basin.

All the data are interpolated to a common set of depths. These depths are closely spaced in the upper waters, with increasing separation toward the bottom. The spacings are chosen to resolve the large structures of the general circulation and the mesoscale variability. Table 1.1 lists the standard depths. Data and interpolation procedures are described here for each cruise.

1.2 Discovery II 1957 IGY Data

There is a detailed description of the cruise in Fuglister (1960). The cruise was carried out between October 6 and October 28, 1957, from 16°20'W to 75°28'W. The total number of stations was 38 and the sampling was done using reversing thermometers and Nansen bottles.

Temperatures are stated to be accurate within ± 0.01°C, depth is accurate within ± 5 m based on reading of paired protected and unprotected thermometers and salinity is accurate to ± 0.005 °/$_{oo}$.

Data were converted from depth to pressure using Saunders's formula (Saunders, 1981). Temperatures were based on IPTS-48 (International Practical Temperature Scale 1948), conversion to IPTS-68 (Barber 1969) is possible by Fofonoff and

	depth	interval
1	0	
2	50	
3	100	
4	150	50
5	200	
6	250	
7	300	
8	400	
9	500	
10	600	
11	700	
12	800	
13	900	100
14	1000	
15	1100	
16	1200	
17	1300	
18	1400	
19	1500	
20	1750	
21	2000	
22	2250	
23	2500	
24	2750	
25	3000	
26	3250	
27	3500	250
28	3750	
29	4000	
30	4250	
31	4500	
32	4750	
33	5000	
34	5500	
35	6000	500

Table 1.1: Standard depths

Bryden (1975) formula. Differences, however are less than 0.01 in surface and less than 0.002 for temperature lower than 4 °C. Such differences are lower than the accuracy of the measurements and therefore the 48 scale were used. Salinities were based on the old scale (part per thousand), before the Practical Salinity Scale, the differences between the two scales are well below the accuracy of the measurements. Therefore, all salinity data used in this research are based in PSS-78 (pss).

For the discrete bottle data, vertical linear interpolation was made between adjacent data points for each station to the standard depths. Data were plotted to check the values and detect errors in interpolation.

1.3 Atlantis II 1981 Long Lines Data

Detailed description of the cruise is in Roemmich and Wunsch (1985). The cruise began August 11 from Las Islas Canarias with the first station off Cape Juby (Morocco). The last station was east of the Bahamas Bank on September 4. Two sections were made across the Florida Current at 26°02' N and 27°23'N to finish on September 6. The mid-Atlantic section was composed of 90 stations sampled by Neil Brown Instrument CTD/O_2. A 24-bottle rosette water sample was used for CTD-O_2 calibrations (Millard, 1982).

Simple averages of nearly continuous CTD/O_2 measurements are made to derive the standard depths values. The 'window' was set 20 m above and 20 m below the standard depths. When the CTD did not reach the bottom to enable interpolation to all available standard depths, linear vertical extrapolation was allowed to estimate one more standard depth from the last two interpolated depths.

1.4 Hespérides 1992 WOCE Data

The 1992 24.5°N section, designated A-5 by WOCE (WOCE Implementation plan), was made by the Spanish B.I.O. *Hespérides* of the Armada Española, (Chief Scientist Gregorio Parrilla, Instituto Español de Oceanografía). The boat departed from Cádiz on July, 14 sailing to Las Islas Canarias; six stations were made in this track for testing CTDs and rosette.

We left Las Palmas on July 20 arriving at station number one (24°29.97'N, 15°58.08'W) the same day. The section was finished at the Bahamas (24°30'N 75°31'W) after 101 stations on August 14. On August 15, a section of 11 stations across of the Florida Current at 26°3'N was done. Figure 1.1 gives the location of the stations.

Two NBIS/EG&G Mark IIIb CTD underwater units each equipped with pressure, temperature, conductivity and polographic oxygen sensors were used throughout the cruise. Their serial number are 1100 and 2326. A General Oceanics rosette fitted with 24 Niskin bottles of 10 or 12 liter of capacity was used with the CTD for collecting water samples. In all cases, data were collected from the ocean surface to within a few meters of the bottom.

Both NBIS/EG&G Mark IIIb CTDs were equipped with titanium pressure sensors manufactured by Paine Instrument. The temperature sensor was a Rosemount platinum # 171. The conductivity sensor is a 3-cm alumina cell manufactured by NBIS/ED&G. The CTD work was supervised by G. Parrilla (IEO) and H. Bryden (WHOI), software and calibrations by R. Millard (WHOI) and hardware by J. Molinero (IEO) and G. Bond (WHOI).

Water sampling included measurements of salinity, oxygen, nutrients (silicate, nitrate, nitrite and phosphate), chlorofluorocarbons (CFC), pH, alkalinity, CO_2,

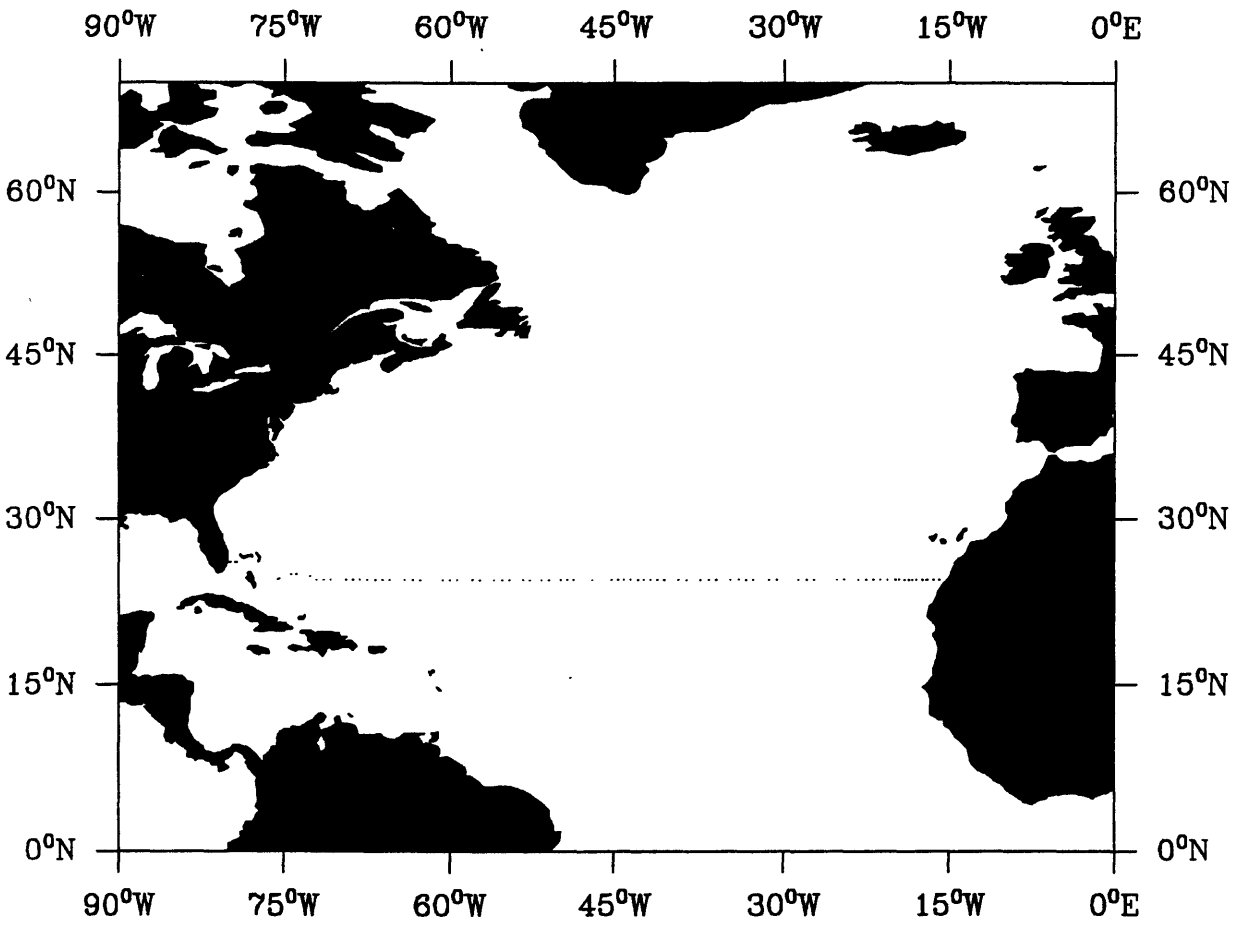

Figure 1.1: Section at 24.5°N in the North Atlantic. Dots denote the location of stations in the 1992 Hespérides cruise. IGY 1957 track was similar, but spacing between stations was larger than in the 1992 section. Atlantis 1981 was also at that latitude west of 24.5°W. For the comparison I have used this common part.

particulate matter, chlorophyll pigments, ^{14}C and aluminum. Underway Acoustic Doppler Current Profiler (ACDP) measurements were also taken. Typically, 24 samples were obtained for each station. The water sample salinities were measured with a Guildline Autosal model 8400A salinometer by R. Molina (IEO). Oxygen determinations were carried out primarily by J. Escánez (IEO). (G. Parrilla, Cruise report in preparation).

Since in this research we have used only CTD/O_2 data, I will describe only these observations. Data acquisition and calibrations were done following the procedures given by Millard and Yang (1993). The EG&G data logging program CTDACQ was used to record down and up profiles and CTDPOST was used to flag spurious data. The remainder of the CTD post-processing was performed using the WHOI PC based CTD processing system as described by Millard and Yang (1993).

The CTD/O_2 profiles require accurate calibration of conductivity, temperature, and pressure sensors in the laboratory. This is particularly important in deep water (below 1500 m) where variations in temperature and salinity are small. CTD pressure, temperature, and conductivity sensors for both CTDs were calibrated at WHOI before and after the cruise. The best fit NBIS/EG&G Mark IIIb CTD sensor calibration is usually found to be linear in conductivity, quadratic in temperature, and quadratic for the titanium pressure transducer (Millard *et al.*, 1993). The polynomial coefficients to calibrate the raw sensor data are determined using standard least squares techniques.

Temperature calibrations are based on the International Practical Temperature Scale 1968 (IPTS-68, Barber,1969). All the comparisons are made in this scale. In pressure, resolution is 0.1 db, with an accuracy of $\pm$ 2.0 db for CTD number 1100 and $\pm$ 5.0 db for CTD number 2326. The temperature resolution was 0.0005°C with an accuracy better than $\pm$ 0.0015°C (Millard and Yang, 1993) over the range 0 to 30°C. A comparison of pre-cruise and post-cruise calibration shows a large (0.01 to 0.015°C)

shift of temperature in the same direction in both CTDs. This shift was traced to a faulty pre-cruise laboratory temperature standardization, and was removed from the calibrations.

For calibration purposes, acquisition programs allow the operator to create a file of CTD observations at the time of bottle closure, and write averaged values of the raw, uncalibrated CTD/O_2 sensor data around that point. An iterative fitting procedure has been developed for determining both conductivity and oxygen algorithm model coefficients (Millard and Yang, 1993) to minimize the differences between the CTD data and the water samples. Pre-cruise calibration data and *in situ* water sample salinity and oxygen were used on board to calibrate conductivity (salinity) and oxygen. These data were considered preliminary until the post-cruise laboratory calibration was completed.

The conductivity sensor resolution was 0.001 Ms/cm and an overall accuracy of the CTD conductivity calibrated to the rosette water bottle salinities is estimated as better than $\pm$ 0.0025 pss. CTD 1100 was used for stations 1-62, 74-80, 89-101 and the Florida Strait section; CTD 2326 was used for stations 63-71 and 81-88. The conductivity calibrations were examined closely at the change of instruments.

After acquiring the CTD data, the four post-processing steps are: editing, pressure averaging, calculation of calibrated data quantities, and pressure centering and data quality control. We edited the raw station data just after the finish of each station. Erroneous CTD observations were flagged and pressure-averaging programs replaced these observations. To match the conductivity data time response to that of the temperature data, an exponential recursive filter was applied to the conductivity sensor data (Millard, 1982). The edited raw CTD data was gridded to form a centered uniform pressure series with calibrated salinity and oxygen data in two steps. The pressure-averaging step replaced the erroneous input data, applied the conductivity-temperature sensor lags, and bin averaged the raw data in uniform pressure steps

of 2 decibars. After that, a pressure centering step converted the data to physical units by applying the calculation polynomial and interpolated the pressure averaged observations to a uniform pressure series.

Data quality control was performed to check the integrity of the calibrations and water sample measurements. Temperature, salinity, oxygen, and potential density anomaly profiles versus pressure were examined, also salinity and oxygen versus potential temperature diagrams of consecutive stations are examined. Calibration data and quality control of this cruise has been done by R. Millard (WHOI), G. Parrilla (IEO), M. J. Garcia (IEO), H. Bryden (Rennel Center, U.K.) and myself.

The 2-db temperature, salinity, and oxygen data have been smoothed with a binomial filter and then linearly interpolated (Mamayev *et al.*, 1991) as required to the standard levels (Table 1.1). When the CTD did not reach the bottom, to enable interpolation to all available standard depths, linear vertical extrapolation were used to estimate one more standard depth from the last two interpolated depths. Figure 1.2 A, B and C present distributions of temperature, salinity, and oxygen for the 1992 Hespérides Section.

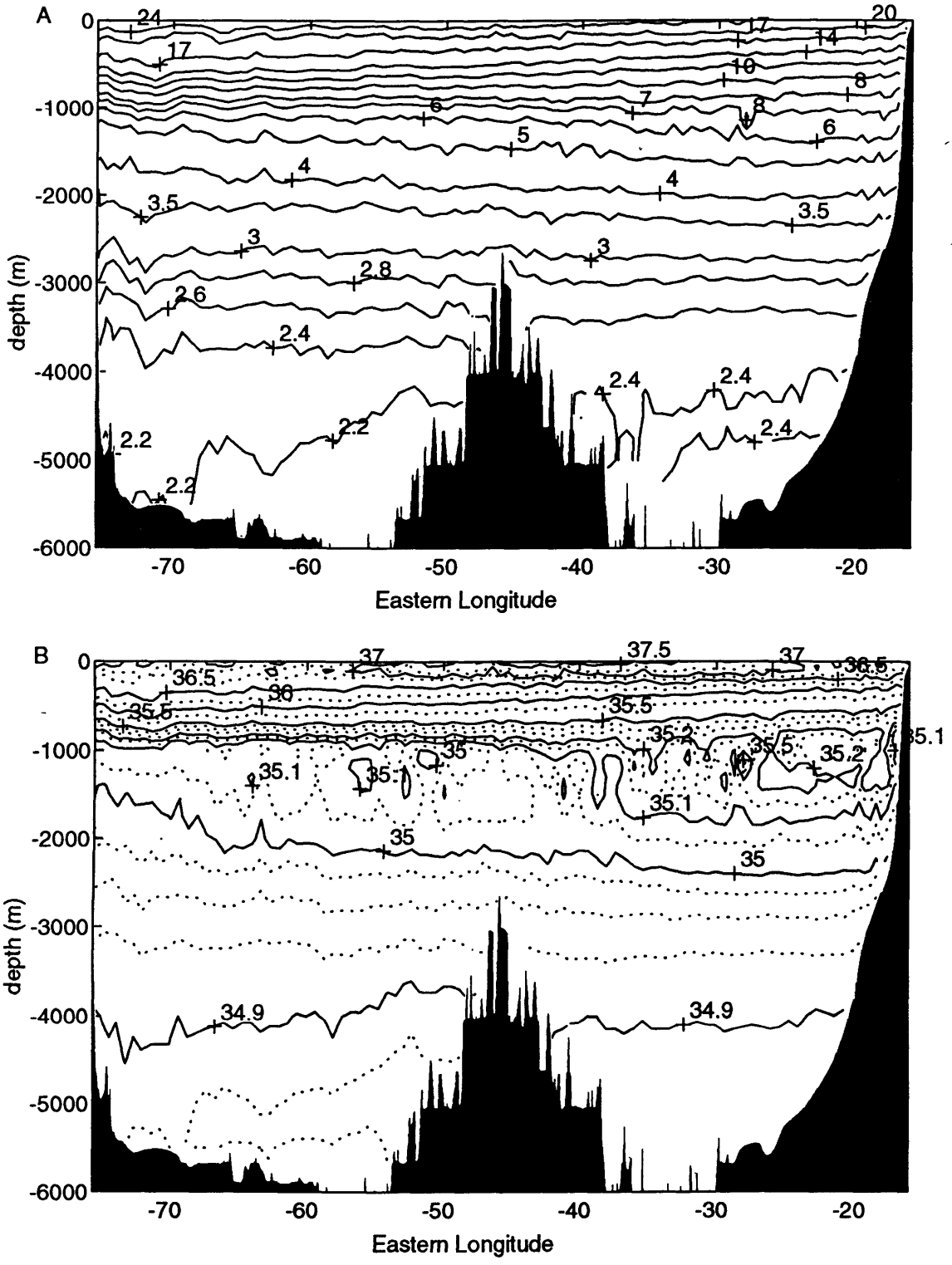

Figure 1.2: Distributions of A) Temperature (°C), B) salinity (pss) C) Potential temperature (°C), and D) oxygen (ml l^{-1}) for the 1992 Hespérides Section

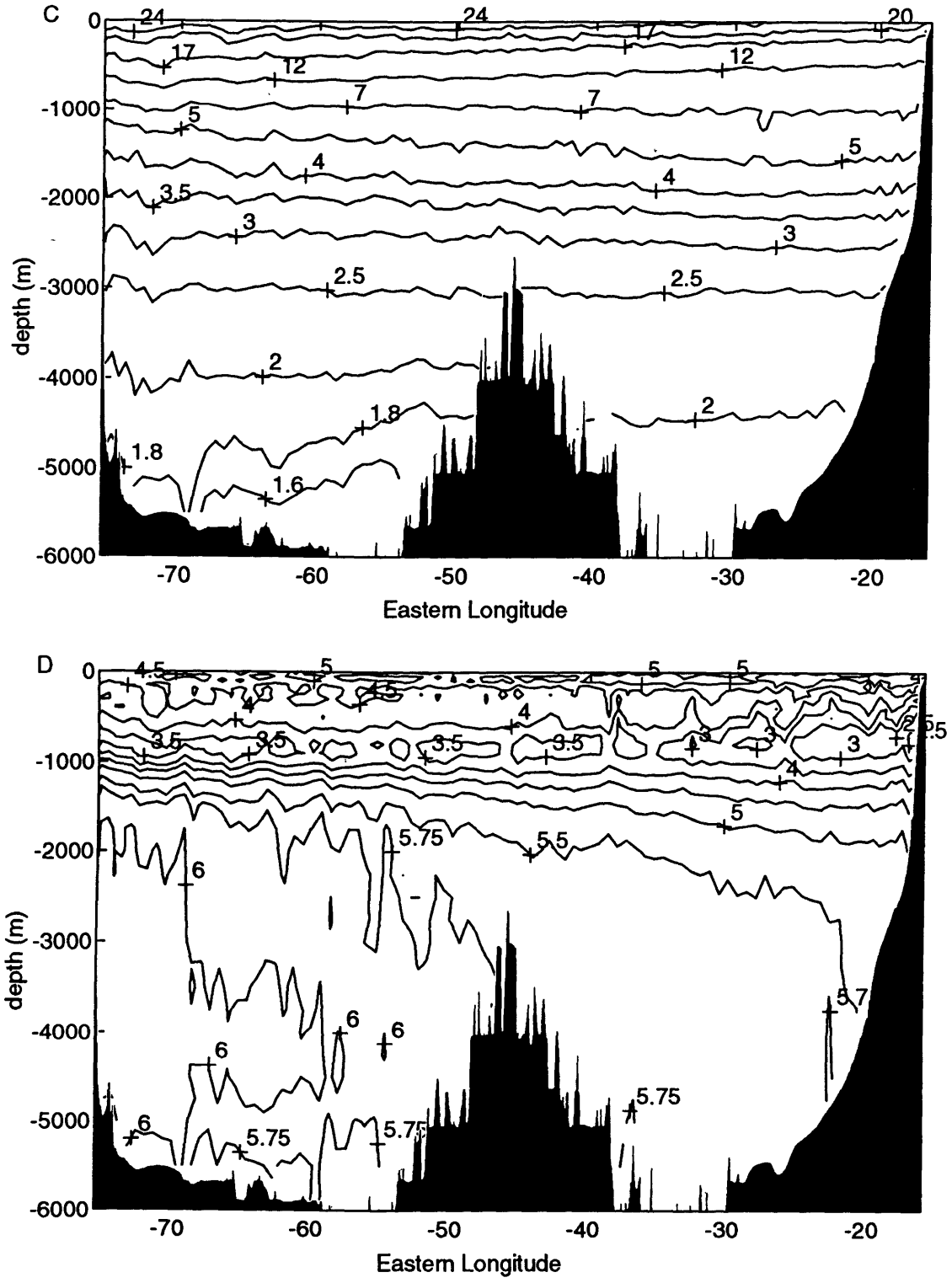
C
D
depth (m)
Eastern Longitude
0
-1000
-2000
-3000
-4000
-5000
-6000
-70
-60
-50
-40
-30
-20

Chapter 2

Comparison over Time of Temperature and Salinity

2.1 Introduction

The objective of this research is to investigate the climatic variations of temperature and salinity over the tropical Atlantic Ocean from the surface to 6000 m depth during the last 35 years. All three available cruises have been done at the nominal latitude of 24.5°N. However, the 1981 cruise started on the African Continental shelf at 27.9°N and angled southwestward to joint 24.5°N at 24.3°W due to the Sahara war which was close to the coast at 24.5°N.

The *nominal* station spacing in the IGY survey was 185 km. On the *Atlantis II*, the spacing varied between 50 and 80 km with shorter spacing when the stations were over the continental slopes and the Mid-Atlantic Ridge. The same criteria were used for the *Hespérides* survey, but the spacing was more regular, between 58 and 67 km. Therefore, in order to compare the variables from the different cruises directly it is necessary to interpolate all the data onto a set of common geographic locations. The data were interpolated onto a two dimensional grid at 24.5°N. The horizontal spacing chosen was 0.5° of longitude. This corresponds approximately to 50 km at

this latitude (0.5 x 60 x 1.85 x cos(24.5) = 50.5 km). The data were placed vertically onto a set of 35 standard depths, defined in Table 1.1

2.2 Methodology

In order to choose a scheme of interpolation, we compared spline interpolation and objective mapping, two methods which could reasonably be used. Here we describe how their advantages and disadvantages led to the decision to use one of them for this work. Between the results of the two methods, discrepancies are within the expected error in all regions except the boundaries. Cubic spline is simpler to use but the advantage of calculating expected errors made objective mapping the most suitable method of interpolation for this analysis.

2.2.1 Spline interpolation

The spline interpolation (Ahlberg *et al.* 1967) assumes the existence of a function $y = f(x_i)$ whose value is known at a set of x_i points, $a = x_0 < x_1 < \ldots < x_n = b$, regularly or irregularly spaced. The cubic spline is the cubic polynomial $f(x)$ that is continuous in the interval $[a, b]$, has continuous first and second derivatives, and passes through the points $f(x_i)$ (i=0,n). The interpolating cubic spline defines a separate cubic polynomial for each interval $x_{i-1} \leq x \leq x_i$, or a total of n polynomials for the n+1 points. We can write the polynomial equation take derivatives and , at each data point equate the first and second derivative of the left-side polynomial to those of the right-side.

Following Thompson (1984), writing the Taylor series for the cubic polynomial for interval i, expanded about the point x_i

$$y(x) = y_i + (x - x_i)y_i^{'} + (x - x_i)^2 y_i^{''}/2 + (x - x_i)^3(y_{i+1}^{''} - y_i^{''})/6h \qquad (2.1)$$

$y_i^{'}$ and $y_i^{''}$ stand for the first and second derivatives evaluated at $x = x_i$, and the third derivative has been replaced by its divided difference form, which is exact for a cubic function (Bevington and Robinson, 1992). At $x = x_i$, we have $y = y_i$, as required. Setting $x = x_{i+1} = x_i + h$ it is possible to solve the equation

$$y(x_{i+1}) = y_i + (x_{i+1} - x_i)y_i^{'} + (x_{i+1} - x_i)^2 y_i^{''}/2 + (x_{i+1} - x_i)^3(y_{i+1}^{''} - y_i^{''})/6h \qquad (2.2)$$

to obtain

$$(y_{i+1} - y_i) = hy_i^{'} + h^2\,[2y_i^{''} + y_{i+1}^{''}]/6 \qquad (2.3)$$

Repeating the calculation, using the equation for $y(x)$ in interval *i-1* and requiring that $y(x) = y(x_i)$ at the i data point we obtain

$$(y_i - y_{i-1}) = hy_{i-1}^{'} + h^2\,[2y_{i-1}^{''} + y_i^{''}]/6 \qquad (2.4)$$

To establish continuity conditions at the data point, we equate first and second derivatives at the boundaries $x = x_i$ and $x = x_{i-1}$. The use of the divided difference form for the third derivative assures continuity of the second derivative across the boundaries and gives the spline equation

$$y_{i-1}^{''} + 4\,y_i^{''} + y_{i-1}^{''} = D_i \qquad (2.5)$$

with

$$D_i = y\,[y_{i+1} - 2y_i + y_{i-1}]/h^2 \qquad (2.6)$$

These equations can be solved for the second derivatives $y_i^{''}$, as long as the values of $y_1^{''}$ and $y_n^{''}$ are known. If those values are set to 0 the *natural splines* are obtained.

In our case we have used *natural splines* for the interpolation. The fitting by cubic splines was done from the longitude of the western-most to the eastern-most station, for each of the 35 standard depths. After fitting, the function was evaluated every 0.5° of longitude. Below 2750 m (standard depth number 24) the North Atlantic is separated by the Mid-Atlantic Ridge in two basins, the North American basin and the Canarias basin. Since the behavior of the basins is different, the fitting was done separately for each.

The set of data obtained after the gridding is for Hespérides 1992 from 75.5°W to 16°W, for Atlantis 1981 from 75.5°W to 13.5°W and IGY 1957 from 75.5°W to 16.5°W. Atlantis-II data, due to the deviation of the track from 24.5°N east of 24.5°W, only compared with the other sections west of 24.5°W. For comparison we only have computed west of this longitude. After gridding for the three cruises, we calculated the differences on the common area:

- 1992-1981: Subtracting 1981 data from 1992 between 75.5°W and 24.5°W.
- 1981-1957: Subtracting 1957 data from 1981 between 75.5°W and 24.5°W. This comparison was also done by Roemmich and Wunsch (1984) using objective mapping.
- 1992-1957: Subtracting 1957 data from 1992 between 75.5 and 16.5 °W.

Because the grid-point temperature differences exhibit large variations due to the presence or absence of eddies during the different surveys, a horizontal gaussian filter of e-folding scale of 300 km has been applied to the temperature differences at each depth.

Behavior of the boundaries

When we apply the gaussian filter at the boundaries, we extend the temperature difference matrices in an unbiased way with zeros past the boundaries so that

smoothed temperature differences are obtained up to the western and eastern boundaries as well as in the Mid-Atlantic Ridge.

Figure 2.1 A, B and C present temperature differences for 1981-1957, 1992-1981 and 1992-1957 obtained with this methodology.

For salinity we have done calculation similar to those for temperature, fitting by cubic splines at each standard depth and using a gaussian filter of the differences. Figure 2.2 A, B and C present salinity differences for 1981-1957, 1992-1981 and finally 1992-1957.

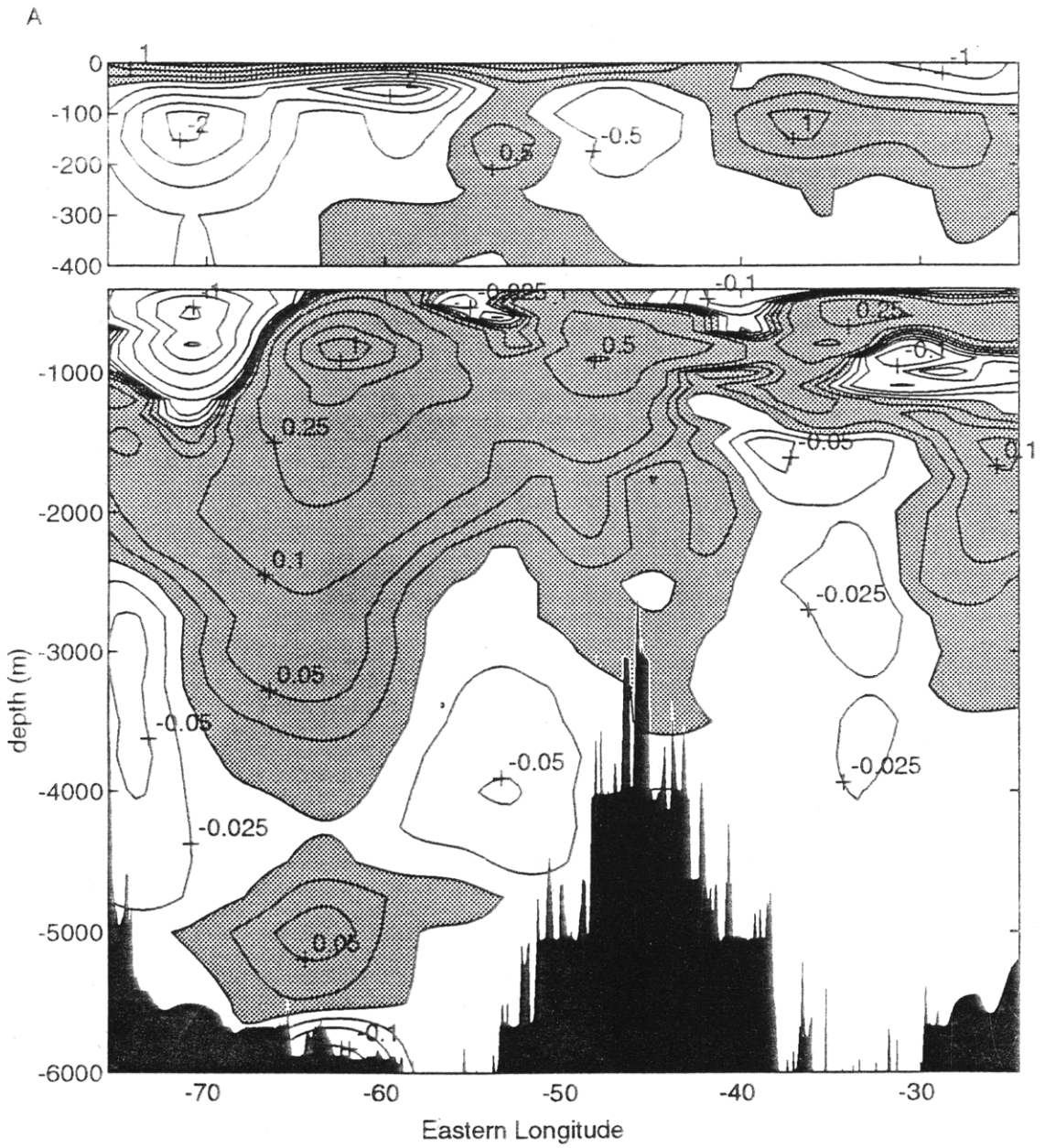

Figure 2.1: Difference of temperature at 24.5°N using spline fitting and interpolating values each 0.5°of longitude. Data were smoothed using a gaussian filter of e-folding scale of 300 km. Differences were calculated for A)1981-1957 B) 1992-1981, and C) 1992-1957. Values are in °C. Shading indicates positive difference.The top plot has expanded vertical scale

B

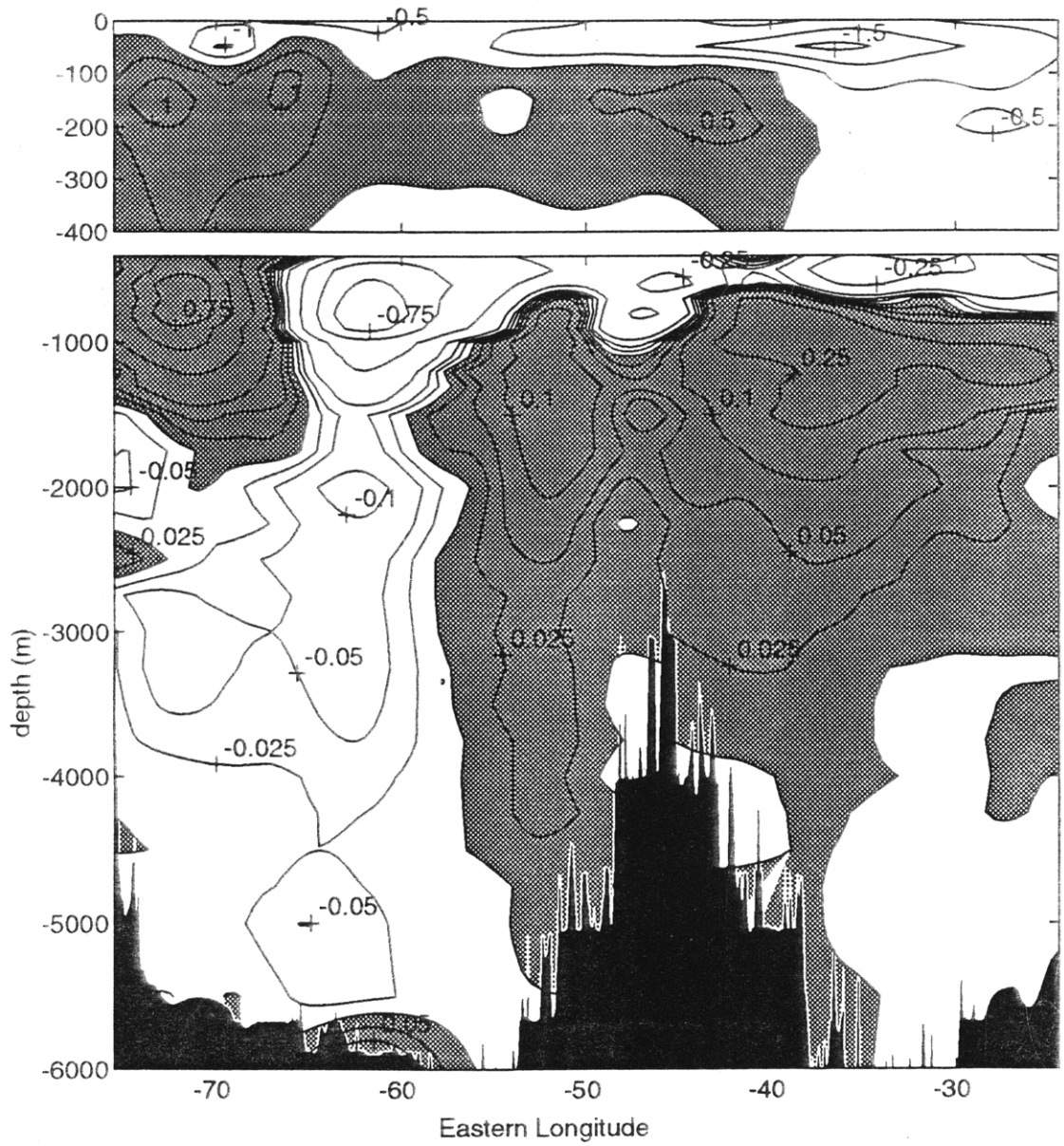
0
-100
-200
-300
-400
-1000
-2000
-3000
-4000
-5000
-6000
depth (m)
-70
-60
-50
-40
-30
Eastern Longitude
-0.5
-1.5
0.5
-0.5
-0.25
0.75
-0.75
0.25
0.1
0.1
-0.05
-0.1
0.025
0.05
0.025
0.025
-0.05
-0.025
-0.05

C

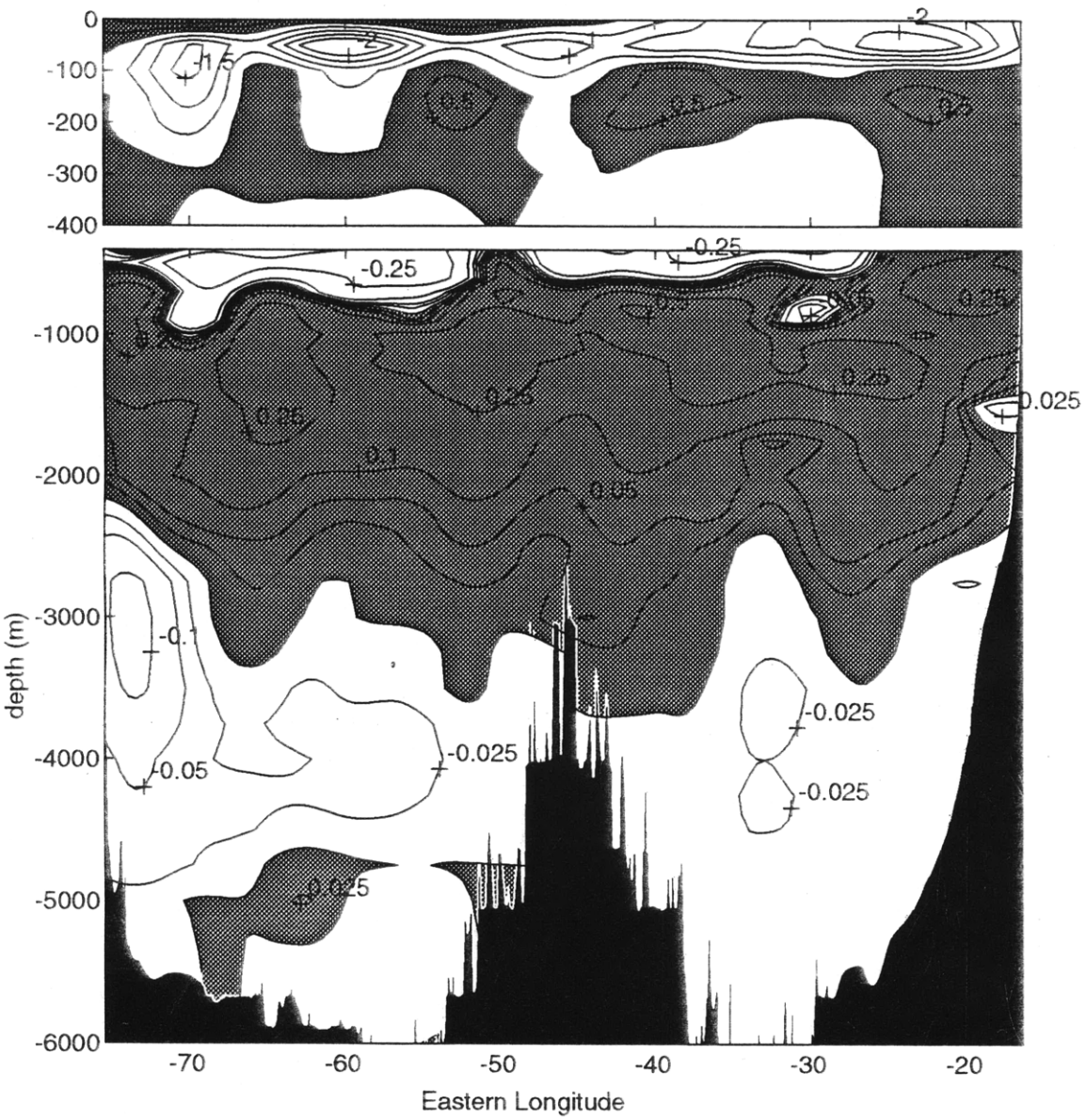
0
-100
-200
-300
-400
-1000
-2000
-3000
-4000
-5000
-6000
depth (m)
-70
-60
-50
-40
-30
-20
Eastern Longitude
-0.25
-0.1
-0.05
-0.025
0.025
0.1
0.25

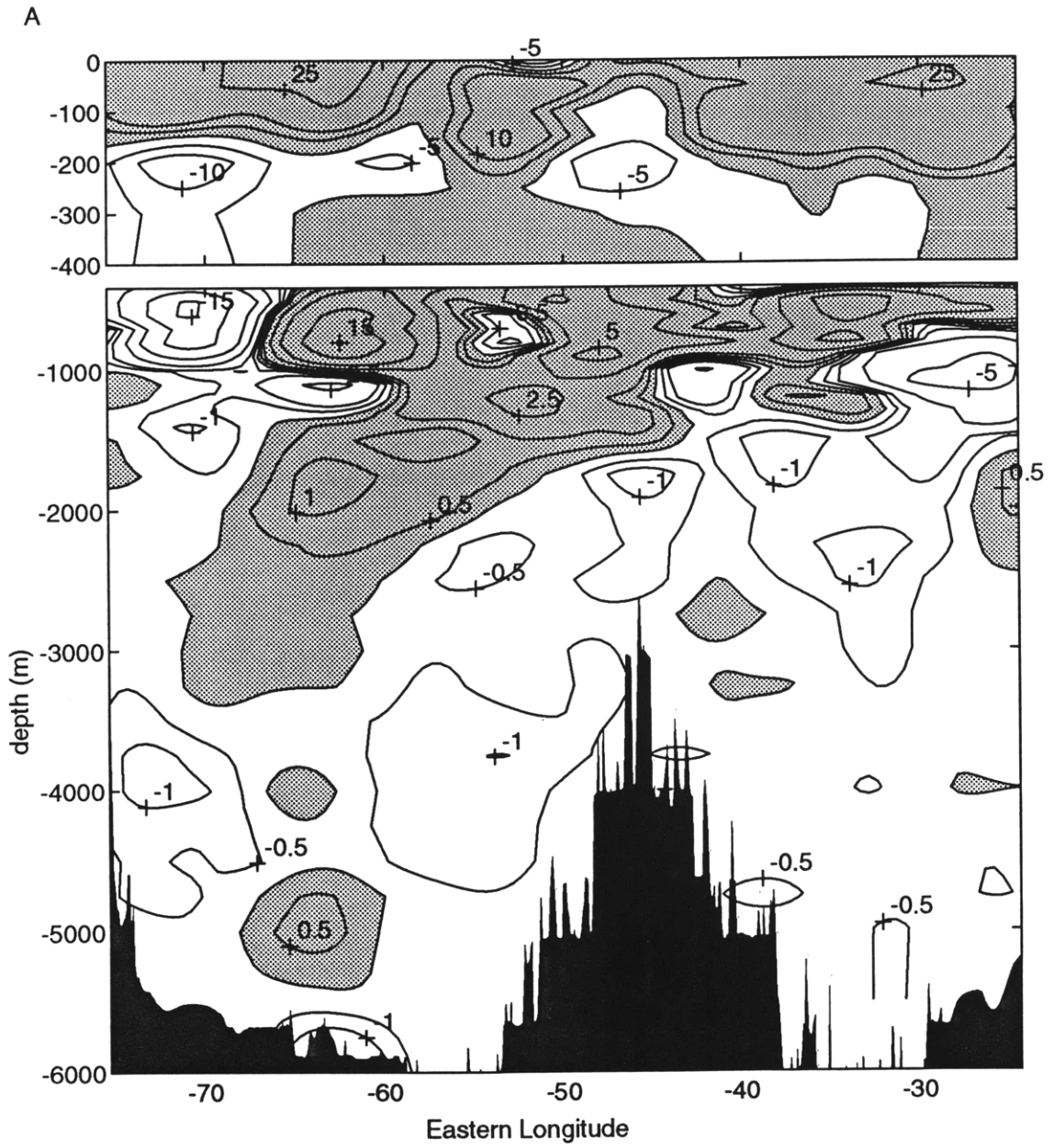

Figure 2.2: Difference of salinity at 24.5°N using spline fitting and interpolating values each 0.5°of longitude. Data were smoothed using a gaussian filter with of 300 km of e-folding scale of 300 km. Differences were calculated for A)1981-1957 B) 1992-1981, and C) 1992-1957. Values are in pss x 100. Shading indicates positive difference. The top plot has expanded vertical scale

B

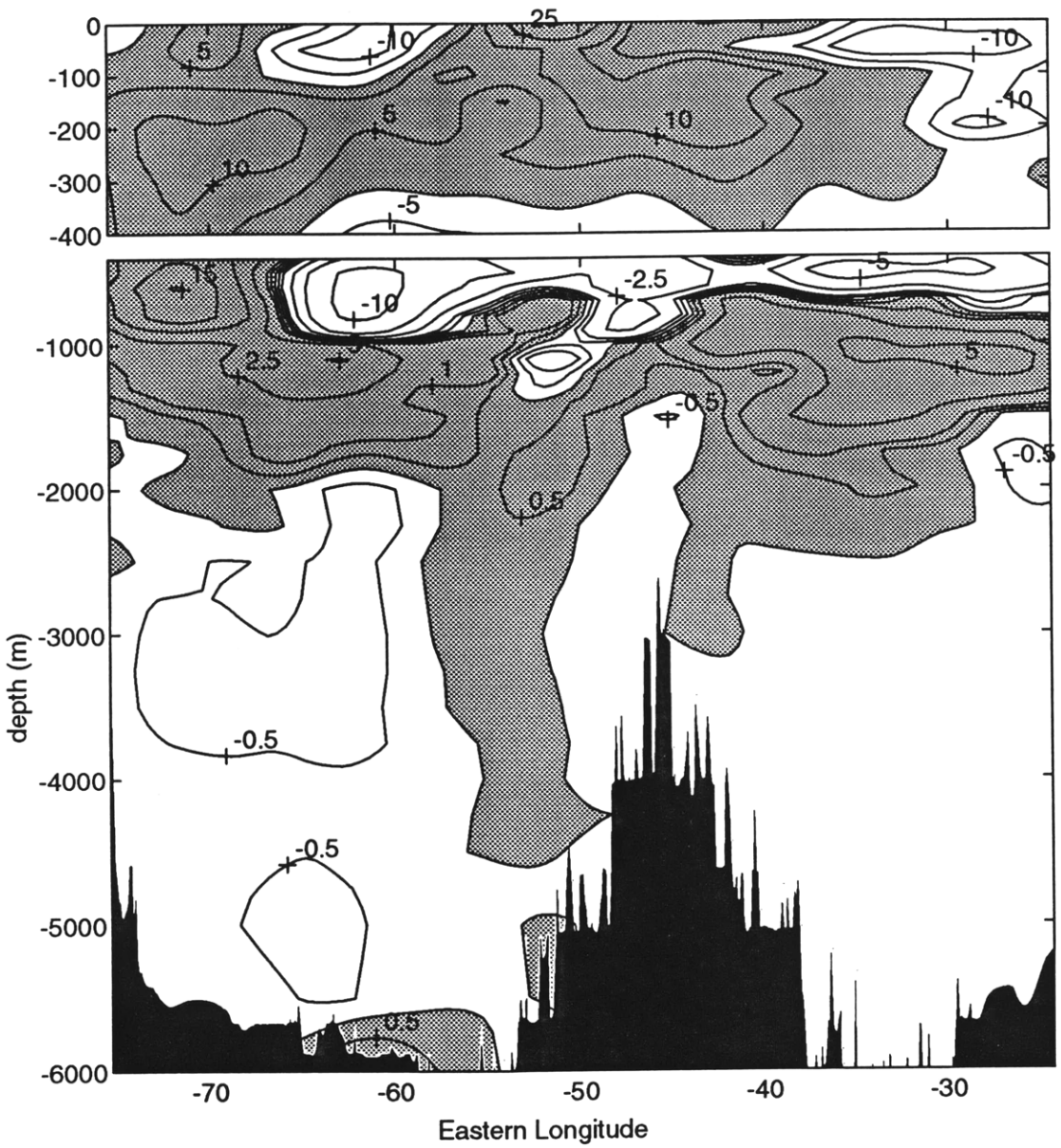
depth (m)
0
-100
-200
-300
-400
-1000
-2000
-3000
-4000
-5000
-6000
-70
-60
-50
-40
-30
Eastern Longitude
25
5
-10
10
-5
2.5
1
-2.5
-0.5
0.5

C

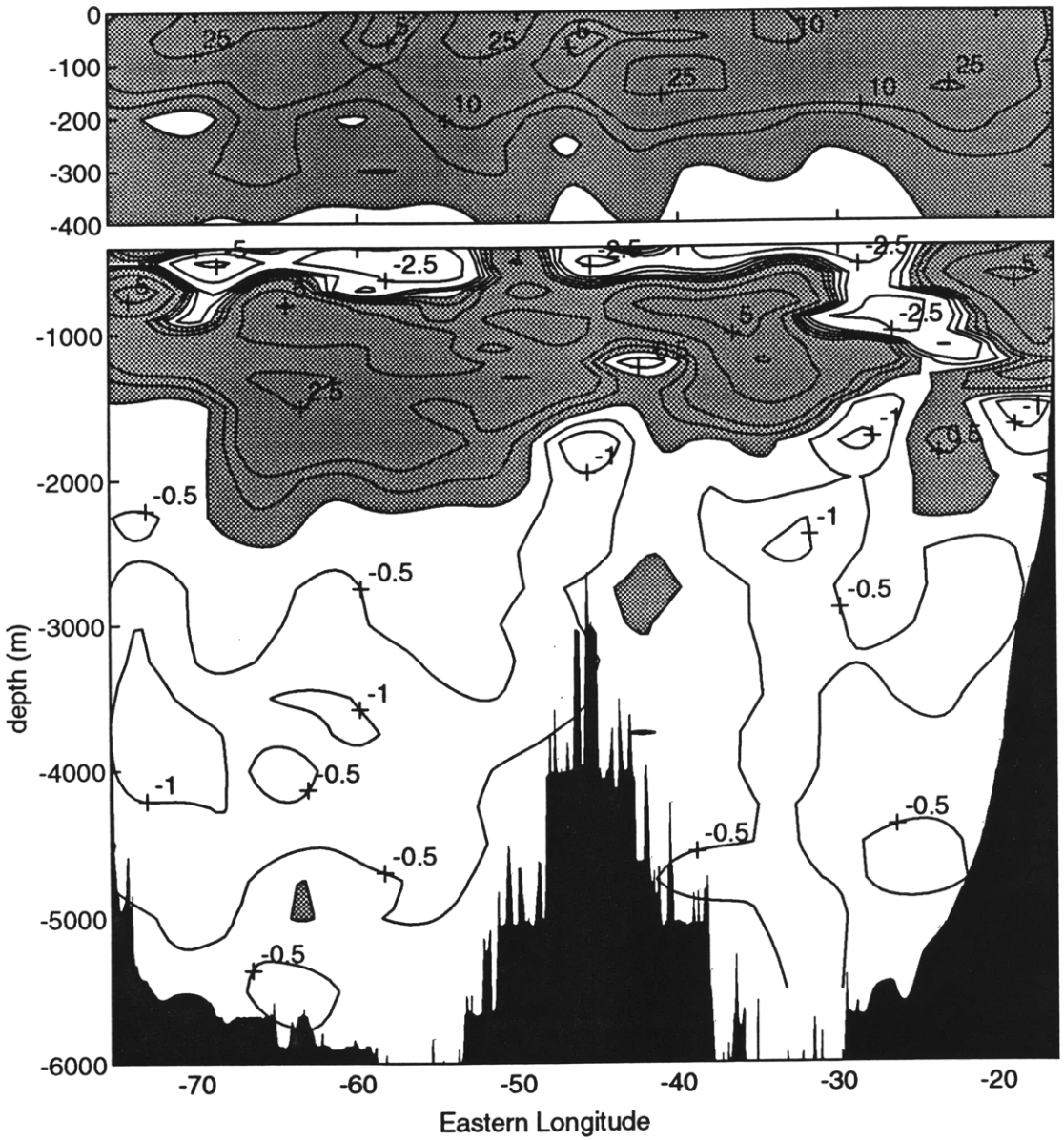
0
-100
-200
-300
-400
-1000
-2000
-3000
-4000
-5000
-6000
depth (m)
-70
-60
-50
-40
-30
-20
Eastern Longitude
25
10
-2.5
-1
-0.5

2.2.2 Objective mapping

The technique for the objective mapping is based on a standard statistical result, the Gauss-Markov Theorem, which gives an expression for the minimum variance linear estimate of some physical variable given measurements at a limited number of data points (Bretherton *et al.* 1976). Objective mapping has been used by a number of physical oceanographers, (e.g.., Roemmich (1983), Wunsch(1985) and (1989), Fukumori *et al.* (1991)); I will give just the basic derivation applied to a hydrographic section.

We are presented with a section of hydrographic stations, in the case of the Hespérides cruise 101 stations, located in a set of longitudes r= $[r_i]$. For each standard depth we have a data series of variables such as temperature, salinity, etc. Let's call them $\{T_i\}$ = T(r_i) where i goes from 1 to the number of stations sampled at that depth.

Because of sloping topography at the boundaries and the Mid-Atlantic Ridge, not all the depths will have 101 values. Below 3500 m, we will have two data series, one for the North American Basin and another for the Canary Basin. We denote the total number of stations by N.

In the case that the mean, $< T_i >= 0$, (usually approximation is obtained by removing the sample mean value at each standard depth), the covariance matrix of T at the data point is given by:

$$\{R_{ij}\} = R(r_i, r_j) \; = \; \{< T_i \, T_j >\} \tag{2.7}$$

where i and j go from 1 to N. The size of this data covariance matrix is an N x N. If T is *spatially stationary* or homogeneous its second moments depend only on the separation of the evaluation points.

$$R_{ij} = R(r_i - r_j) \tag{2.8}$$

The set $\hat{r} = \{\hat{r}_i\}$ contains the points where the values of T_i are required. In this case the points will be from the western coastline (75.5°W) to the eastern coastline (16°W) with an interval of 0.5°. The number of interpolated values, M, is 120. The objective is to estimate the variable value $\hat{T}(\hat{r})$ from observations. $S(r_j) = T(r_j) + n(r_j)$ where n is the observational noise, with zero mean and known covariance.

$$< n(r_i)\, n(r_j) >= N(r_i - r_j) \tag{2.9}$$

Then $R(\hat{r}_k, r_i)$ is the covariance matrix of T at the interpolation points with its value at any data point. The field we seek to map has the statistics given by R. Suppose the noise is uncorrelated with the value of T:

$$< T(r_i)\, n(r_j) > = \ 0 \text{ all } i, j \tag{2.10}$$

Suppose further, that the interpolated value is a weighted average of the observations:

$$\hat{\mathbf{T}}(\hat{r}_k) = \sum_j \mathbf{B}(\hat{r}_k, r_j)\, \mathbf{S}(r_j) \ = \ \mathbf{B}(\hat{r}_k)\, \mathbf{S} \tag{2.11}$$

where **B** is an M x N matrix. We then evaluate the variance of the difference between the correct value at $\hat{r}_k$ and the interpolated value

$$\mathbf{P} \ = < (\hat{\mathbf{T}}(\hat{r}_k) - \mathbf{T}(\hat{r}_k))^2 > = < (\mathbf{B}\, \mathbf{S} - \mathbf{T}(\hat{r}))^2 > \tag{2.12}$$

The Gauss-Markov theorem states that the minimum of this difference is reached when **B** is chosen as

$$\mathbf{B} \ = \ \mathbf{R}(\hat{r}_k, r_i)\, [\mathbf{R}(r_i, r_j) + \mathbf{N}(r_i, r_j)]^{-1} \tag{2.13}$$

and the minimum possible expected error is,

$$\mathbf{P_{min}} \ = \ \mathbf{R}(\hat{r}_k, \hat{r}_k) - \mathbf{R}(\hat{r}_k, r_i)\, [\mathbf{R}(r_i, r_j) + \mathbf{N}(r_i, r_j)]^{-1}\, \mathbf{R}^T(r_j, \hat{r}_k) \tag{2.14}$$

One of the important uses of the mapping is the determination of a mean value. Let the measurements of a variable, temperature for example, be denoted by y_i and

suppose that each is made up of a large-scale mean, m, plus a deviation from that mean of θ_i (Wunsch, 1989), so that we can write

$$m + \theta_i = y_i, i = 1 \text{to} N \tag{2.15}$$

or

$$\mathbf{D}m + \theta = \mathbf{y}, \mathbf{D}^T = [1, 1, ..1] \tag{2.16}$$

We seek a best estimate, $\hat{m}$, of m. Suppose an *a priori* estimate of the size of m exists, and is called m_0, i.e. $< m^2 >= m_0^2$. If $\mathbf{R}$ is the spatial covariance of the measured field about its true mean, the best estimate of the mean (Liebelt, 1967, Eq. 5-26) can be written

$$\begin{aligned} \hat{m} &= [\frac{1}{m_0^2} + \mathbf{D}^T\mathbf{R}^{-1}\mathbf{D}]^{-1}\mathbf{D}^T\mathbf{R}^{-1}\mathbf{y} \\ &= \frac{1}{\frac{1}{m_0^2} + \mathbf{D}^T\mathbf{R}^{-1}\mathbf{D}}\mathbf{D}^T\mathbf{R}^{-1}\mathbf{y} \end{aligned} \tag{2.17}$$

($\mathbf{D}^T\mathbf{R}^{-1}\mathbf{D}$ is a scalar). The expected error of the estimate is

$$\begin{aligned} \mathbf{E} &= (\frac{1}{m_0^2} + \mathbf{D}^T\mathbf{R}^{-1}\mathbf{D})^{-1} \\ &= \frac{1}{\frac{1}{m_0^2} + \mathbf{D}^T\mathbf{R}^{-1}\mathbf{D}} \end{aligned} \tag{2.18}$$

the goal of the analysis is to retain and separate the large-scale time-averaged features from the time-dependent features and errors.

Objective mapping requires a statement of the expected *a priori* measurement error, and mapped field covariances (Bretherton *et al.* 1976). We must define what is signal and what is noise, the variance of the data contains the signal variance as well as the noise variance. We assume that the noise includes two components: the first component, n_e, is the variation caused by mesoscale eddies; the second one n_i is the variance caused by the local measurement error (including errors due to navigation, interpolation, instrumentation, etc) (Wunsch, 1989). Assuming the component are

independent of one another, the total variance $< T_i^2 >$ can be written,

$$< T_i^2 > = < s_i^2 > + < n_e^2 > + < n_i^2 > \tag{2.19}$$

where the total variance of the data is given by the signal variance $< s_i^2 >$, the eddy noise variance $< n_e^2 >$ and the intrinsic noise variance $< n_i^2 >$.

Signal and eddy noise covariances will be modeled by a gaussian covariance function; n_i is modeled by a delta function, n_e on the other hand, has a finite correlation distance, but this distance is smaller than the correlation distance of the signal we are trying to map.

To estimate the e-folding scale of these distributions I have calculated the correlation function. I will describe the calculations done for the 1992 cruise. Because of the different station spacing, we have used 3 sets of data: the Canary Basin between station 11 and 41; the Mid-Atlantic Ridge between stations 42 and 64 and the North American Basin between stations 65 and 96. The distance between stations was 58 km for the Mid-Atlantic Ridge region and 67 km on the other two regions. To estimate the dominant length scales of the eddies we compute the spatial correlation function

$$P(\Delta x) = \frac{< T'(x)T'(x+\Delta x) >}{\sqrt{< (T'(x))^2 >< (T'(x+\Delta x))^2 >}} \tag{2.20}$$

where T' are the data values once we have subtracted the linear trend.

We have computed the function for Δx = 0, 58, 67, 116, 134,... km. Figure 2.3 A, B and C present the values for depths of 100, 900 and 5000 m. For these plots we can see short scale correlations over the Mid-Atlantic Ridge for the shallower plots (there are no 5000 m depths over the Mid-Atlantic Ridge). The zero-crossing distance is between 75 and 100 km. In deep water, for the eastern basin, this distance is around 150 km, and between 150 and 200 km for the western basin. We have taken a value of 175 km for e-folding distance of the gaussian noise covariance. The scale is perhaps somewhat too large, but it has been chosen to make the plots smoother.

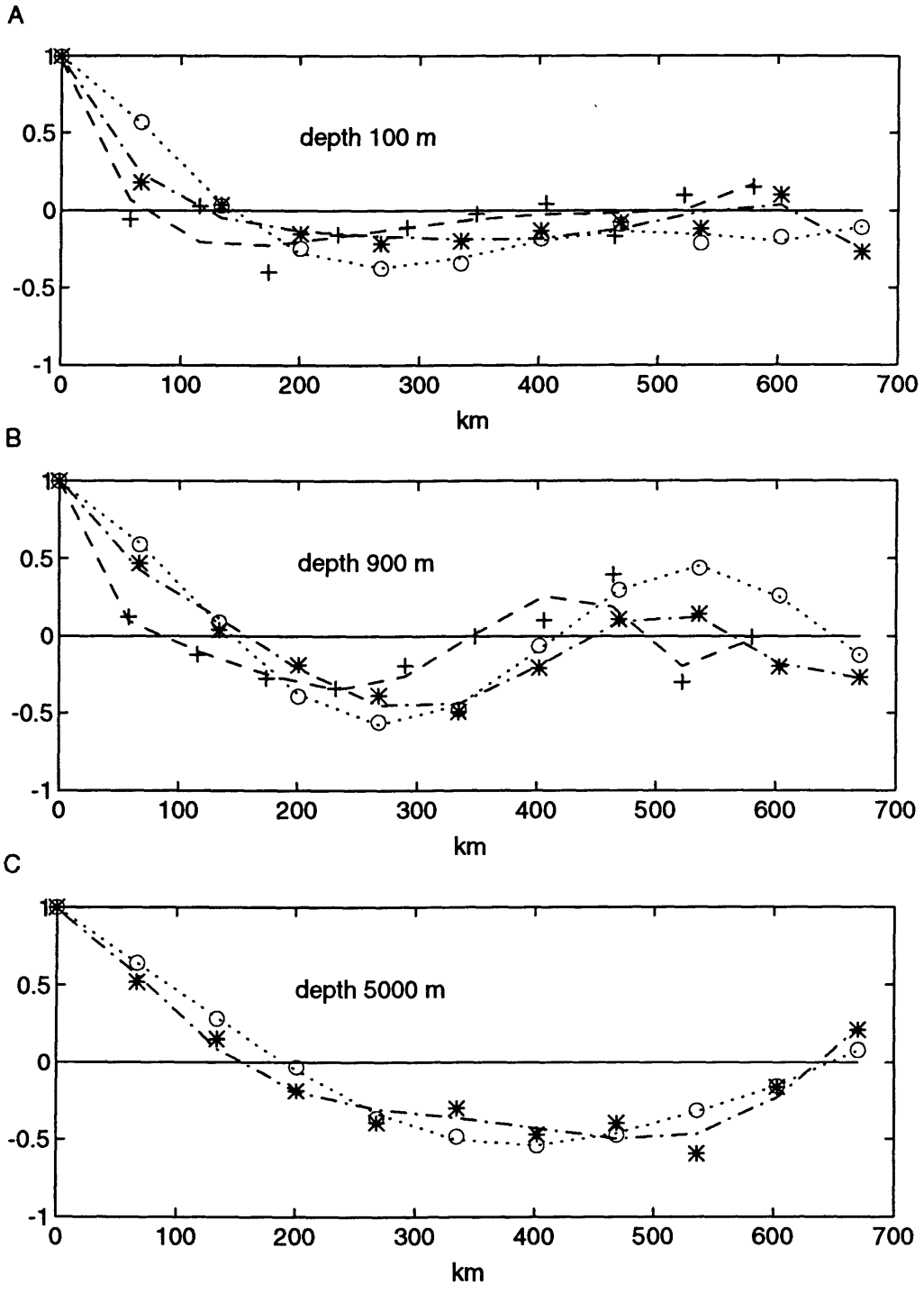

Figure 2.3: Correlation function (equation 2.20) for the North American Basin (o), Mid-Atlantic Ridge(+) and Canary Basin (x) for some depths A) 100 m, B) 900 m and C) 5000 m

Same as Fig 2.3 but with eddy motion filtered out was done for the the signal correlation function. Figure 2.4 A, B and C show the signal correlation function for depths of 0, 1200 and 4250 m. We have taken an e-folding scale of 400 km for the signal covariance at all depths. The zero-lag covariances have been estimated following the method described by Fukumori *et al.* (1991). Let T_j the data at station j at a certain depth, with signal s_j, eddy noise n_{ej} and intrinsic noise n_{ij}

$$T_j = s_j + n_{ej} + n_{ij} \tag{2.21}$$

The mean square difference from a neighboring station $(j+1)$ is,

$$\begin{aligned} < (T_j - T_{j+1})^2 > &= < (s_j - s_{j+1} + n_{ej} - n_{ej+1} + n_{ij} - n_{ij+1})^2 > \\ &= < (s_j - s_{j+1} + n_{ej} - n_{ej+1})^2 > + 2 < n_i^2 > \end{aligned} \tag{2.22}$$

where we have assumed the intrinsic noise is uncorrelated over the distance and has uniform variance. If the signal and the eddy noise have much longer correlation distances than the station separation, it is possible to neglect the first term on the right hand side of equation 2.22 with respect to the second term which yields

$$< (T_j - T_{j+1})^2 > \approx 2 < n_i^2 > \tag{2.23}$$

In the same way, let $< (T_j - T_k)^2 >_L$ denote the mean square difference of data between two points, j and k, separated by L km, then

$$\begin{aligned} < (T_j - T_k)^2 >_L &= < (s_j - s_k + n_{ej} - n_{ek} + n_{ij} - n_{ik})^2 > \\ = 2 < s^2 > - 2 < s_j s_k >_L + 2 < n_e^2 > - 2 < n_{ej} n_{ek} >_L + 2 < n_i^2 > \end{aligned} \tag{2.24}$$

If the signal s, has a length scale much longer than L, the second term will be similar to the first and they will partially cancel. Using a distance of 400 km, these two terms cancel; if the eddy noise covariance has a length scale smaller than that distance, then equation 2.24 will be approximated by

$$< (T_j - T_k)^2 >_{400km} = 2 < n_e^2 > + 2 < n_i^2 > \tag{2.25}$$

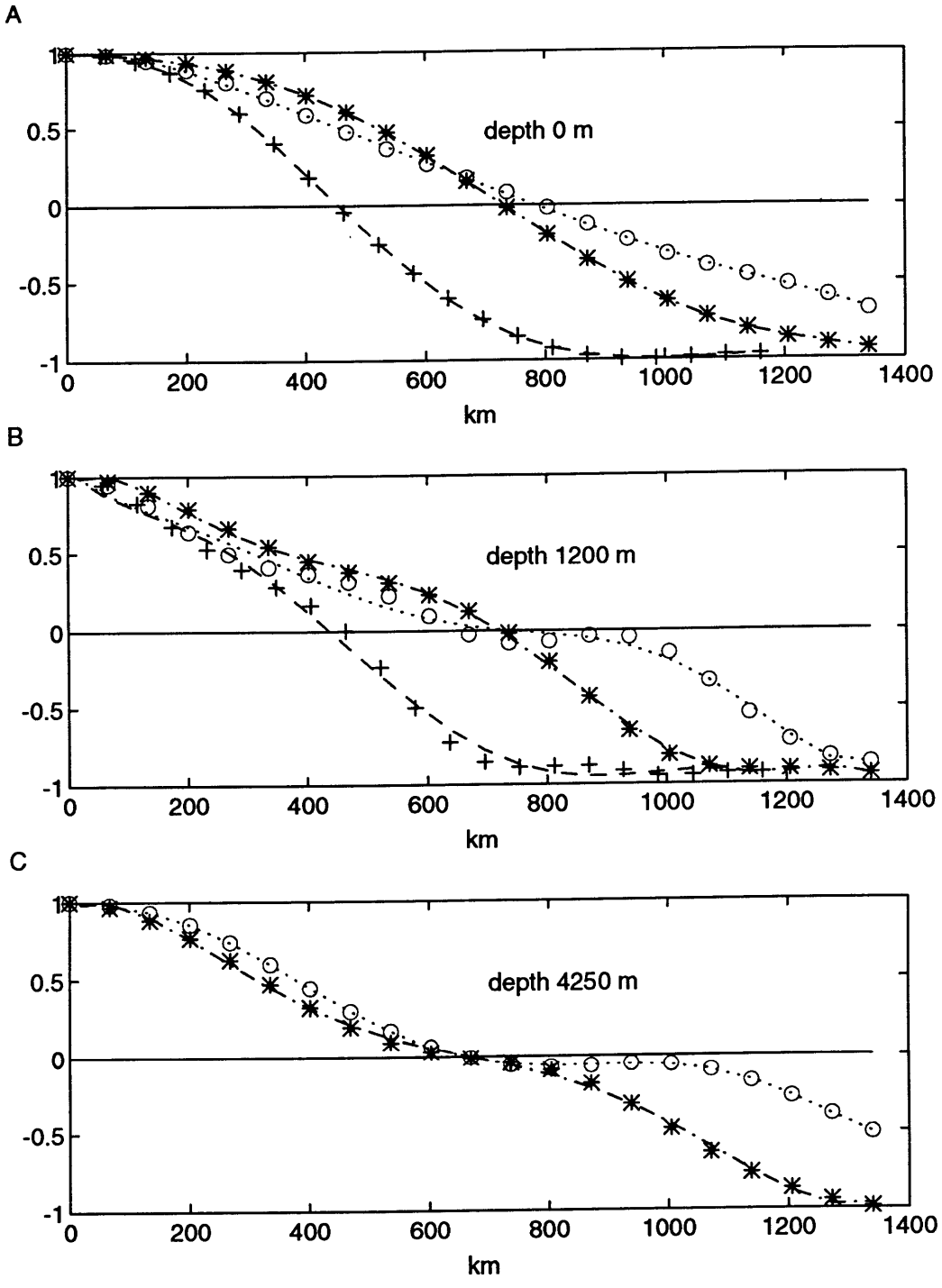

Figure 2.4: Signal correlation function (same as Fig 2.3, but with eddy motion filtered out) for the North American Basin (o), Mid-Atlantic Ridge(+) and Canary Basin (x) for depths A) surface , B) 1200 m and C) 4250 m

Signal variances have then been calculated by equation 2.19.

For computing the expected difference for a spatial separation, we have taken the data set between station 11 and station 96, where the spacing is homogeneous. The distance between a station and the neighboring one is less than 70 km. Due to the different behavior of the deeper part of the North American and the Canary Basins the variance calculations for depths below 2750 m (the depth of the shallowest station in the Mid-Atlantic Ridge) have been computed separately for each basin.

At 900 m the signal variance is smaller than the noise variance. The mapping is practically using the mean temperature value for most of the section. In the Canary Basin, values below 4750 are scarce. For the computations of the eddy noise variance we have used a distance of 200 km, and for the intrinsic noise a value of 0.004°C at 4750 m and 6000 m. On the Western Basin at 6000 m we have used a value 0.002°C. These values are slightly higher than the value for instrumental noise of a Mark III CTD given by Millard *et al.*, 1990.

The variances used are:

$$< s_i^2 > = < T_i^2 > - \frac{1}{2} < (T_i - T_j)^2 >_{400Km} \tag{2.26}$$

$$< n_e^2 > = \frac{1}{2} < (T_i - T_j)^2 >_{400Km} - < n_i^2 > \tag{2.27}$$

$$< n_i^2 > = \frac{1}{2} < (T_i - T_{i+1})^2 >_{70Km} \tag{2.28}$$

The variance of the temperature signal (s_i^2), eddy noise (n_e^2) and measurement noise (n_i^2) are summarized in Table 2.1 at the standard depths for all the North Atlantic Basin shallower than 2750 m., Table 2.2 below 3000 m for the North American Basin and Table 2.3 below 3000 m for the Canary Basin.

The variance of the salinity signal (s_i^2), eddy noise (n_e^2) and measurement noise (n_i^2) are summarized in Table 2.4 at the standard depths for all the North Atlantic

depth (m.)	s_i °C	n_e °C	n_i °C
0	2.41	0.33	0.17
50	1.94	0.81	0.64
100	1.54	0.73	0.65
150	1.10	0.69	0.71
200	1.04	0.44	0.47
250	1.15	0.29	0.30
300	1.34	0.23	0.25
400	1.59	0.29	0.24
500	1.50	0.35	0.24
600	1.17	0.33	0.24
700	0.85	0.33	0.24
800	0.50	0.28	0.23
900	0.19	0.24	0.19
1000	0.22	0.15	0.16
1100	0.36	0.10	0.23
1200	0.45	0.10	0.21
1300	0.46	0.11	0.14
1400	0.43	0.10	0.12
1500	0.37	0.08	0.11
1750	0.22	0.06	0.06
2000	0.13	0.05	0.05
2250	0.09	0.04	0.04
2500	0.06	0.03	0.03
2750	0.03	0.02	0.03

Table 2.1: Signal (s_i), eddy noise (n_e) and measurement noise (n_i) square root variances for mapping temperature data at the indicated depth at 24.5 °N for all the North Atlantic Basin shallow than 2750 m. Data are given in °C

depth (m.)	s_i °C	n_e °C	n_i °C
3000	2.57	1.31	2.97
3250	3.42	1.55	2.62
3500	3.59	1.90	2.68
3750	1.56	1.53	1.96
4000	2.70	1.70	1.56
4250	3.65	2.39	1.74
4500	4.92	3.31	1.69
4750	5.48	4.48	1.87
5000	6.15	7.15	2.96
5500	5.62	6.20	3.75
6000	1.17	0.11	0.20

Table 2.2: Signal (s_i), eddy noise (n_e) and measurement noise (n_i) square root variances for mapping temperature data below 3000 m at 24.5 °N for the North American Basin. Data are given in °C x 10^{-2}

depth (m.)	s_i °C	n_e °C	n_i °C
3000	1.24	1.55	1.57
3250	1.10	1.60	1.00
3500	2.31	0.96	0.99
3750	2.51	1.15	1.16
4000	2.22	0.96	1.04
4250	0.98	1.42	1.04
4500	1.70	0.27	0.59
4750	0.49	0.13	0.40
5000	1.17	0.72	0.53
5500	1.22	1.38	0.78
6000	0.67	0.37	0.40

Table 2.3: Signal (s_i), eddy noise (n_e) and measurement noise (n_i) square root variances for mapping temperature data below 3000 m at 24.5 °N for the Canary Basin. Data are given in °C x 10^{-2}

Basin shallow than 2750 m., Table 2.5 below 3000 m for the North American basin and Table 2.6 below 3000 m for the Canary Basin.

Since the distance $(r_i - r_j)$ in our covariance functions is given in longitude degrees, we have used 4° and 1.75°, which is equivalent to 400 and 175 km (at this latitude 1°x 60' x cos(24.5)=101 km). Then the covariances are:

$$\mathbf{R}(r_i - r_j) = < s_i^2 > \exp(-(r_i - r_j)^2/4^2) \tag{2.29}$$

$$\mathbf{N}_e(r_i - r_j) = < n_e^2 > \exp(-(r_i - r_j)^2/1.75^2) \tag{2.30}$$

$$\mathbf{N}_i(r_i - r_j) = < n_i^2 > \delta(r_i - r_j) \tag{2.31}$$

Behavior of the mapping function on the boundaries

As you approaches the boundaries not all data point are available and the mapping function given by equation 2.13 becomes one sided. The mapping function reduces the variability of the data, errors increase and the expected value tends to the mean.

Figure 2.5 presents values of raw data and mapped data with its error at 5000 m depth in the North American and Canary Basins. It is possible to see the different behavior of the temperature in both basins and the associated error. The uncertainty is around 0.04°C in the North American Basin and only about 0.005°C in the Canary Basin. Errors are slightly increased near the boundaries. In this case the mapped values are practically within the sampled area. Near the boundaries of the basins where due to the irregular topography there are some gaps, we have mapped values outside the sampled area.

The mapping values of temperature for the 1992 cruise are presented in Figure 2.6. The expected error in the temperature mapping (Bretherton *et al.* 1976) as a function of depth is shown on the right side. Below 3000 m, the error is given separately for the North American and Canary Basins. These errors have been computed

depth (m.)	s_i pss	n_e pss	n_i pss
0	4.21	1.93	1.24
50	3.36	1.18	0.99
100	2.10	0.90	1.11
150	1.12	0.73	1.31
200	0.93	0.46	0.81
250	1.47	0.39	0.56
300	1.96	0.33	0.44
400	2.40	0.43	0.38
500	2.09	0.49	0.36
600	1.42	0.42	0.35
700	0.91	0.42	0.34
800	0.49	0.34	0.34
900	0.36	0.29	0.25
1000	0.42	0.22	0.24
1100	0.50	0.20	0.50
1200	0.59	0.18	0.39
1300	0.60	0.19	0.25
1400	0.59	0.19	0.22
1500	0.51	0.17	0.19
1750	0.35	0.12	0.10
2000	0.22	0.07	0.06
2250	0.15	0.04	0.04
2500	0.10	0.03	0.03
2750	0.06	0.02	0.02

Table 2.4: Signal (s_i), eddy noise (n_e) and measurement noise (n_i) square root variances for mapping salinity data at the indicated depth at 24.5 °N for all the North Atlantic Basin shallow than 2750 m. Data are given in pss x 10^{-1}

depth (m.)	s_i pss	n_e pss	n_i pss
3000	1.71	1.91	2.14
3250	1.32	1.93	1.89
3500	2.29	2.25	2.08
3750	3.21	2.42	1.98
4000	5.29	3.19	1.66
4250	6.19	4.06	2.41
4500	7.61	5.20	2.21
4750	8.35	5.72	2.45
5000	7.77	8.51	3.62
5500	6.76	7.50	4.79
6000	1.58	0.41	0.91

Table 2.5: Signal (s_i), eddy noise (n_e) and measurement noise (n_i) square root variances for mapping salinity data at the indicated depth at 24.5 °N Below 3000 m for the North American Basin. Data are given in pss x 10^{-3}

depth (m.)	s_i pss	n_e pss	n_i pss
3000	2.28	1.18	1.57
3250	0.70	1.57	1.08
3500	1.25	0.84	0.87
3750	1.73	1.23	1.30
4000	1.23	1.11	1.00
4250	0.49	1.28	0.99
4500	1.28	0.57	0.78
4750	0.47	0.34	0.57
5000	0.98	1.05	0.63
5500	1.22	1.61	0.76
6000	0.39	0.51	0.85

Table 2.6: Signal (s_i), eddy noise (n_e) and measurement noise (n_i) square root variances for mapping salinity data at the indicated depth at 24.5 °N Below 3000 m for the Canary Basin. Data are given in pss x 10^{-3}

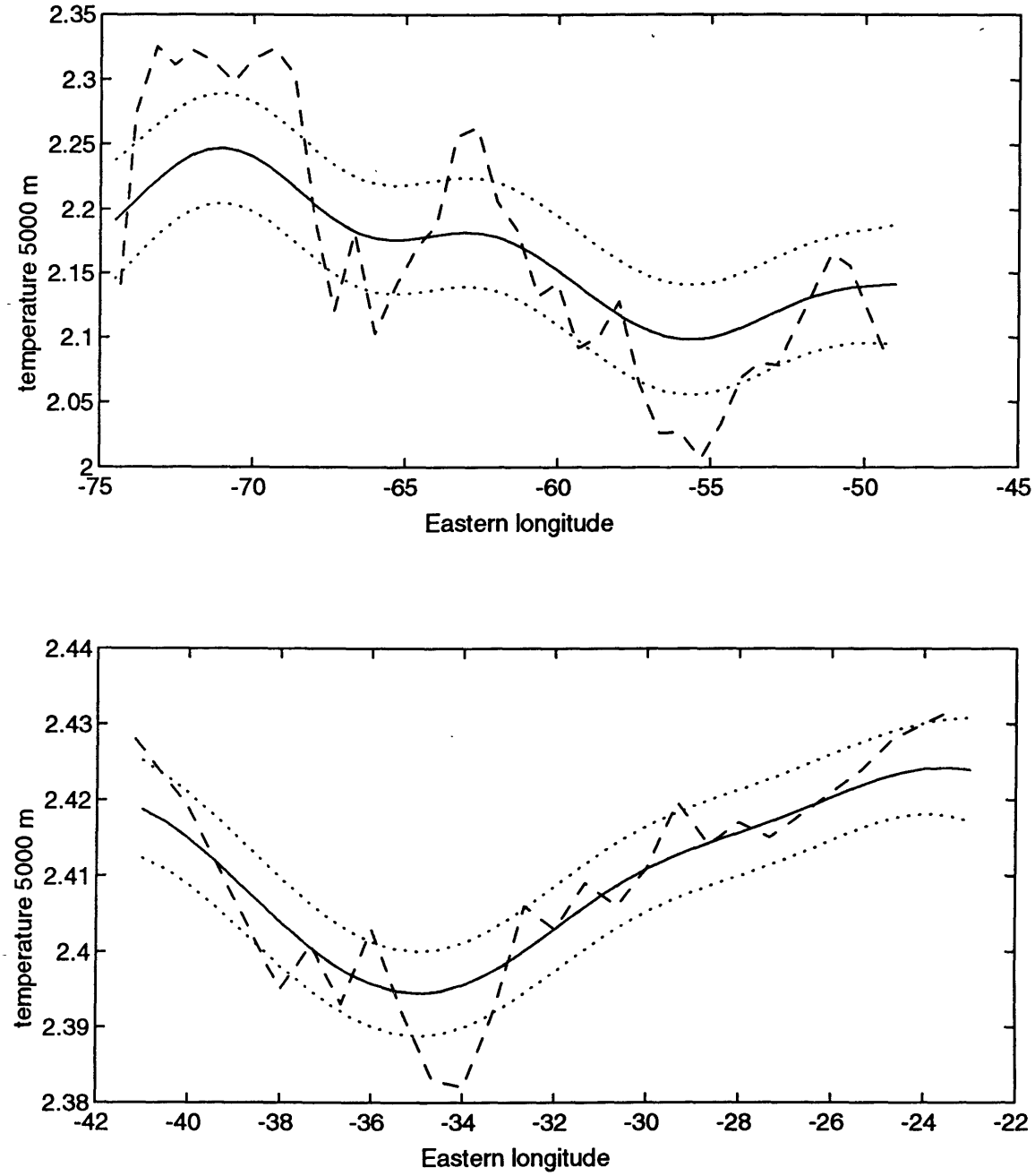

Figure 2.5: 1992 cruise raw data (dashed), mapping data (solid) plus/minus the error in the mapping (dotted) for A)North American basin and B) Canary Basin. data are in °C.

by the square root of the diagonal of P_{min} in (2.14) . The highest values appear at 50 m, where the highest eddy noise variance was found (Table 2.1). Between this depth and the middle of the thermocline ($\sim$ 850 m), the error decreases to 0.2°C. Below $\sim$2000 m, the expected error is less than 0.05°C, for all the cruises. Errors in the Canary basin are less than 0.02°C while in the North American one they are between 0.01 and 0.04°C with the highest values appearing between 5000 and 5500 m.

Salinity mapping has been done in the same way as the temperature mapping, we present in Figure 2.7 salinity mapping for the 1992 cruise including the expected error for this mapping. Expected errors in salinity are largest at the surface and reduce with depth.

Calculations of covariances and mapping were performed for 1981 and 1957 datasets the same as it was described for 1992 dataset. After this interpolation to a common grid, we have calculated the differences for the three cruises for the same extension we did for spline interpolation. Figure 2.8 A presents the temperature difference between the 1981-1957 cruises. Figures 2.8 B and 2.8 C give the temperature differences from 1992-1981 and 1992 and 1957.

The expected error of the differences is the sum of the expected errors of the mapping values for each map. We have adding the values of P_{min} in equation (2.14) for each set of data and taking the square root of the diagonal. On the right side of the figures the expected error in function of depth is presented. Figure 2.9 A, B and C presents the difference in salinities for 1981-1957, 1992-1981 and 1992-1957. Expected errors have been calculated in the same way as for temperature.

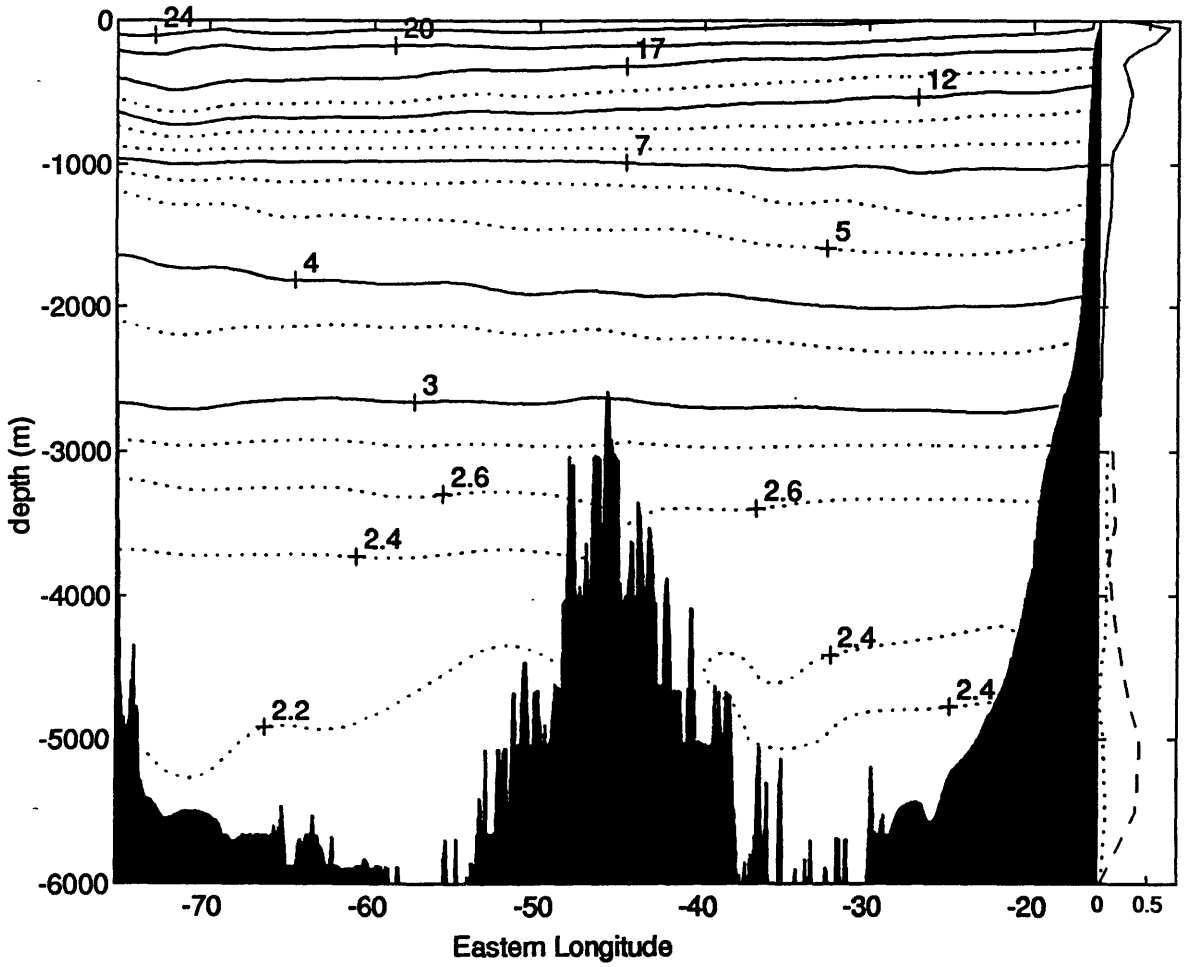

Figure 2.6: Temperature values for the 1992 cruise using objective mapping, Data are in °C. The expected error in the temperature mapping in function of depth is shown on the right side. Below 3000 m, the error is given separately for the Canary (dotted) and North American (dashed) Basins and values are multiplied by 10). Expected errors are in °C.

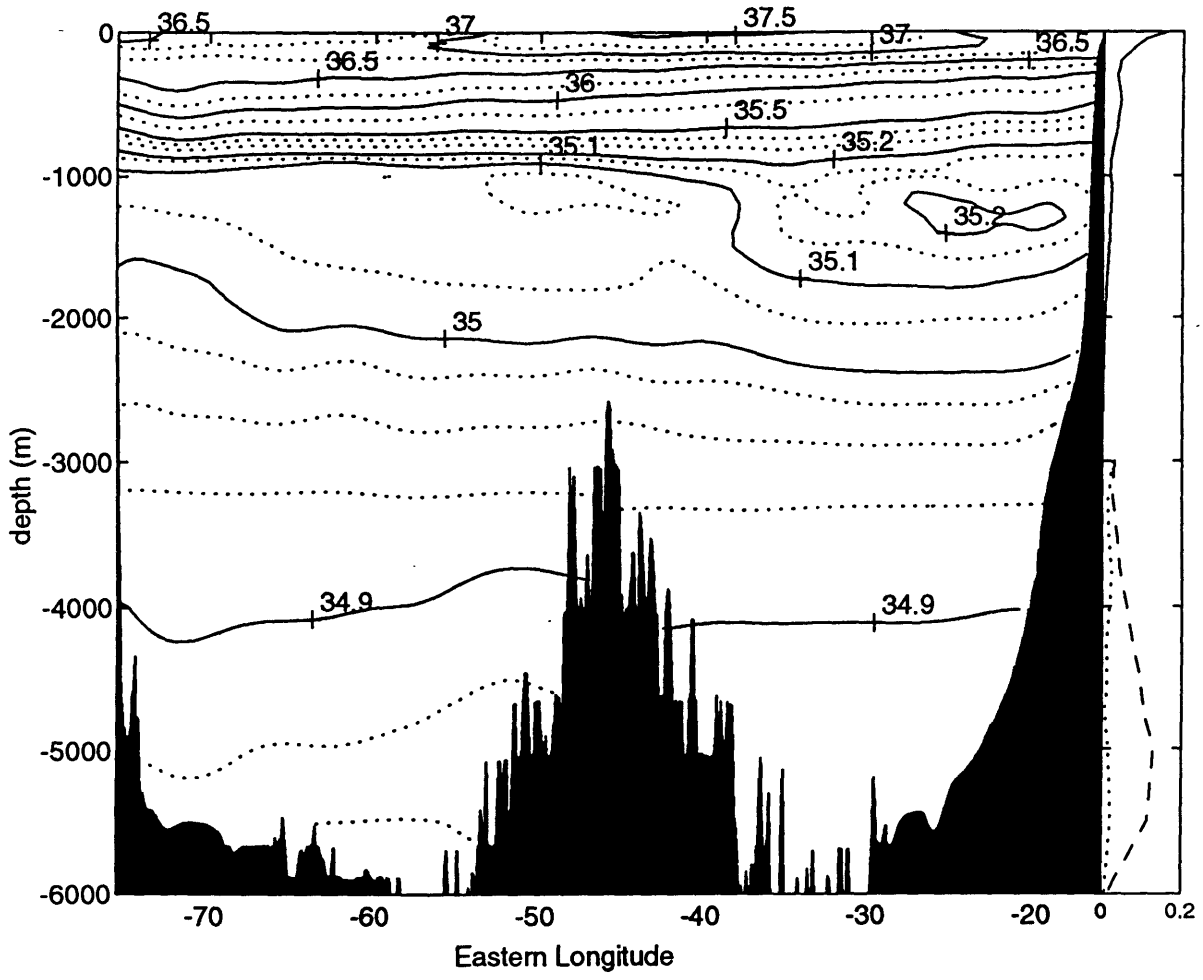

Figure 2.7: Salinity values for the 1992 cruise using objective mapping. The expected error in salinity mapping in function of depth is shown on the right side. Below 3000 m, the error is given separately for the Canary (dotted) and North American (dashed) basins and values are multiplied by 25). Data are in pss.

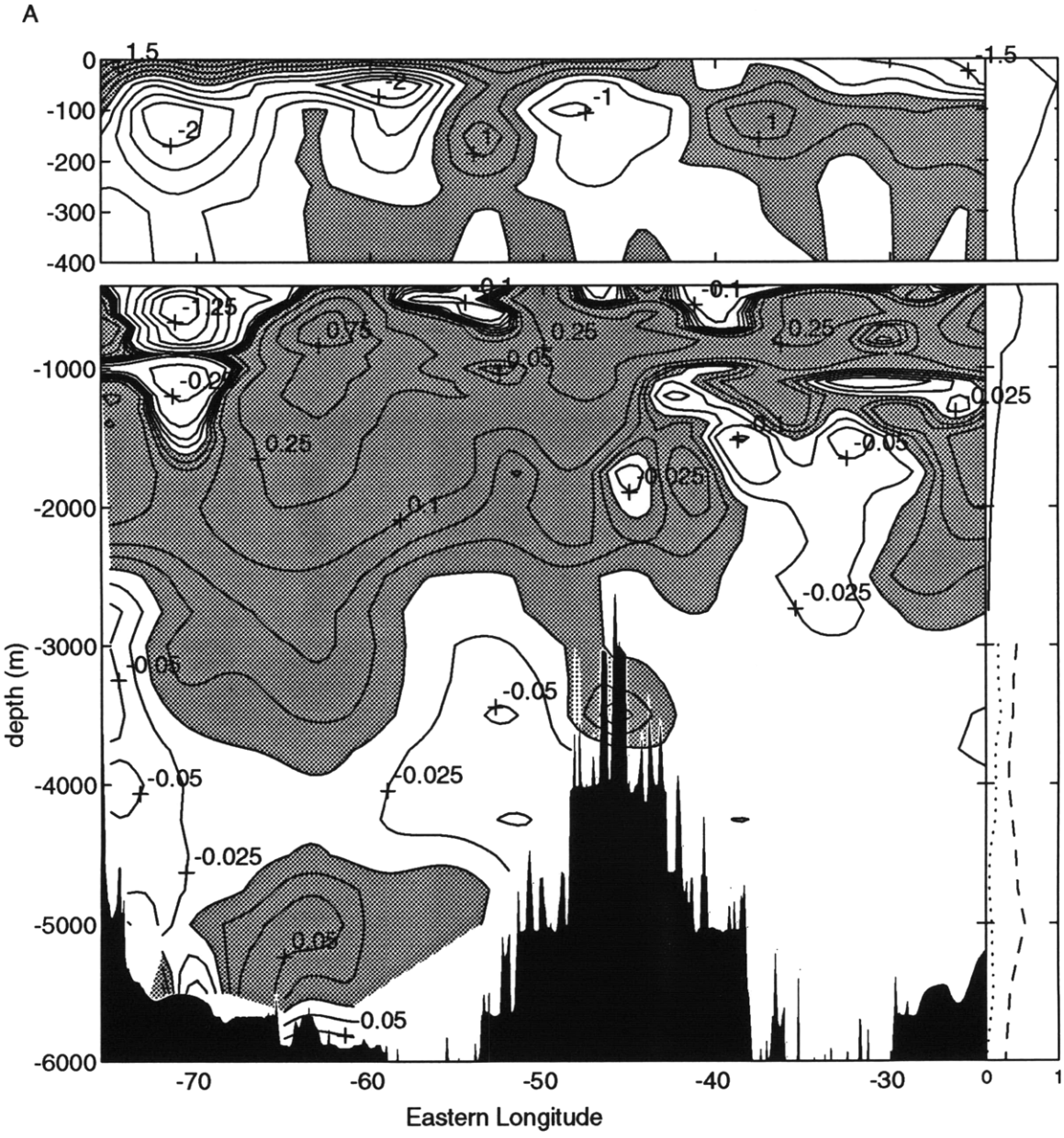

Figure 2.8: Difference of temperature by objective mapping, A) 1981-1957, B) 1992-1981 and C) 1992-1957. Data are in °C. The expected error in the temperature difference in function of depth is shown in the right side. Below 3000 m, the error is given separately for the Canary (dotted) and North American (dashed) basins and values are multiplied by 10). Expected errors are in °C. The shaded indicates positive difference. The top plot has expanded vertical scale.

B

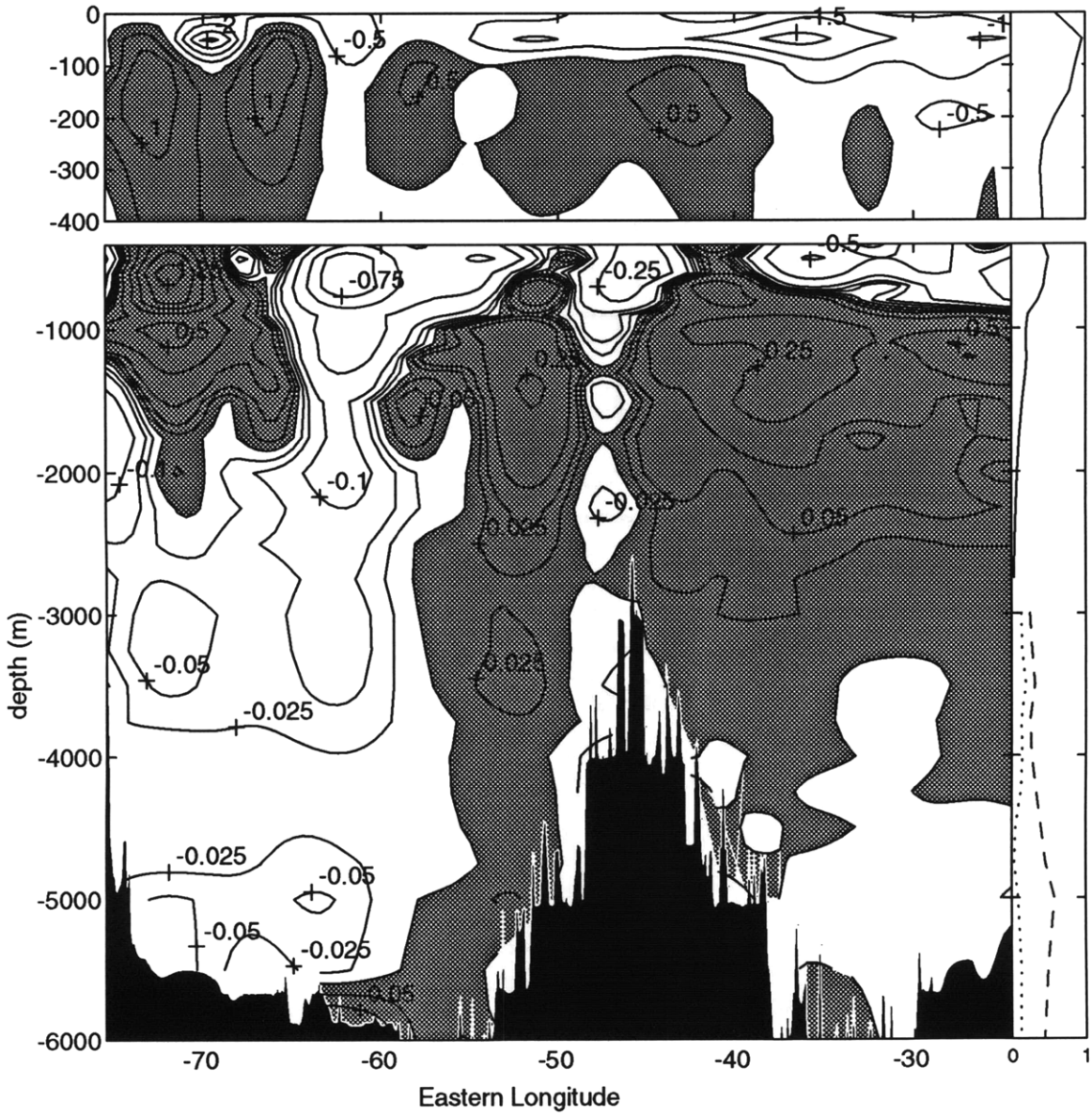
depth (m)
Eastern Longitude
0
-100
-200
-300
-400
-1000
-2000
-3000
-4000
-5000
-6000
-70
-60
-50
-40
-30
0
1
-0.5
0.5
-1.5
-1
-0.75
-0.25
0.25
-0.1
-0.05
-0.025
0.05
0.025

C

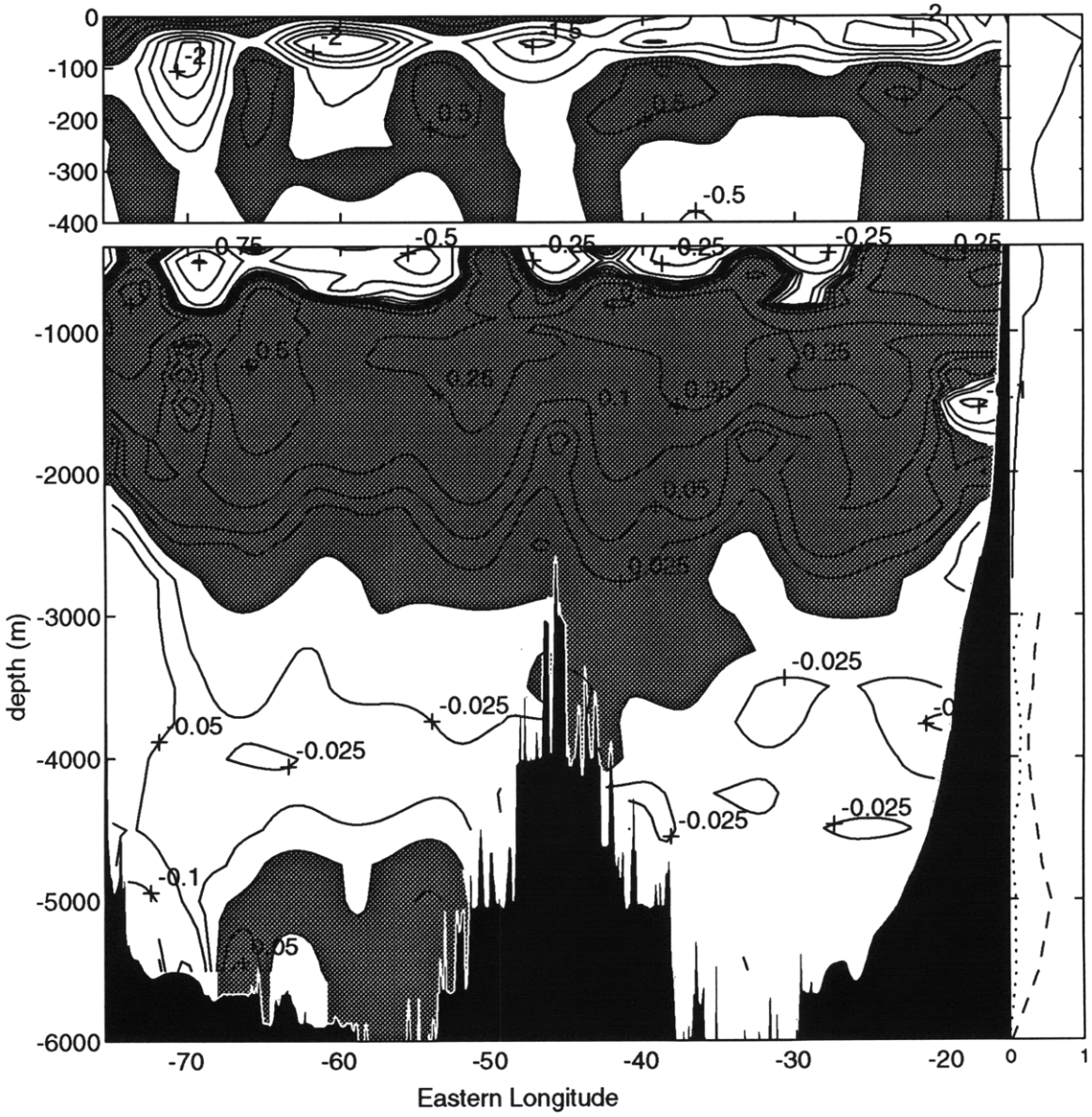
depth (m)
Eastern Longitude
0
-100
-200
-300
-400
-1000
-2000
-3000
-4000
-5000
-6000
-70
-60
-50
-40
-30
-20
0
1
-0.5
-0.25
0.25
0.05
-0.025
-0.1

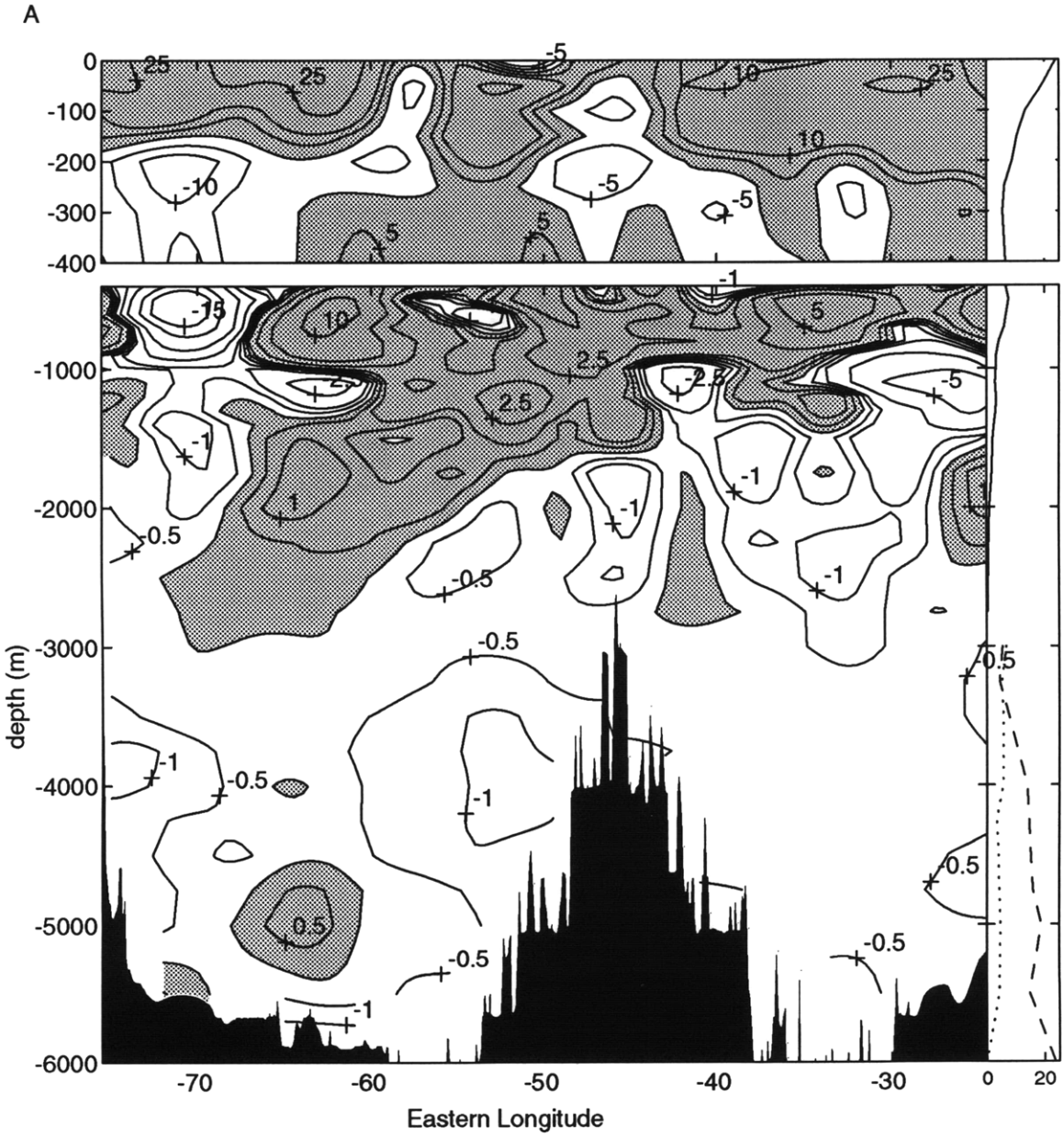

Figure 2.9: Difference of salinity by objective mapping, A) 1981-1957, B) 1992-1981 and C) 1992-1957. Data are in pss x 100. The expected error in salinity difference in function of depth is shown in the right side. Below 3000 m, the error is given separated for the Canary (dotted) and North American (dashed) basins and values are multiplied by 25. The shaded area indicates positive differences. The top plot has expanded vertical scale.

B

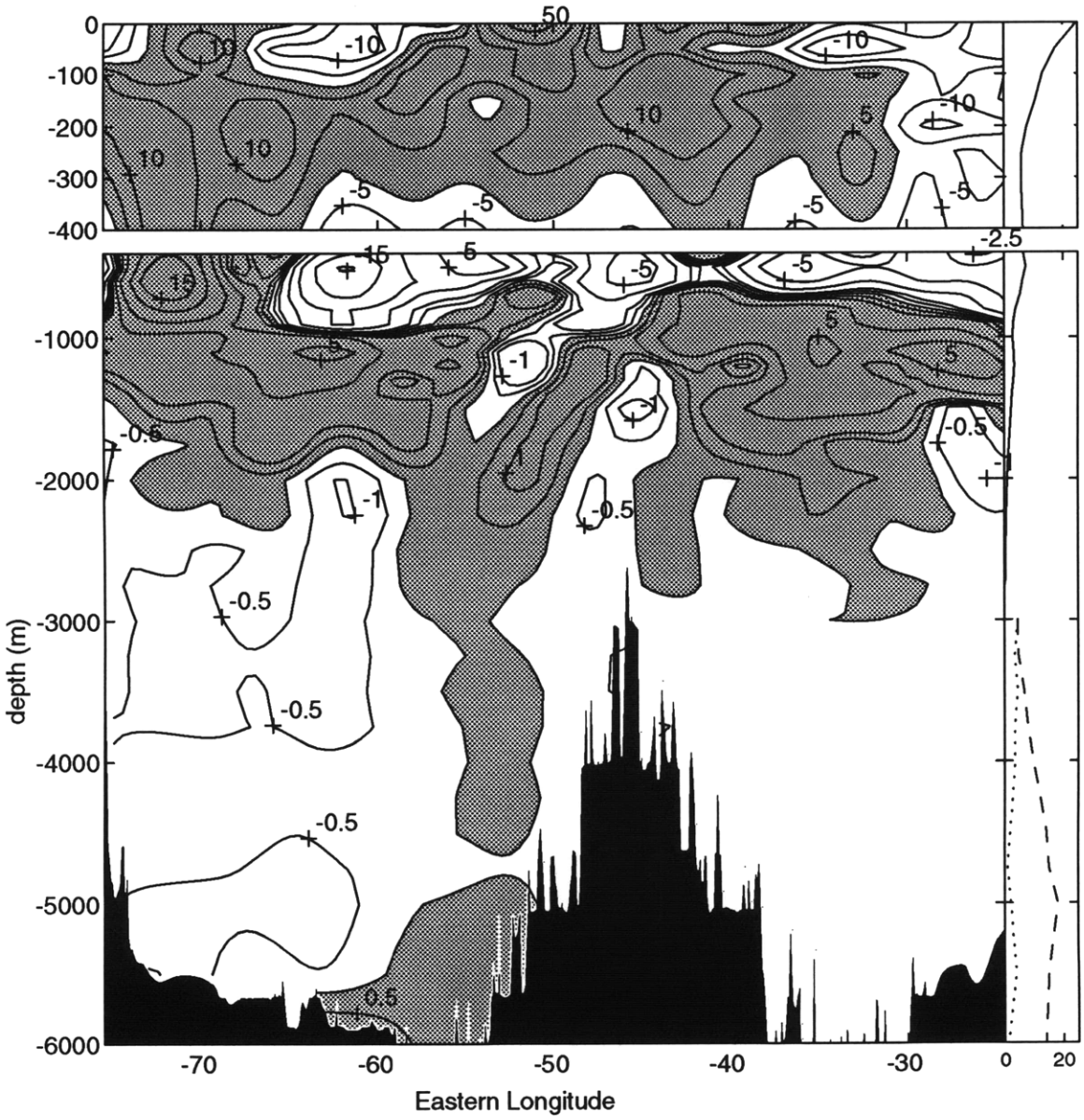
depth (m)
Eastern Longitude
0
-100
-200
-300
-400
-1000
-2000
-3000
-4000
-5000
-6000
-70
-60
-50
-40
-30
0
20
50
-10
10
5
-5
-2.5
15
-1
-0.5

C

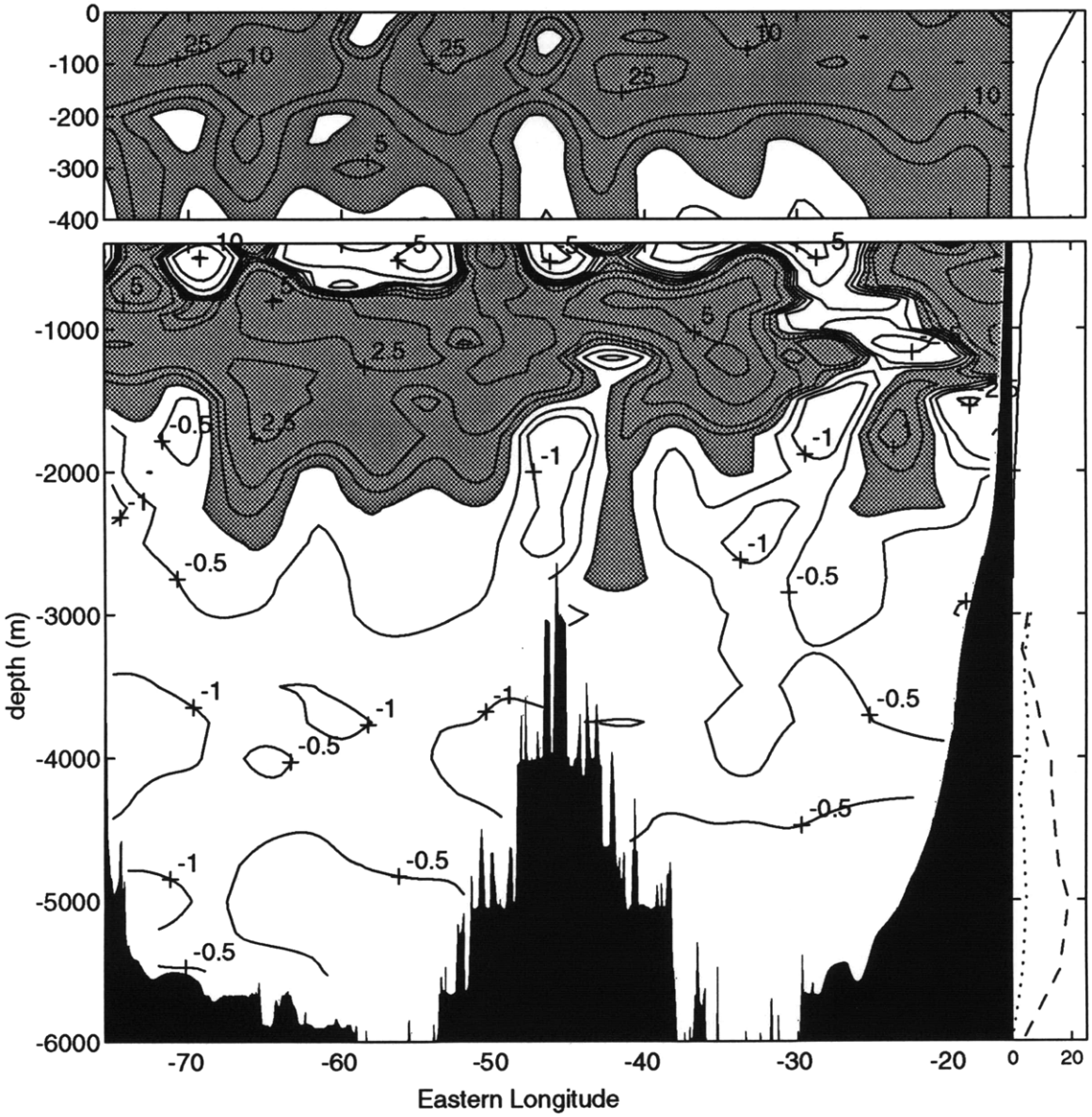
depth (m)
Eastern Longitude
0
-100
-200
-300
-400
-1000
-2000
-3000
-4000
-5000
-6000
-70
-60
-50
-40
-30
-20
0
20

2.2.3 Discussion

I have compared the use of cubic spline interpolation and objective mapping to interpolate the data to a regular grid. The most significant differences between the two methodologies are that the spline interpolation with the gaussian filter gives a large scale vision of the features, but smooths over the small scale features, and that the maximum values are reduced in most of the cases.

The behavior of the gaussian filter on the boundary data is to smooth these values and tends to reduce the differences in this region. The objective mapping also smoothes the values and reduces the differences in the boundaries, but to a lesser extent; so that the objective mapping slightly increases differences relative to the gaussian filter.

This effect can be seen in the eastern boundary 1992-1957 difference (Fig 2.1 C, Fig 2.8 C). In the North American Basin, we can find most of these effects on the two boundaries (Continental shelf and Mid-Atlantic Ridge) and at the bottom of the basin. Even when we are looking at the large scale effects, I think it is convenient maintain these boundary differences.

Due to the behavior of polynomial functions, when the fitting has to be extended outside the sampled area, values calculated by splines change very quickly. In these regions, values given by objective mapping are more realistic than values given by spline interpolation.

There is a high degree of similarity among cubic spline smoothing with a gaussian filter and objective mapping methods using the convenient parameters. The discrepancies are within the expected error in all regions but the boundaries.

Advantages of using cubic spline

- fast, and does not need much memory
- there exist fast routines in software, i.e., in packaged form.
- it doesn't require any *a priori* knowledge about the data or the measurement error.
- gives the real value on the sampled locations
- the results are reasonable, discrepancies are within the expected error, in this application.

Disadvantages of using cubic spline

- there is no estimate of uncertainties

Advantages of using objective mapping

- extrapolated values near the continental slopes or the bottom topography are better determined.
- the most important advantage is the expected error given by the method in the form of an error map.

In this case, when we are attempting to perform data comparison, the error maps are a fundamental requirement. Without the expected errors, we can not recognize whether or not the differences are significant.

Disadvantages of using objective mapping

- It requires a lot more work and computing time, matrices are usually big and demands large computer memory.

- It requires previous knowledge of the covariance functions or assuming the correlation matrices.
- not available in packaged form. One must build it from the start.

The possibility of calculating expected errors has made objective mapping the most suitable method of interpolation for this analysis.

2.3 Differences in Temperature and Salinity

In this section we will describe the features found in the comparison of data carried out by the objective mapping techniques shown in the previous section.

2.3.1 Temperature differences

1981-1957 (Fig 2.8 A)

This comparison was already done by Roemmich and Wunsch (1984). They found warming above about 3000 m and cooling below it. We have calculated differences in temperature using the same dataset and obtained similar results.

The most notable feature has been a large warming mainly in the North American Basin between 55°W and 68°W. Although this feature was the most relevant, I will describe the main differences beginning with the surface water and continuing down through to the water column.

At the surface, there are positive differences in a very thin layer west of 40°W and negative differences east of that longitude. Between this layer and 500 m we found negative differences in the whole area except in the Canary Basin. There is also an area of large cooling in the western part of the North American Basin, centered around 70°W, between 100 and 1500 m. Differences are as large as -2°C at 150 m and -1.25°C at 600 m. East of 60°W there is a cooler layer between 200 and 600 m and a warmer one below it.

In the North American Basin, there was a large warming between 55°W and 68°W. Warming penetrates deeply down to 4000 m and dominates the zonal average temperature change. Maximum positive difference is centered in 62 °W, with values of 0.75 °C between 700 and 800 m. Warming also affects the Canary Basin between

700 and 2500 m. The highest positive differences in this area are about 0.5°C between 800 and 900 m. Below 2500 m on both sides of the North American Basin, and below 4000 m on the central portion, water has cooled, with slightly larger cooling along the western boundary. In the central part of the Canary Basin negative difference is found below 1500 m.

The values of the differences are of the same order of magnitude as the uncertainty in the measurements. Trying to justify that the differences are statistically significant, we have plotted (Figure 2.10) the temperature correlation, function B in equation (2.13) for a point situated at 50°W for 500, 1200 and 5000 m depth (the last one in both basins). The horizontal correlation is around 5 longitude degrees. The scale of most of the features discussed above is larger than this value. Since the calculations have been done independently for each standard depth, features are not artificially correlated at each depth. These two factors increase the reliability of the calculated differences.

1992-1981 (Fig 2.8 B)

The substantial area of warming in the central North American Basin during 1981-1957 has cooled between 1981 and 1992. So that the area of Roemmich and Wunsch (1984) of large warming is now a large cooling region. Similarly, the area of substantial cooling during 1981-1957 centered at about 70°W, has now warmed. Thus, there appears to be an oscillation in temperature with a zonal half-wavelength of about 1000 km. The Canary Basin has warmed considerably down to 4000 m.

The surface layer down to 50 m has cooled. Below this layer, the differences are positive down to 300 m west of 40°W; this warming trend reaches 2000 m in the western part of the North American Basin.

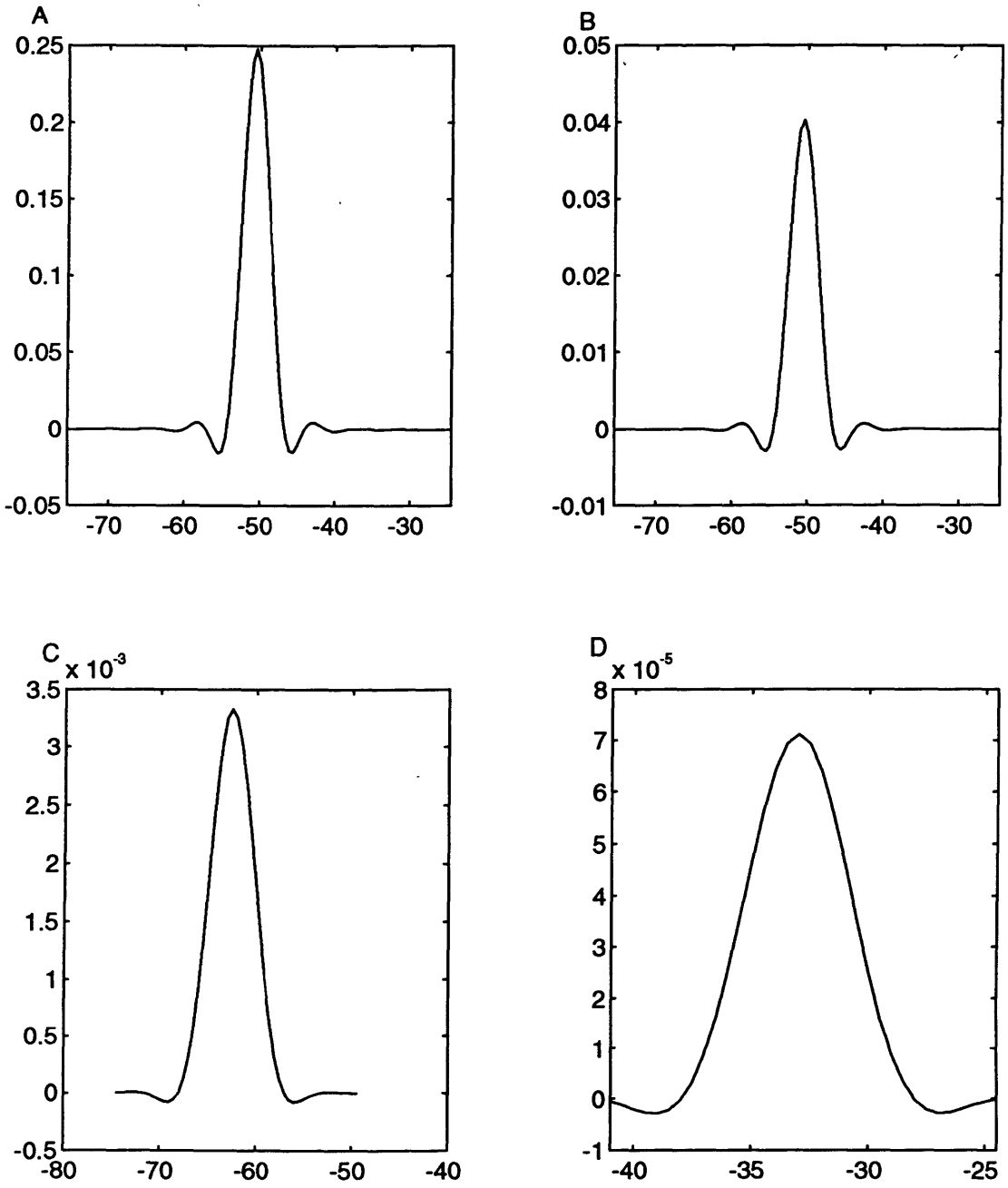

Figure 2.10: Correlation function of a point situated at 50°W for A) 500 m, B) 1200 m, C) 5000 m in the North American Basin and D) 5000 m in the Canary Basin. Correlation is in °C and distance in degrees of longitude.

Colder water appears between 400 and 800 m. Differences are greater, up to a peak value of -0.75°C at 61°W. This is where Roemmich and Wunsch (1984) found warming. Below 800 m, there is generally warmer layer with differences larger than 0.5°C around 1000 m. The warmer water reaches 4000 m in the Canary Basin and the bottom on the eastern part of the North American Basin. In the rest of the North American Basin differences are negative below 2000 m and below 4000 m in the eastern part. In the western boundary, cooling occurs between 1500 and 2000 m. Below that depth, the cooling presented in the previous period has reduced in a large amount.

1992-1957 (Fig 2.8 C)

A remarkable regular warming occurred between 700 and 3000 m from 1957 to 1991. The contours of temperature are nearly horizontal across most of the section. Both the North American and Canary Basins have been warmed by about the same rate. Peak values are larger than 0.5 °C at around 1000 m.

The surface layer is warmer between 0 and 50 m in the North American Basin. Negative differences occur above 100 m, in the North American Basin below the warmer surface layer. This feature can result from seasonal variability, (measurements were done in July-August 1992 and during October 1957). Seasonal variations in this area affect above 100 m. The negative differences are deepening to 900 m on the western part of the North American Basin. While the Canary Basin presents two well defined layers one colder and one warmer above 200 m, the North American Basin has alternating cold and warm rings in longitude. The negative ones are located at 46, 60 and 70°W.

There is a large area of negative temperature difference centered around 500 m. Peak values are between -0.75 °C and -0.5 °C in the North American Basin and -0.5

°C in the Canary Basin. Those values are significantly higher than the uncertainty at this depth.

Near the western boundary region, below 2000 m, negative differences greater than -0.05°C appear west of 70°W. The negative differences extend all over the North American Basin between 3000 and 5000 m. Most of these values are statistically significant. (Note that the error values on the temperature plots are multiplied by 10 below 3000 m.)

The Canary Basin also has been cooled in the last 35 years. The cooling has been stronger around 4000 m, and at the eastern boundary. The uncertainty is less than 0.01°C for most of the values in this basin. The differences are statistically significant. At the eastern boundary, between 1300 and 1800 m an area of cooling appears. This area is situated just below the northward eastern boundary current cited by Roemmich and Wunsch (1985). They interpreted this current as the eastern flow of Antarctic Intermediate Water in the tropics, which feeds an eastern boundary current flowing into the Mediterranean salt tongue.

2.3.2 Salinity differences

Salinity in the 1957 cruise was measured by water samples, and data have been interpolated for the water column. All values are in the Practical Salinity Scale (pss).

1981-1957 (Fig 2.9 A)

Saltier water was found on the area of warming noticed by Roemmich and Wunsch (1984). Salinity differences are positive all over the section from the surface to 200 m depth, and generally negative in a band between 200 and 500 m. Deeper than 500 m, as for temperature, there is substantial zonal variability. The western part of the

section shows negative values to the bottom, with differences as large as -0.15 pss between 500 and 700 m. Positive differences are found between 300 and 3000 m in the central part but only down to 2000 m in the eastern part of the North American Basin. In the Canary Basin, fresher water is found between 1000 and 1500 m and near the bottom. At 4000 m depth, water is fresher at both boundaries of the North American Basin. Around 5000 m in the central part of the North American Basin, water appears saltier than in the previous cruise. Differences are significant over most of the basin, except for the deep water in the North American Basin. Even when the uncertainty given by the mapping is very small, as in the Canary Basin, problems with the salinity determination from the batch of Standard Sea Water prevent the plotting of smaller salinity differences.

1992-1981 (Fig 2.9 B)

Salinity differences present a zonal distribution similar to that of temperature except near the surface where the difference is positive. Positive differences are found between 50 and 350 m, and negative (fresher water) from that layer until 800 m. The water is saltier between 800 m and about 2500 m for all of the section. This saltier water reaches the bottom over the western part of the Mid-Atlantic Ridge with an interruption around 5000 m. The rest of the deep regions appears to be fresher. This freshening is strongest around 3000 and 5000 m in the central and western parts of the North American Basin.

1992-1957 (Fig 2.9 C)

The most important feature is the increase in salinity occurring between 600 and 2500 m, with maximum values of 0.05 pss. The salinity section gives generally positive differences above 300 m. The differences are predominantly negative between 300 and

600 m with values as high as -0.1 pss in the western part and -0.05 for the remainder except near the eastern boundary where the differences are positive down to 1400 m depth.

Below 2000 m the differences are negative, peak values are found at 4000 m, at the western boundary and over the Mid-Atlantic Ridge. In those areas fresher water is shallower than in other locations In the Canary Basin the least freshening occurs around 4000 m. Below 4250 m there is a significant freshening to the bottom, with differences larger than 0.005 pss.

2.3.3 Zonal Averages

To determine the average of the temperature and salinity differences at each standard depth, we have used the technique for determination of a mean value by objective mapping.

For this calculation we assume that the error in the mapping of two different cruises is uncorrelated one with the other. The covariance functions of the cruises are $\mathbf{R}_{\theta\theta}$ and Rrr respectively. These covariance have been calculated using equation (2.7). The spatial covariance function, $\mathbf{R}$, of the difference of the two mapping will be the sum of the covariance functions of each of them,

$$\mathbf{R} = \mathbf{R}_{\theta\theta} + \mathbf{R}rr \tag{2.32}$$

We have estimated the zonal average of the differences by $\hat{m}$ in equation (2.17) and the expected error of the mean by taking the square root of $\mathbf{E}$ in equation (2.18) for each standard depth.

Since we have no previous hypothesis about the mean difference, we take the limit $m_0 \to \infty$ in equations (2.17) and (2.18). The calculated values are presented in the next section.

Temperature

In Figure 2.11 we present the zonal average temperature plus/minus error estimate for the three differences A) 1981-1957, B) 1992-1981 and C) 1992-1957 from surface down to 3000 m (upper plot), and for the North American and Canary Basins deeper than that depth (down right and left plots). The more notable effects are:

- 1981-1957 (Fig 2.11 A)

  As noted by Roemmich and Wunsch (1984) the average warming begins at 400 m, and all values are significantly warmer between 600 and 2500 m, with a peak value of 0.22°C at 800 m. In the North American Basin water was significantly cooler between 3750 and 4500 m, with values around -0.025°C. In the Canary Basin, cooling occurred all over the deep basin. Values are statistically significant below 3750 m. At 6000 m values in the 1957 dataset were scarce, principally in the Canary Basin.

- 1992-1981 (Fig 2.11 B)

  The zonal average values above 800 m have opposite signs from the results obtained from the previous period. Significant cooling occurs between 500 and 600 m with values around −0.20°C. Continuous warming between 900 and 2750 m is statistically significant between 1000 m and 1750 m. Below 3000 m, in the North American Basin we found cooling above 5500 m, which is statistically significant between 3000 and 4250 m, with values ranging from −0.025°C to −0.013°C. At 6000 m there appears to be a significant warming, but at this

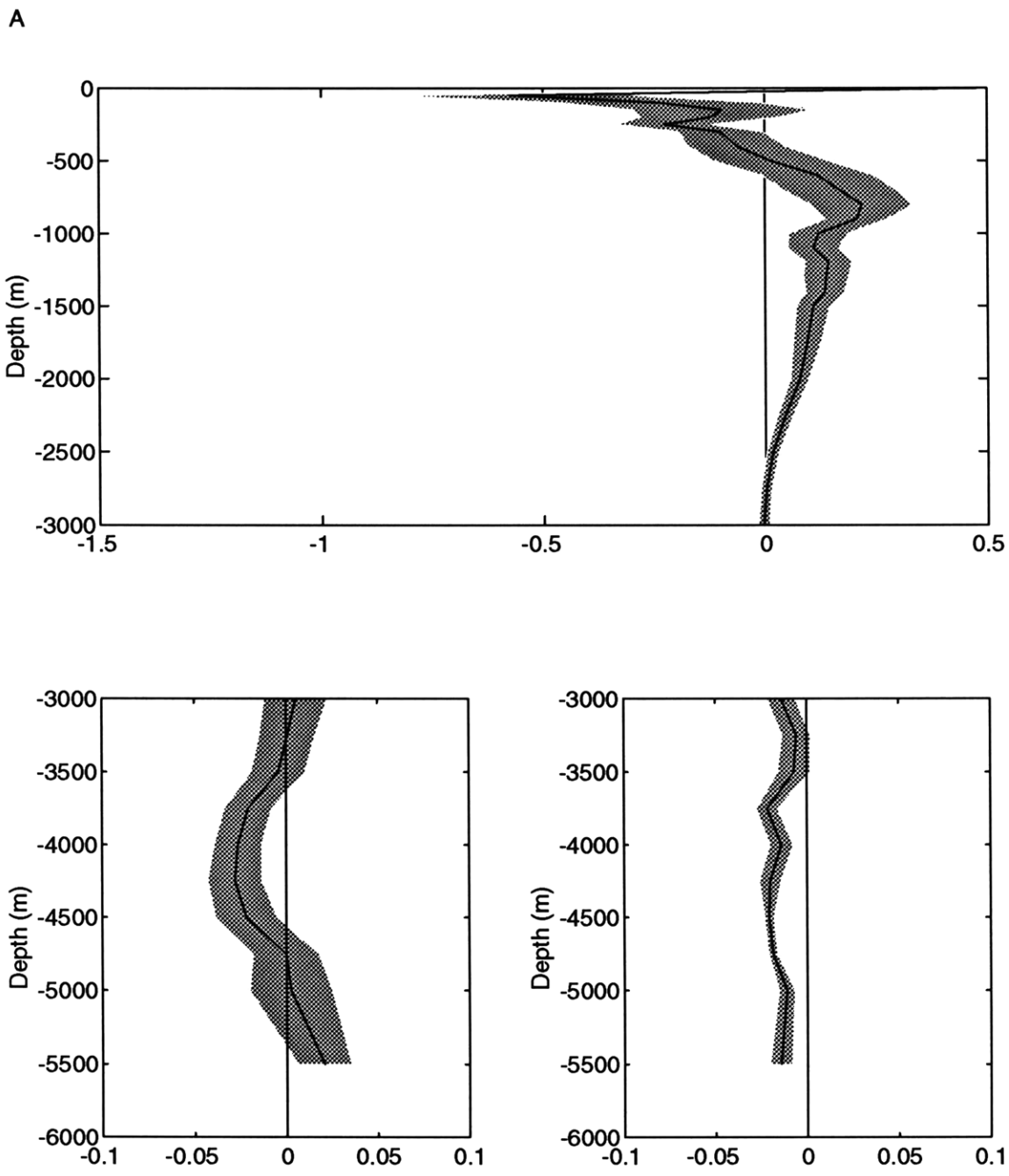

Figure 2.11: Zonal average temperature differences plotted plus/minus the error estimate (shading) for A) 1981-1957, B) 1992-1981 and C) 1992-1957 from surface to 3000 m for all the Atlantic Basin (upper plot) and deeper than that bottom left figure North American Basin and bottom right Canary Basin. Data are in °C.

B

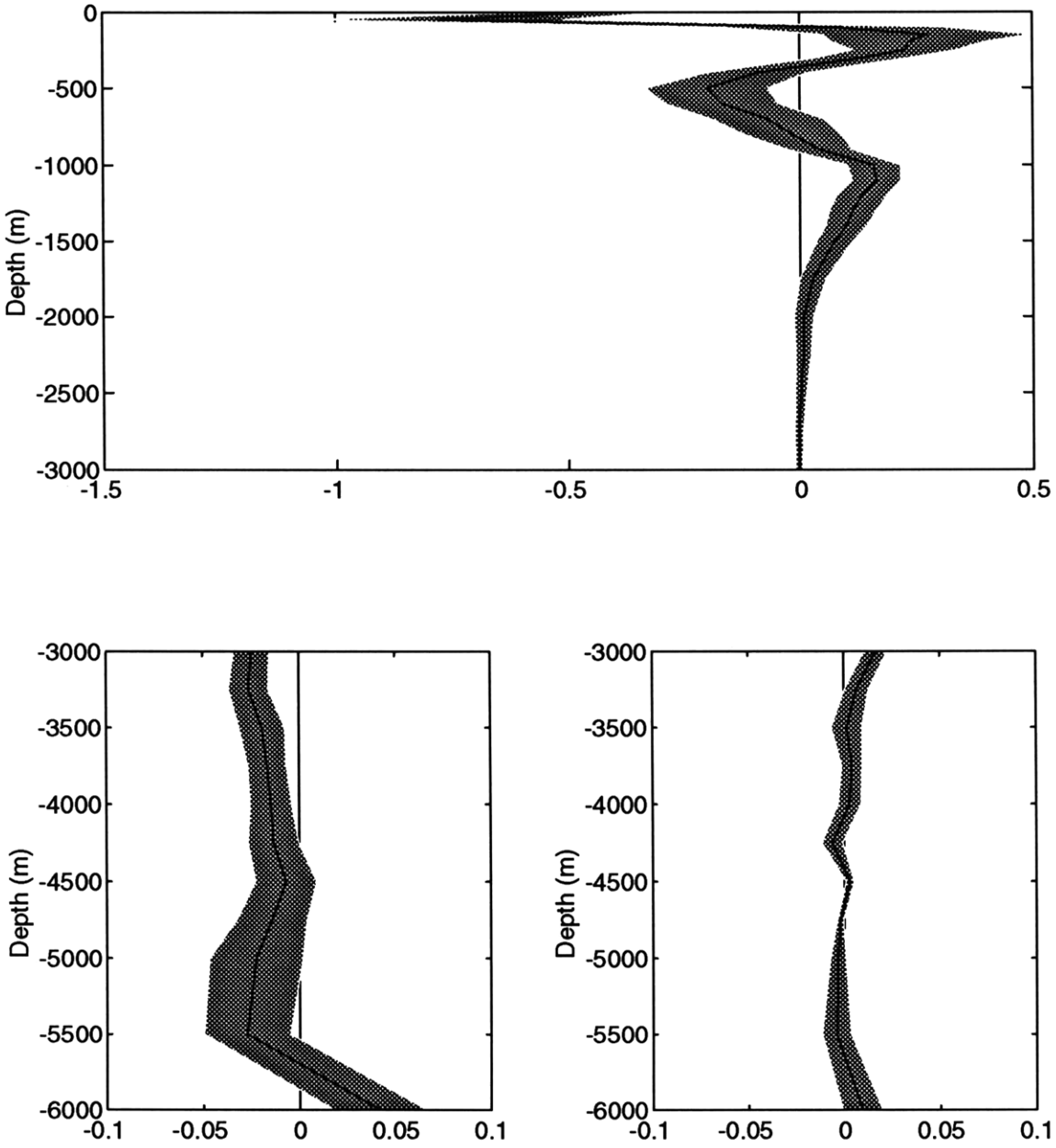
0
-500
-1000
-1500
-2000
-2500
-3000
Depth (m)
-1.5
-1
-0.5
0
0.5
-3000
-3500
-4000
-4500
-5000
-5500
-6000
Depth (m)
-0.1
-0.05
0
0.05
0.1
-3000
-3500
-4000
-4500
-5000
-5500
-6000
Depth (m)
-0.1
-0.05
0
0.05
0.1

c

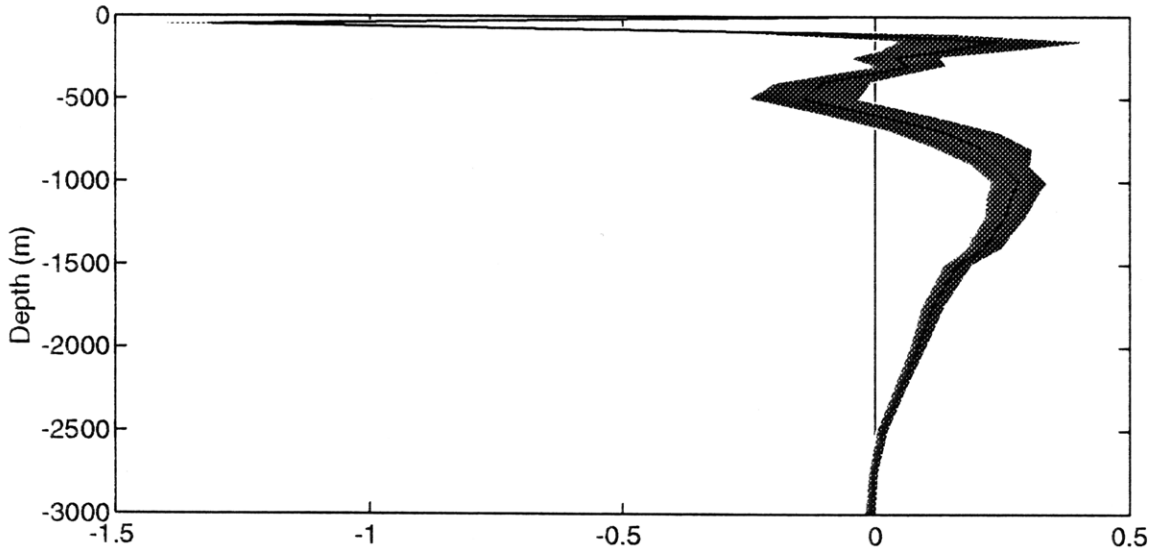
0
-500
-1000
-1500
-2000
-2500
-3000
Depth (m)
-1.5
-1
-0.5
0
0.5

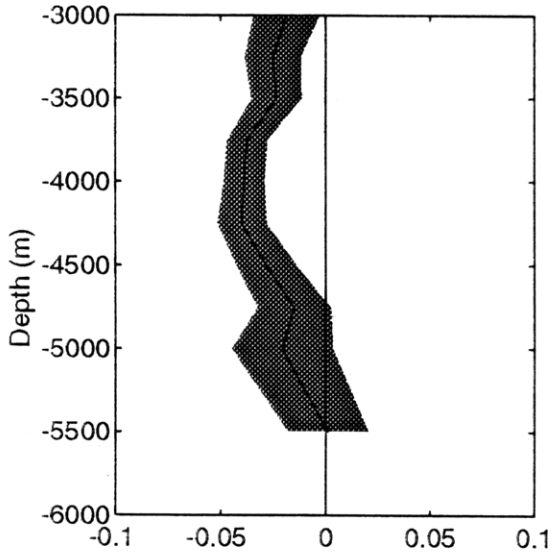
-3000
-3500
-4000
-4500
-5000
-5500
-6000
Depth (m)
-0.1
-0.05
0
0.05
0.1

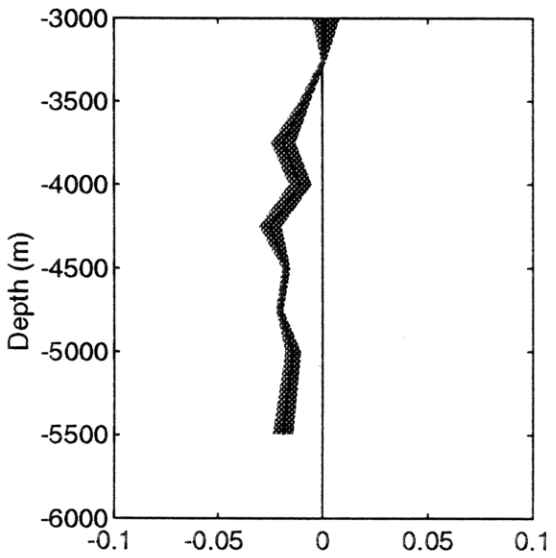
-3000
-3500
-4000
-4500
-5000
-5500
-6000
Depth (m)
-0.1
-0.05
0
0.05
0.1

depth values are scarce and calculation of variances for the mapping are also problematic producing poor statistics. In the Canary Basin, warming occurred above 3250 m. Very small and statistically insignificant changes appear below this depth.

- 1992-1957 (Fig 2.11 C)

  Positive values are found for zonal averages between 600 and 2750 m and between 200 and 400 m. Cooling occurred between 400 and 500 m and below 2750 m. Values are significant between 700 m and 2500 m depths. Values are as large as 0.2 °C between 800 and 1400 m. The peak value is 0.28 °C at 1000 m. In the North American Basin we found significant cooling between 3250 and 5500 m, with a maximum difference of -0.03 °C at 4250 m. In the Canary Basin, cooling is significant in waters below 3500 m, with a peak difference of -0.02 °C at 5000 m.

Salinity

In Figure 2.12 we can see the zonal average salinity plus/minus error estimate for the three differences A) 1981-1957, B) 1992-1981 and C) 1992-1957 from surface down to 3000 m, and for the North American and Canary Basins deeper than that. The more notable features are.

- 1981-1957 (Fig 2.12 A)

  Saltier water is found between 400 and 900 m. Deeper than 1000 m differences are not significant until 2000 m. At this depth where the water is fresher by -0.003 pss. The freshening continues in the North America Basin down to 5000 m. Significant values in the intermediate part are around 0.006 pss. In the Canary Basin freshening occurs until the bottom, with zonal average values around -0.004 pss.

A

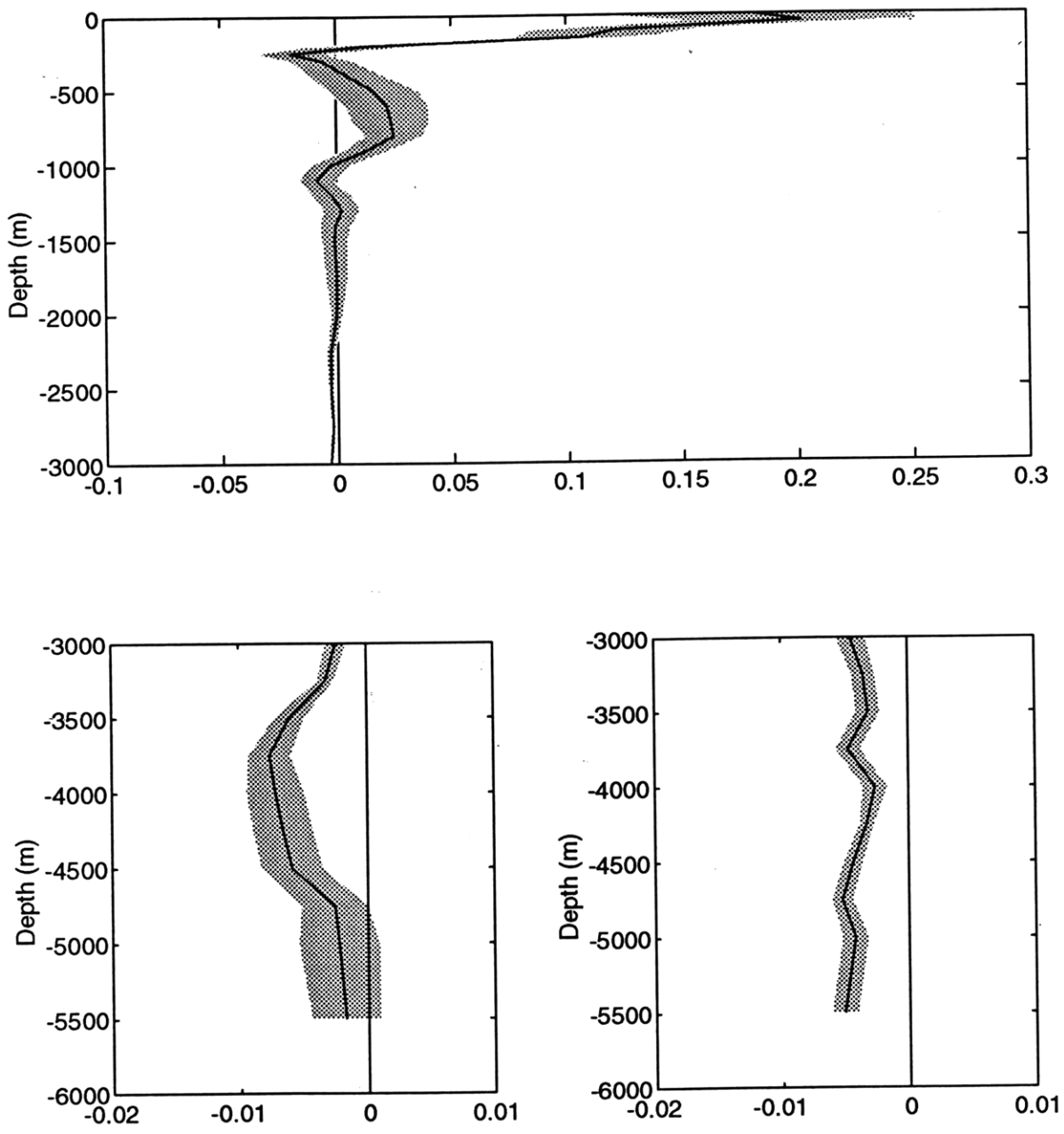

Figure 2.12: Zonal average salinity differences plotted plus/minus the error estimate (shading) for A) 1981-1957, B) 1992-1981 and C) 1992-1957 from surface to 3000 m for all the Atlantic basin (upper plot) and deeper than that bottom left figure North American Basin and bottom right Canary Basin. Data are in pss.

B

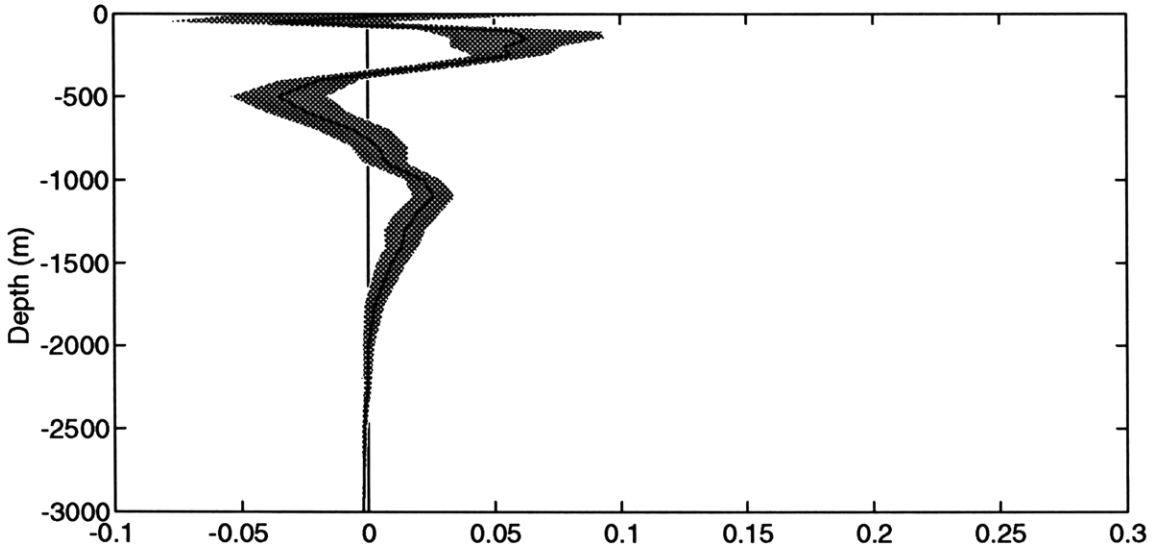
0
-500
-1000
-1500
-2000
-2500
-3000
Depth (m)
-0.1
-0.05
0
0.05
0.1
0.15
0.2
0.25
0.3

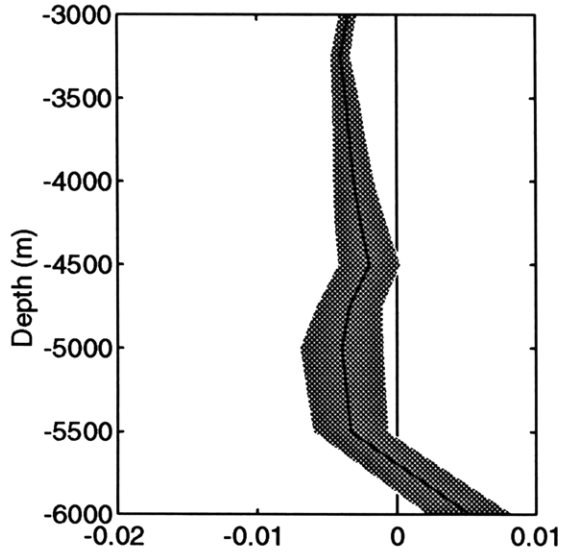
-3000
-3500
-4000
-4500
-5000
-5500
-6000
Depth (m)
-0.02
-0.01
0
0.01

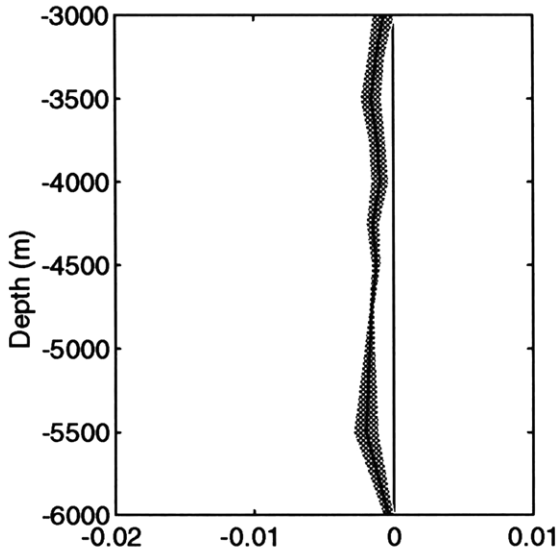
-3000
-3500
-4000
-4500
-5000
-5500
-6000
Depth (m)
-0.02
-0.01
0
0.01

C

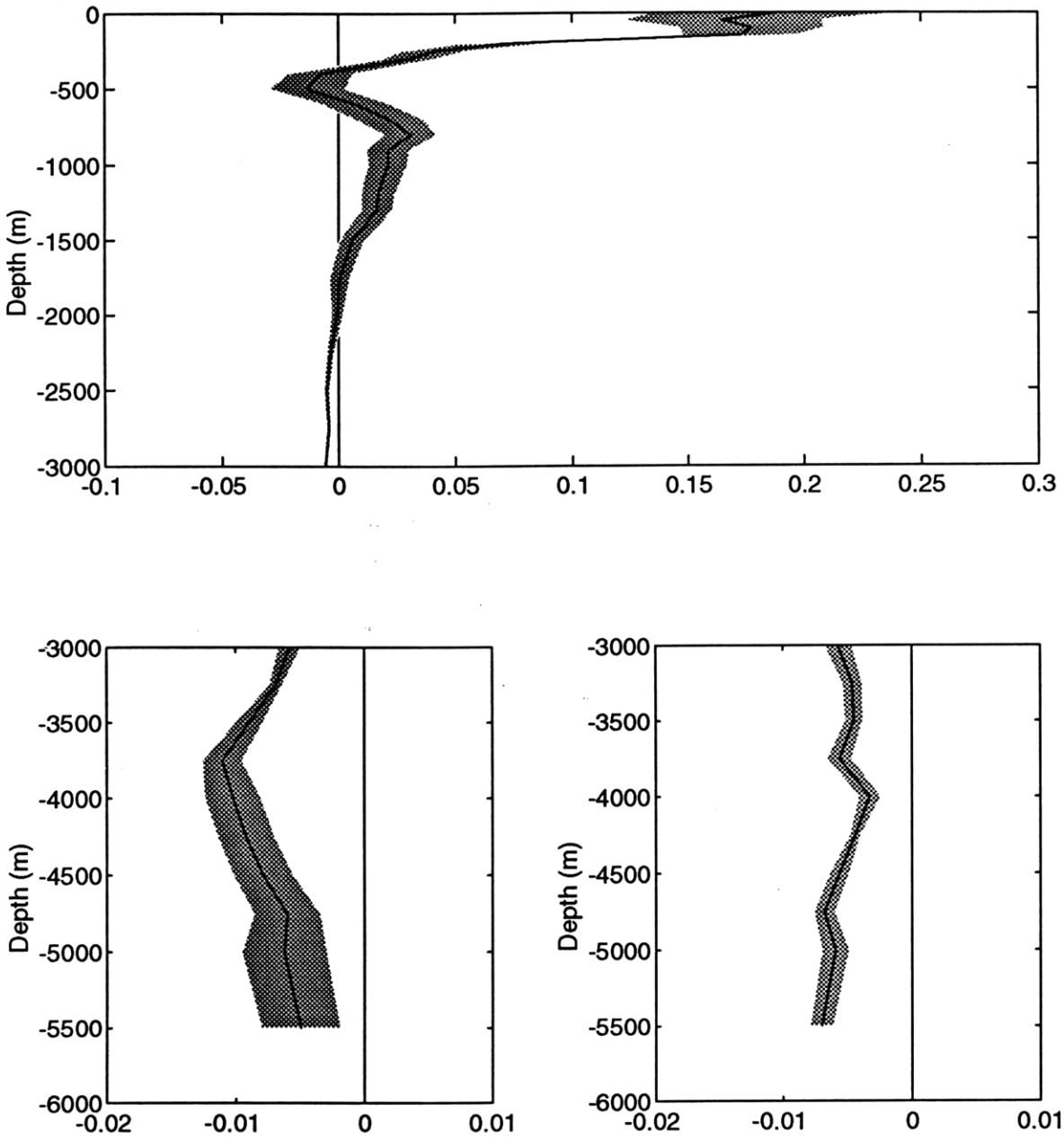
0
-500
-1000
-1500
-2000
-2500
-3000
Depth (m)
-0.1
-0.05
0
0.05
0.1
0.15
0.2
0.25
0.3
-3000
-3500
-4000
-4500
-5000
-5500
-6000
Depth (m)
-0.02
-0.01
0
0.01
-3000
-3500
-4000
-4500
-5000
-5500
-6000
Depth (m)
-0.02
-0.01
0
0.01

- 1992-1981 (Fig 2.12 B)

  The most significant part is the saltier water between 1200 and 1750 m. The maximum increase in salinity was 0.026 pss at 1100 m. Saltier water is also found between 100 and 300 m, below that appears fresher water. Most of the differences are insignificant in this layer. Below 2500 m, water is significantly fresher until 5500 m in the North American Basin. At 6000 m the zonally averaged difference is significantly positive with a value of 0.005 pss. In the Canary Basin the water became fresher but the values are smaller than in the North American Basin.

- 1992-1957 (Fig 2.12 C)

  Saltier water occurs between 600 and 1750 m. The maximum value was 0.031 pss at 800 m. Water is also saltier at depths shallower than 300 m. Differences are significantly negative below 2000 m, where the differences are around -0.004 pss. In the deep North America Basin differences are between -0.008 and -0.005 pss and in the deep Canary Basin between -0.006 and -0.004 pss.

2.3.4 Discussion

In the western part of the North American Basin, the horizontal temperature variation reverses sign between the two periods 1981-1957 and 1992-1981. In the area east and north of the Bahamas, the flow seems to have a C-shaped circulation (Schmitz *et al.*,1992), and the recirculation is described by Schmitz and McCartney (1993) (Figure 8 for water above 7 °C and Figure 10 below 7 °C of their paper). Schmitz and Richardson, (1991) found that 45% of the transport of the Florida Current is of South Atlantic origin. This water is fresher and warmer than the water of North Atlantic origin. Variations in the origin of the water carried by the recirculation may be responsible for the varying behavior found in this area in the sampled periods.

Joyce(1993), in a study of a long-term hydrographic record at Bermuda (32.17°N, 64.50°W), shows that the variations in temperature and salinity on interannual time-scales are largely independent of each other in the surface layer (0-500 m depth), and highly correlated in the thermocline. Between 500 and 1500 m, correlation between temperature and salinity changes is due to vertical oscillations of the thermocline with amplitudes of ± 50 m. Within his records (1955-1988), he found a long-term negative trend in temperature for the layer between 500 and 1000 m, and a positive trend between 1500 and 2500 m (Figure 2 of his paper). This result is consistent with the trend calculated in this study for the zonal average of the 24.5°N section with negative differences around 500 m and significant warming found below 700 m. He extended the time series from 1932 to 1990 (figure 3, of his paper) and found that the long-term trend in the shallow layer disappears, while the one in the deep layer persists. The long-term trend is about 0.5°C/century, with oscillations on the deep layer of approximately 0.05°C over decadal time scales.

In the Roemmich and Wunsch (1984) comparison of 36°N and 24°N sections, the cooling of the upper layers penetrates to 700 m at 36°N but only to 500 m at 24°N. The Bermuda station is situated between them, the cooling there being found between 500 and 1000 m.

Integrating from 100 m (the depth of the seasonal variability at 24.5°N) down to 3000 m the changes in temperature, provides a barely significant value of 0.096 ±0.09 °C. This value gives a trend of warming in this upper part of the North Atlantic of 0.03 °C/decade. The changes in temperature integration for the two periods reveals practically the same values for these rates 0.025°C/decade for the first 24 years and 0.027 °C/decade for the last 11 years. The upper 1000 m present high variability between the three difference datasets, but below that a significant warming of 0.1±0.02 °C has been observed. The rate of warming between 1000 and 3000 m is statistically significant at a rate of 0.028±0.007°C/decade. This value is similar to the rate for

the whole water column between 100 and 3000 m. In my opinion, there is a nearly steady tendency of warming in the North Atlantic above 3000 m. The rate of change of temperature is around 0.03 °C/decade.

For the calculation of the uncertainty in the deep-averaged variation of temperature, I have considered the standard depths as independent of each other. I have done all the calculation at each standard depth without considering any vertical correlation. Looking the structures found in these section, we could assume 6 independent layers in the upper 3000 m. Using these degree of freedom, the change in temperature is 0.09 with uncertainty ± 0.2°C. Assuming 2 independent layers between 1000 and 3000 m, a still significant warming of 0.1 ± 0.05 °C is obtained.

The tendency in salinity for the upper 3000 m was 0.011 ± 0.013 pss or a trend of 0.003 pss/decade. The rates of change in salinity over time are less regular than in temperature and values of 0.002 and 0.005 pss/decade for the periods 1981-1957 and 1992-1981 were calculated. Since uncertainties are larger than the values, the values are not statistically significant.

In the North Atlantic, the deep water, below 3000 m exhibits a significant cooling of -0.027 ± 0.016 degrees C in the North America Basin and -0.013 ± 0.005 degrees C in the Canary Basin. The rates of variation of temperature over the total period of time were -0.008 °C/decade in the North American Basin and -0.004°C/decade in the Canary Basin. The rates for changes in temperature over time are different for the two periods. The North American Basin was cooling principally during 1992-1981 by -0.015°C/decade and somewhat less during the previous period. In the Canary Basin most of the cooling occurred between 1981 and 1957 with a rate of -0.006 °C/decade. Using 2 degrees of freedom the rate of change in temperature in the North American Basin is -0.027 ± 0.03°C and in the Canary Basin is 0.013 ± 0.011°C.

The total change of salinity in deep water during the last 35 years was $-0.008\pm$ 0.002 pss in the North American Basin and -0.005±0.001 pss in the Canary Basin. Freshening was quite homogeneous over time in both basins, with values of -0.002 pss/decade on the North American Basin and -0.0015 pss/decade in the Canary Basin. The change in salinity using 2 degrees of freedom in the deep water is -0.008±0.004 for the North American Basin and -0.005±0.002 in the Canary Basin.

Levitus (1989b) found at 1750 m depth an increase in temperature of approximately 0.1 °C and salinity 0.025 pss for most of the North Atlantic for a 15-year period (1970-1974 - 1955-1959). Also in the upper layers (Levitus 1989a), the variations over the 15-year period at 24.5 °N are similar to those presented here. Behavior of this part of the subtropical North Atlantic is quite different from that of the northern part. In a Levitus's (1989a) comparison between 1970-1974 and 1955-1959 at 1000 m depth, warmer water is found throughout the 24°N section except near the boundaries, with differences larger than 0.2 °C between 30°and 55°W. This value is consistent with the value calculated in this study of 0.28 °C at 1000 m during 35 years. North of 24°N, differences are negative for the entire subtropical gyre.

Before discussing what these changes mean for the general circulation of the North Atlantic, we will present variations in volume of water masses and θ/S relationship.

2.4 Comparison of water masses

To study the variation of water masses between the cruises, we have split the water column into several potential temperature classes.

2.4.1 Water masses

In this area of the North Atlantic the principal layers and water masses identified by Worthington (1976), and Schmitz and McCartney (1993) are:

- *Warm water*, warmer than 17 °C. This water occasionally reaches depths of more than 600 m in the western area but is very shallow in the eastern side of the section.

- *Upper thermocline*, water between 12 and 17 °C. This water lies above the depth of influence of the Mediterranean Overflow. The 17 °C isotherm marks the top of the main thermocline in the Sargasso Sea.

- *Mid-thermocline*, water between 7 and 12 °C. This water is influenced by the Mediterranean Overflow Water (MOW). The salinity of this water is higher in the eastern side of the section than in the western part.

- *Lower thermocline.* Water between 7 °C and a potential temperature of 4 °C. In the tropical region this layer is dominated by South Atlantic Water (Wright and Worthington, 1970), but farther north in the eastern North Atlantic this water mass gives way to the saline Mediterranean water. Worthington (1976) situated the transition between these two water masses at 35.0 pss. Subpolar Mode Water (SMW) and Labrador Sea Water (LSW) can be found in the deeper segment of this layer (McCartney and Talley, 1982).

- *Deep Water.* Water colder than a potential temperature of 4 °C. In this layer we find a series of water masses:

  - *Upper North Atlantic Deep Water.* (UNADW) Wüst (1935) designated this water as the intermediate salinity maximum derived from and including the Mediterranean Overflow Water. Temperature intervals are between 3 and 4 °C.

  - *Lower North Atlantic Deep Water.* (LNADW) Described by Wüst (1935); this water mass is situated around 3700 m. Its source may be the Denmark Strait Overflow Water (Edmond and Anderson, 1971, Reid and Lynn, 1971). The Denmark Strait Overflow has 34.91 pss and temperature below 1.8 °C. (Worthington and Wright, 1970). The potential temperature range at 24.5°N is between 2 and 3 °C.

  - *Antarctic Bottom Water* (AABW) (Wüst, 1935). The transition between the NADW and the AABW begins at about 2 °C (Broecker *et al.*, 1976); Wright, 1970). This water follows a θ /S curve from 1.8 °C and 34.89 pss to 0.5 °C and 34.74 pss (Worthington and Wright, 1970). In the Canary Basin the characteristics are $\theta \sim 1.95$°C S $\sim$ 34.88 pss and $\sigma_4 \sim 45.87$ (Tsuchiya *et al.*, 1992). In the North American Basin the AABW characteristics face progressively northward and tend to be stronger in the eastern half of the basin at mid-latitudes (Wüst, 1933 and 1935; Mantyla and Reid, 1983; McCartney, 1993).

2.4.2 Comparison of water masses

In this section, we want to study the expansions and contractions of water masses over time. Based on the previous definition of water masses, we have chosen a

	1992	1957	1992*	1981*	1957*
17	316	319	334	334	341
12	597	597	616	626	619
7	989	952	985	964	952
4	1810	1747	1795	1776	1729
3	2460	2436	2450	2449	2424
2w	3948	4070	3948	3982	4070
2e	4424	4584	4442	4455	4599
1.8w	4736	4745	4736	4733	4745

Table 2.7: Average depths (in m.) of the potential temperature surfaces for the total section (75.5 °W - 16 °W) for 1992 and 1957 cruises and from 75.5 °W to 24.5 °W (denoted by *) for 1992, 1981 and 1957. Below 3 °C data are separated for the North American (denoted by w) and Canary (denoted by e) basins

series of potential temperature surfaces. All the values of temperature are potential temperature in this section.

Table 2.7 gives the average depths of several temperature surfaces between 75.5 °W - 16 °W for 1992 and 1957 cruises and from 75.5 °W to 24.5 °W for 1992, 1981 and 1957 cruises. The 7°C isotherm is deepening by 30 m and the 4°C is deepening by 60 m. In the North American Basin 2°C isotherm is shallowing by about 100 m and in the Canary Basin 2°C isotherm is shallowing by about 150 m from 1957 to 1992. Standard deviation of the difference in depths are around $\pm$15 m at 7°C and around $\pm$40 m below 4°C. For the standard deviation of the difference on depth, the mean depth at 2°C in the North American Basin for the IGY 1957 data was not used because it gives a standard deviation of $\pm$40 m. This value is twice the others values.

Table 2.8 gives the intervals of potential temperature we have chosen with the area occupied by the corresponding water mass for each cruise. We present areas for the complete section for 1957 and 1992 (75.5 °W to 16 °W), and areas between the western coast and 24.5 °W for comparison with the 1981 cruise.

	1992	1957	1992*	1981*	1957*
Sup-17	1901	1924	1725	1723	1763
17-12	1688	1668	1455	1507	1434
12-7	2335	2116	1903	1744	1715
7-4	4844	4694	4164	4173	3993
4-3	3791	4022	3356	3450	3566
3-2w	4252	4656	4280	4377	4690
3-2e	4898	5280	3977	4005	4304
2-1.8w	2129	1818	2129	2028	1818
1.8-botw	2321	2295	2321	2329	2295
2-bote	2175	1829	1988	1961	1698

Table 2.8: Areas for the intervals of potential temperature for the total section (75.5 °W - 16 °W) for 1992 and 1957 cruises and from 75.5 °W to 24.5 °W (denoted by *); for 1992, 1981 and 1957. Units are km^2. Below 3 °C data are separated for the North American (denoted by w) and Canary (denoted by e) Basins. The last interval in both basins is the area from this isotherm to the bottom of the basin (denoted by bot).

We have calculated the differences in area for the water masses defined previously. Considering the depth error ± 5 m for IGY data and ± 2.5 m for CTD data, the error for the calculated areas across the section is as big as 45 km^2. Systems of positioning at stations were poor in 1957, and this increase the error by about 5 km^2. For the deep part of the North American and Canary Basins, the error is less than 25 km^2 due to the small zonal extent of the deep basins at 2°C and below. Values of the difference in area are significant below the upper thermocline water. Table 2.9 gives the differences in area between the cruises.

Roemmich and Wunsch (1984) found expansion in bottom water (< 2 °C), contraction in deep water (2-4 °C) and expansion in middle and lower thermocline water (4-12 °C) over the period from 1957 to 1981. We find essentially the same results for the period from 1981 to 1992. Since we have studied two periods, we can compute the rates of change in both periods.

	1992-1957		1981-1957*		1992-1981*		1992-1957*	
	dif	%	dif	%	dif	%	dif	%
Sup-17	-23	-1.2	-40	-2.3	2	0.1	-38	-2.2
17-12	20	1.2	73	4.8	-52	-3.6	21	1.4
12-7	219	9.4	29	1.7	159	8.4	188	9.9
7-4	150	3.1	180	4.3	-9	-0.2	171	4.1
4-3	-231	-6.1	-116	-3.3	-93	-2.8	-210	-6.3
3-2 w	-405	-9.5	-314	-7.2	-98	-2.3	-412	-9.6
3-2 e	-382	-7.8	-299	-7.5	-28	-0.7	-328	-8.2
2-1.8w	311	14.6	210	10.4	101	4.7	311	14.6
1.8-botw	26	1.1	34	1.5	-8	-0.3	26	1.1
2-bote	346	15.9	263	13.4	27	1.4	290	14.6

Table 2.9: Difference of area for the intervals of Potential Temperature for the total section (75.5 °W - 16 °W) for 1992-1957 and from 75.5 °W to 24.5 °W (denoted by *); for 1992-1957, 1981-1957 and 1992-1981. Below 3 °C data are separated for the North American (denoted by w) and Canary (denoted by e) Basins. Units are km^2.The last interval in both basins is the area from this isotherm to the bottom of the basin (denoted by bot).

Figure 2.13 presents the expansion-contraction for the section between 75.5°W and 24.5 °W for the three periods 1957-1981, 1981-1992 and 1957-1992. Values are plotted in the middle of each interval of potential temperature. Values include both basins.

In the North American Basin, the deeper water mass expansion has occurred between 1.8 and 2 °C, the total expansion being 311 km^2 over all the period or 14.6 % of the occupied area. The rate of change is maintained in both periods, the expansion being 210 km^2 in the first 24 years and 101 km^2 in the last 11 years. The rate is around 9 km^2/year for the total period. In the Canary basin the expansion has been of 346 km^2, or 15.9% of the area, but most of this expansion has occurred in the first period between 1957 and 1981.

The region between the temperature surfaces of 1.8°C and 2°C in the North American Basin is the transition zone between the LNADW and the AABW Wright

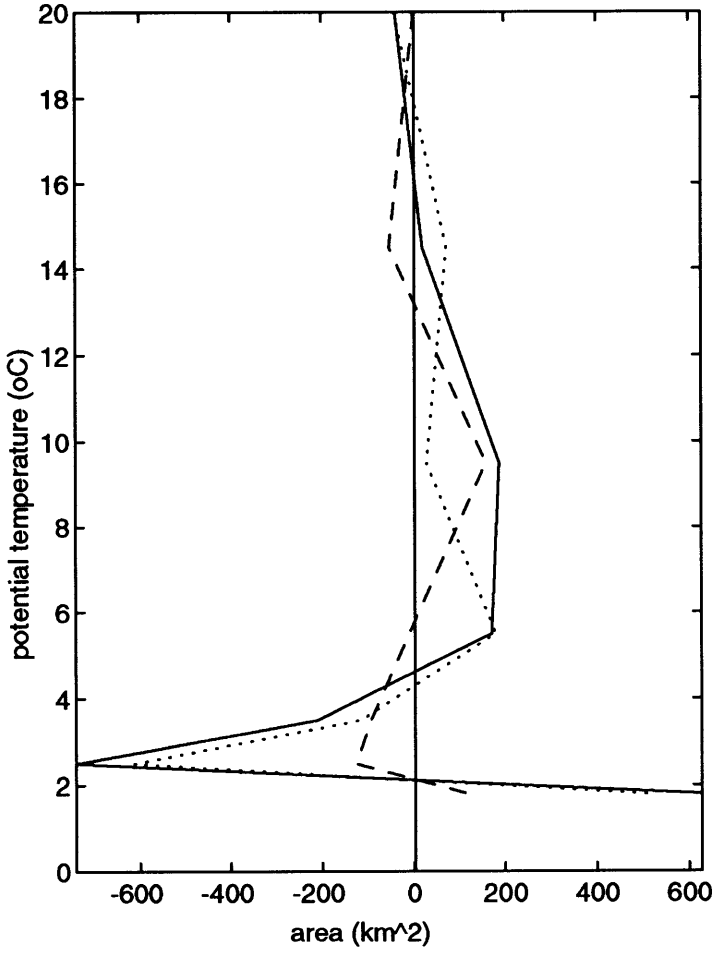

Figure 2.13: Expansion-contraction areas for the intervals of potential temperature for the section from 75.5 °W to 24.5 °W) for 1992-1957 (solid), 1982-1957 (dotted) and 1992-1981 (dashed). Values are plotted in the middle of each interval of potential temperature and include both basins. Units are km^2.

and Worthington (1970) define the lower boundary for the LNADW at 1.8 °C and 34.89 pss for all of the North Atlantic basins except the European Basin. This water comes from the Denmark Strait overflow. Whitehead and Worthington (1982) consider that water in the North American Basin with the properties of 1.9 °C and salinity $\sim$ 34.9 pss must consist almost wholly of NADW with only the smallest tinge of pure AABW. Looking at the θ/S diagram for the North American Basin (Figure 2.20), the transition between NADW and AABW is situated around 1.9 °C. Schmitz and McCartney (1993) found a recirculation of AABW over this area. They say that the AABW rises into NADW to form a weakly stratified water mass at 1.9 °C.

Below 1.8 °C, in the North American Basin, the relatively fresh AABW and the more saline water from the Denmark Strait Overflow are geographically distinct (Worthington and Wright 1970), and only AABW affects the 24.5°N section below 4250 near the Mid-Atlantic Ridge and below 5000 m at the western boundary. The AABW that was beside the western boundary south of the Equator is found against the Mid-Atlantic Ridge, which is the eastern boundary of the basin (Fuglister 1960). Warren (1981) explained this transposition as being a result of the sharp northward increase in the depth of the North American Basin. Expansion in this area from 1957 to 1992 is 26 km^2, only 1.1 % of the area occupied locally by the AABW.

With respect to the contraction area, I can separate two regions corresponding to intervals of potential temperature: 2-3 °C for the North American and Canary Basins and 3-4 °C for the total North Atlantic Basin. These layers give us an indication of the LNADW and the UNADW.

The largest contraction occurred in the UNADW (2-3°C) for the two basins. In the North American Basin, this reduction was -400 km^2, a reduction of -9.5% of the area occupied in 1957. In the Canary Basin the reduction was -380 km^2, or -7.8% of the area. Most of that reduction occurred from 1981 to 1957 in the Canary Basin. In the North American Basin the rate of change was relatively constant decreased

from -130 km^2/decade in the first period to -90 km^2/decade for the period 1981-1992. The contraction of the upper UNADW (3-4°C) was 231 km^2, or 6.1 % of this area. The contraction occurred during the two periods, but was larger from 1981 to 1992. In 1992, the 2°C isotherm was situated at an average depth of 3948 m on the western basin, and 4424 m on the eastern one.

Looking at the distributions of temperature difference (Figure 2.8), we can see that around 4000 m there is an area of more intense cooling, with values of -0.05°C on the eastern side of the North American Basin. This is the mixing area where the LNADW and the AABW are in close contact. Also in the deep western boundary current, the cooling is notable between 2500 m and the bottom. The upper part of this area is covered by the Norwegian-Greenland Sea Overflow Water (2500-4000 m) coming through the Faeroe Bank Channel, Iceland-Scotland Ridge, and Denmark Strait (Pickart, 1988). This reduction in temperature is associated with a reduction in salinity. Salinity differences around 4000 m are -0.01 pss. In 1992 the 2°C isotherm was on average situated 120 m shallower in the North American Basin and 160 m shallower in the Canary Basin than in 1957, but the depth of the 1.8°C isotherm does not change significantly.

This significant reduction of UNADW (3-4°C) might be related to reduced production of deep water during the period studied. Lazier (1980) presents a series of historical data from 1964-1974 of the Weather Ship Bravo in the Labrador Sea where there was a decrease in surface salinity, and only shallow winter-time convection occurred during the 1970's. He attributed these facts to a reduction in the formation of deep water by convection.

Weiss *et al.,* (1985), using a simple dilution model, showed that CFM-bearing waters originating in the region of the Labrador Sea have reached the Equator in a well defined western-boundary undercurrent located at a depth of about 1600 m. They calculate that this water has taken about 23 years to reach the equatorial region.

Since our section is located closer to the source region the time taken for arriving at the subtropical region will be shorter. Changes in the production of NADW occurred in the 1960's may affect the 24.5°N section during the 1980's.

The expansion of water masses in the upper layers (main thermocline) corresponds to the band of positive temperature differences seen all over the transect as presented in the previous section (Figure 2.8). This expansion occurs first in the lower thermocline, with an expansion of 180 km^2 from 1957 to 1981, and with no significant change later from 1981 to 1992. In the mid-thermocline most of the expansion has occurred in the last 11 years, when the rate of expansion was 145 km^2/decade. The warmer area produces isotherms deeper by about 50 m between 7 and 3.5 °C.

2.5 Comparison of θ/S characteristics

In the previous sections, we analyzed the changes in temperature, salinity and volume of water masses which occurred in the North Atlantic during the 35-year period under study. The differences in temperature and salinity were positively correlated; increases in temperature were associated with increases in salinity. However, there is another important and related question. Has the potential temperature/salinity relationship θ/S changed over time?. Roemmich and Wunsch (1984) believed that the historical temperature/salinity correlation was maintained during the period 1957-1981, even though changes in the individual variables occurred.

The 1981 and 1992 CTD measurements have an accuracy greater than ± 0.002 °C in potential temperature and ± 0.0015 pss in salinity, which is much better than the ± 0.01°C and ± 0.005 pss associated with the IGY 1957 data.

For this comparison, we have taken the linear part of the θ/S curve in the temperature intervals that corresponds to the *water masses* defined in the previous section. In the UNADW and Lower Thermocline Water, the dispersion of values is large. In this case, the comparison was performed between the average salinity value for each cruise data. All the temperatures quoted in this section are potential temperatures. Since the IGY values originated from bottle data, we have plotted the original θ/S points, rather than the interpolated ones.

Figure 2.14 gives the θ/S relationship for the 1992 Hespérides cruise in the deep and bottom waters (LNADW and AABW). The change in θ/S characteristics in the LNADW over longitude is evident. Salinity decreases westward (from the Canary Basin to the North American Basin) above 2.3°C due to the influence of mixing with the Mediterranean overflow water, and increases in the lower portion. The turning point between these effects occurs at about 2.3°C and 34.925 pss. In the North American Basin, below 1.9 °C, the AABW is clearly evident with its

characteristic lower temperature and salinity as a knee in the θ/S relationship. In the western and eastern boundaries and in the region of the Mid-Atlantic Ridge, θ/S characteristics have more variability than in the central portion of either basin. For the θ/S comparison between cruises, we try to avoid these transition zones and the changes in longitude. We have compared distributions in θ/S between 55°W and 75°W in the North American Basin and between 24.5°W and 44.5°W in the Canary Basin. We describe θ/S for the three cruises beginning with the deep water in the North American Basin and continuing up through to the water column before describing the θ/S characteristics in the Canary Basin.

2.5.1 North American Basin

Antarctic Bottom Water

Figure 2.15 presents the θ/S relationship for AABW in the North American Basin for each of the data sets, 1992, 1981 and 1957. The IGY data are considerably saltier and/or colder than the other two data sets. The 1957 values were on average -0.03°C colder for constant salinity or 0.005 pss saltier at constant temperature than the 1992 values. As mentioned previously, the 1957 salinity data have an associated uncertainty of ± 0.005 pss. In these calculations, we have used more than 25 pairs of independent values, so that the uncertainty is reduced by at least a factor of 5. Uncertainty in temperature is reduced by the same factor. The number of CTD values used for the regression is quite large (more than a hundred), the uncertainty in 1981 and 1992 data is much less than in 1957. In the cold region, the 1981 θ/S characteristics are similar to those of 1992. At temperatures higher than 1.6°C, the 1981 water seems to be colder and saltier than it was in 1992. Around 1.8°C, the 1981 waters were -0.014°C colder or 0.002 pss saltier than in 1992. Variations over time occur in a greater degree in the warmer/upper portion of the curve rather than in the colder/lower portion.

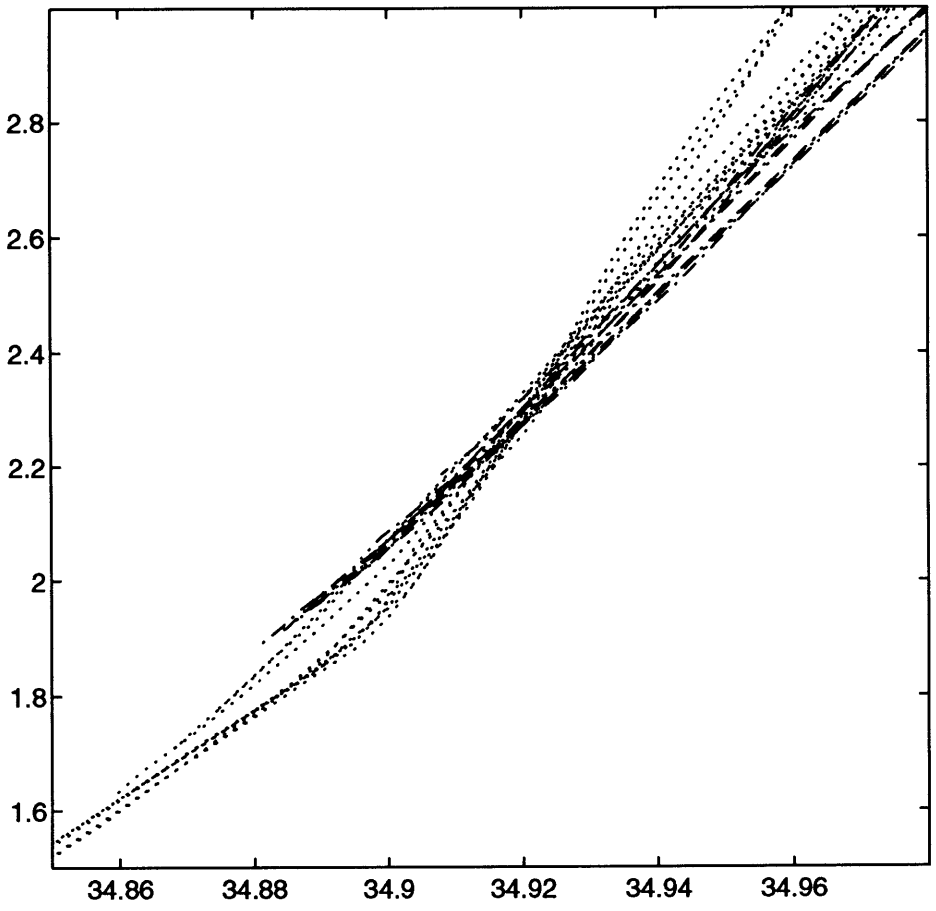

Figure 2.14: θ/S relationship for Lower North Atlantic Deep Water and Antarctic Bottom Water at 24.5 °N, North American Basin (dotted) and Canary Basin (dash-dotted) data are from 1992 cruise . Salinity data are in pss and potential temperature in °C. The plot contains one out of every four stations.

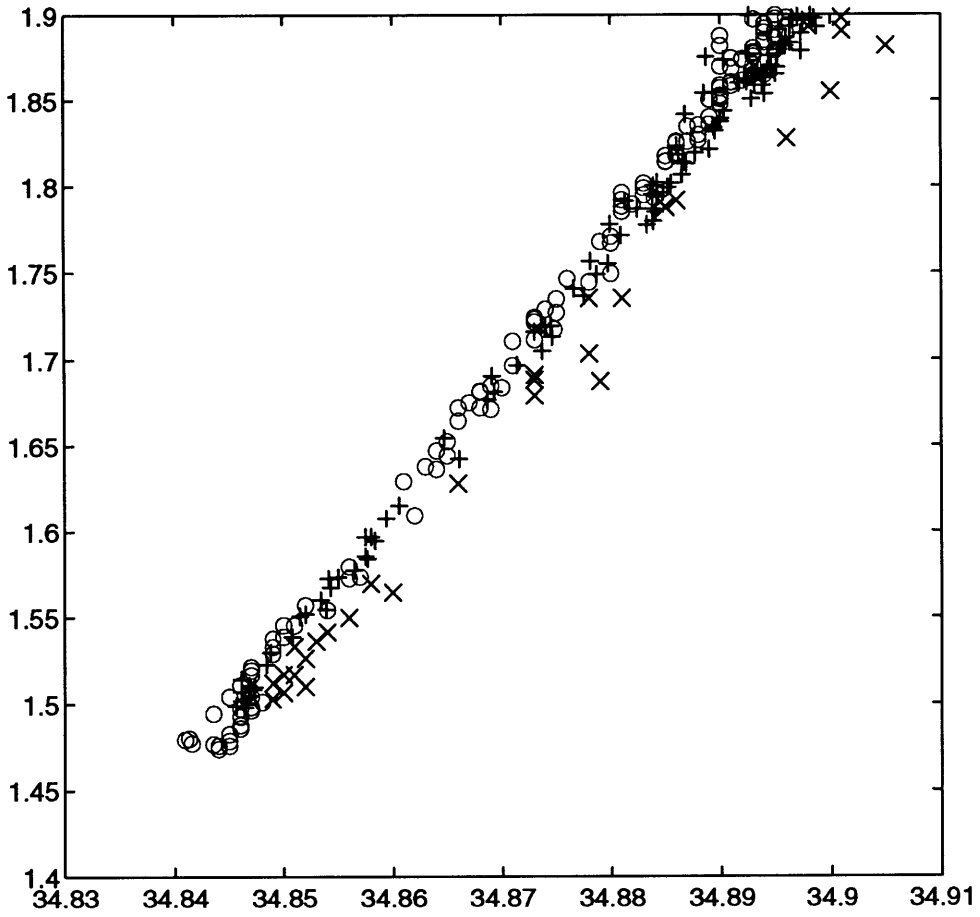

Figure 2.15: θ/S relationship for Antarctic Bottom Water in the North American Basin, data are from 1992 (o), 1981(+) and 1957 (x). Salinity data are in pss and potential temperature in °C.

Statistically significant differences between the θ/S characteristic of the three cruises were found.

Lower North Atlantic Deep Water

Figure 2.16 presents the θ/S relationship for LNADW in the North American Basin for 1992, 1981 and 1957. The comparison has been done in the same way as was done for the AABW. Variations in the θ/S are found in the lower portion of this water mass. At 2°C, the 1957 data were -0.08 °C colder or 0.005 pss saltier than the 1992 data. This tendency is reduced with increasing temperature. The 1981 θ/S regression indicates a reduction in the tendency toward saltier or colder water and reaches a cross over point at a temperature of 2.8 °C and about 34.955 pss with the 1992 θ/S relationship.

Upper North Atlantic Deep Water and Lower Thermocline Water

At 24 °N, in the subtropical North Atlantic, the UNADW is influenced by waters originating both in the Mediterranean Sea and in the region of the Labrador Sea. The salinity maximum of the UNADW is of Mediterranean origin, although south of 24°N, AAIW coming from the south overly this water mass. Toward the east, temperatures and salinities increase in response to the influence of the MOW. This effect is more pronounced at the western boundary current where Labrador Sea Water is flowing southward.

Figure 2.17 presents the θ/S relationship for the UNADW and the Thermocline Water in the North American Basin for 1992, 1981 and 1957, from which we infer a change in water mass characteristics over time. In this part of the water column, the 1981 data seems to be fresher than the 1992 data. Between 4.5°C and 7.5°C an increase in salinity over time is evident. The mean salinity between 5°C and 7°C was

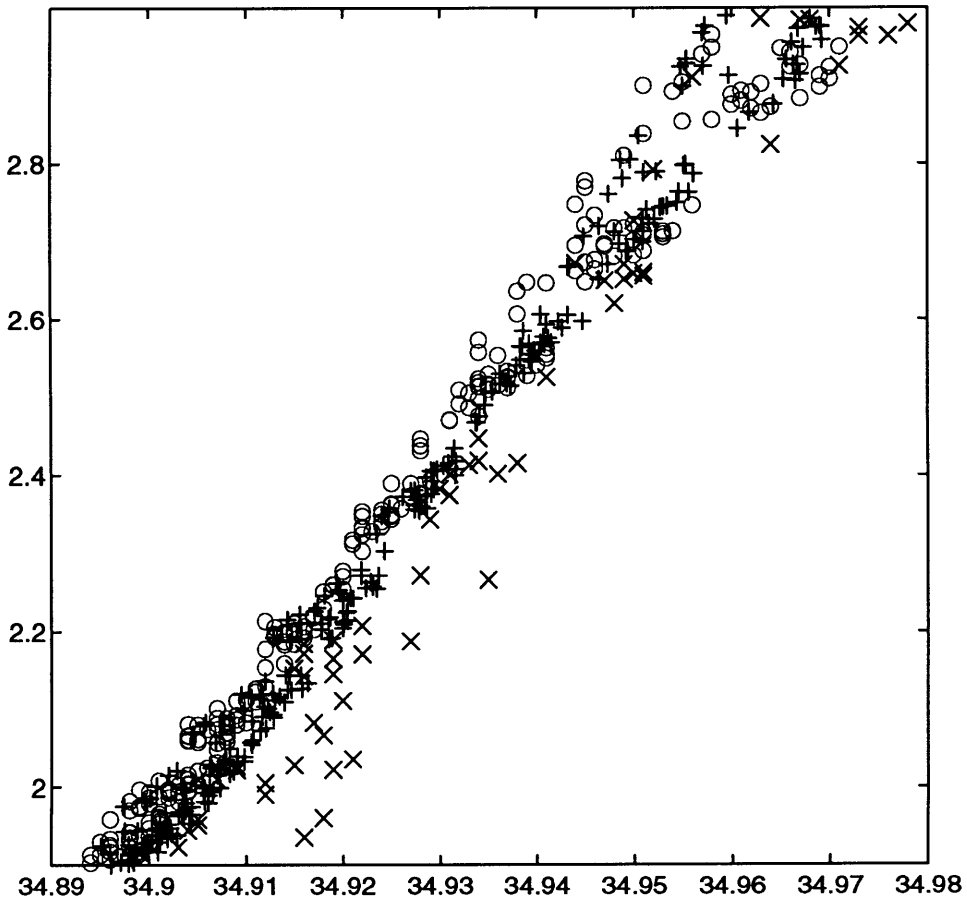

Figure 2.16: θ/S relationship for Lower North Atlantic Deep Water in the North American Basin, data are from 1992(o), 1981(+) and 1957(x). Salinity data are in pss and potential temperature in °C.

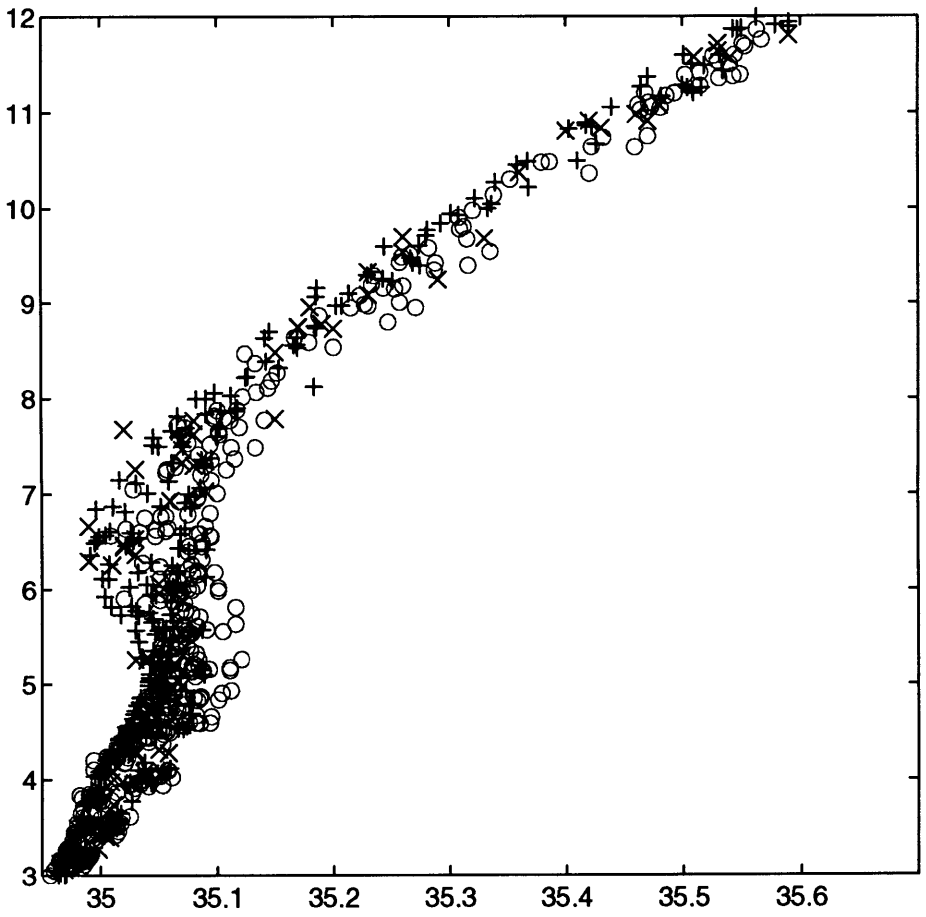

Figure 2.17: θ/S relationship for Upper North Atlantic Deep Water and Thermocline Water in the North American Basin, data are from 1992(o), 1981(+) and 1957(x). Salinity data are in pss and potential temperature in °C.

35.037 pss in 1957, 35.048 pss in 1981 and 35.073 pss in 1992, i.e. an increase of 0.011 pss for the first 24 year period and of 0.025 for the last 11 year.

Mid and Upper Thermocline Water

At 24 °N in the mid-thermocline Water, the θ/S relationship does not seem to have changed significantly between 1957 and 1981. However from 1981 to 1992, mid-thermocline water became 0.02 pss saltier or -0.13°C colder . In the Upper Thermocline Water, the θ/S relationship changes from 1957 to 1981, becoming -0.13°C colder or 0.02 pss saltier. No appreciable change appears to have taken place since the 1981 cruise. So generally, in the thermocline, water tends to be colder or saltier over time. Such changes occurred from 1957 to 1981 in the upper thermocline layer and from 1981 to 1992 in the mid-thermocline layer at 24.5°N in the North Atlantic.

2.5.2 Canary Basin

Lower North Atlantic Deep Water

Figure 2.18 presents the θ/S relationship for LNADW in the Canary Basin for 1992, 1981 and 1957. In this basin, the deepest LNADW is influenced by the presence of AABW. Tsuchiya *et al.* (1992) show that this water comes from the Guiana Basin through the Vema fracture zone across the Mid-Atlantic Ridge flows to the Cape Verde Basin. By the time it reaches the Canary Basin it is characterized by a potential temperature of 1.95 °C and a salinity of 34.88 pss.

For the purposes of this comparison, we have computed water with temperature between 2°C and 3°C for each of the three cruises as LNADW. There is a clear tendency over time toward warmer or fresher water, similar for both periods. At

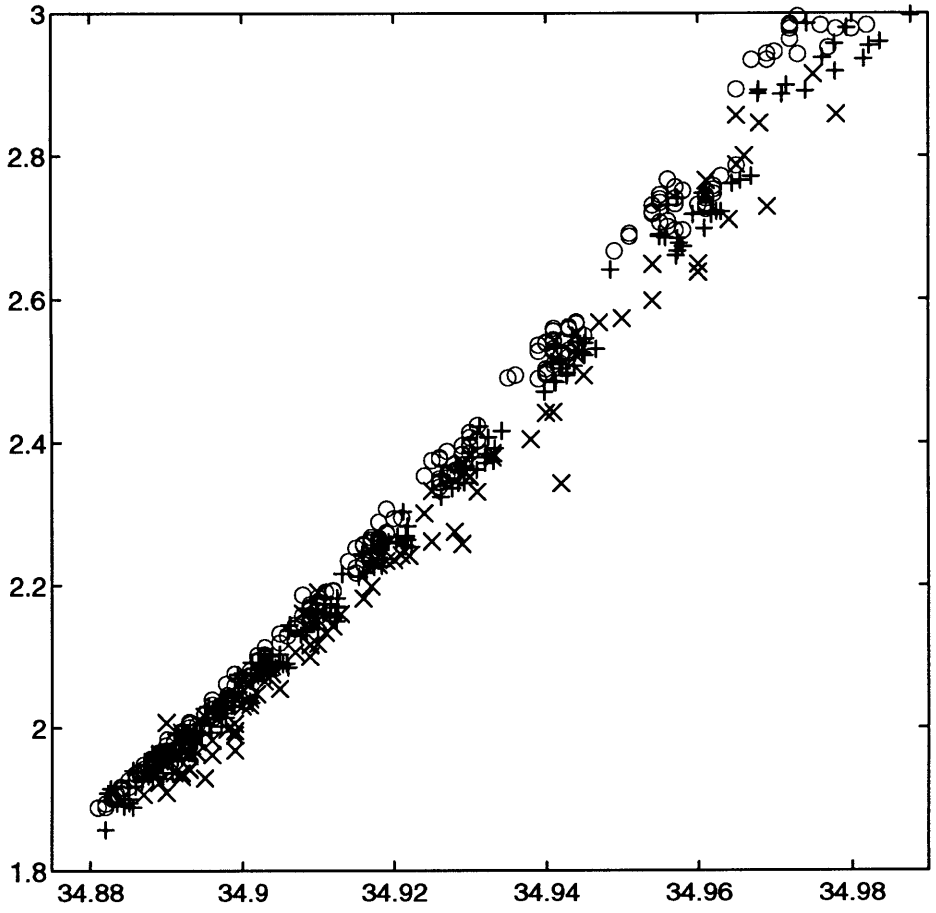

Figure 2.18: θ/S relationship for Lower North Atlantic Deep Water in the Canary Basin, data are from 1992(o), 1981(+) and 1957(x). Salinity data are in pss and potential temperature in °C.

2.6°C, the salinity of the 1992 dataset is -0.006 pss fresher than in the 1957 dataset, or in terms of a constant salinity, 0.06°C warmer. Comparing the θ/S values over the last period, we found LNADW -0.0035 pss fresher and 0.035 °C warmer. This tendency of the water to be warmer or fresher is similar as that of in the LNADW in the North American Basin.

Upper North Atlantic Deep Water and Lower Thermocline Water

Figure 2.19 presents the θ/S relationship for UNADW and thermocline water in the Canary Basin for 1992, 1981 and 1957.

As in the North American Basin, temperature and salinity increases eastward. The 1957 water seems cooler or saltier than in 1992, and 1981 appears warmer or fresher than 1992 waters. The change in the mean value of the salinity in the temperature range 4°- 7°C appears to oscillate. The mean salinity in 1957 was 35.127 pss. It decreases to 35.104 pss in 1981 but increases back to the previous value in 1992. For the temperature interval between 5-7 °C, where the AAIW is likely to have more influence on the θ/S characteristics, the mean salinity values are 35.12 pss in 1957, 35.103 pss in 1981 and 35.131 pss in 1992. Again an oscillation is present, but the values at the end of the period are larger than in the beginning. Whether this is truly an oscillation or a trend with variations cannot be determined with only three points.

Thermocline Water

In the Thermocline Water, there are no significant changes between 1981 and 1992. The 1957 waters change from being colder or saltier at 8 °C (-0.12 °C, 0.01 pss) to being warmer or fresher at 12 °C (0.12 °C, - 0.01 pss) compared with the 1992 data.

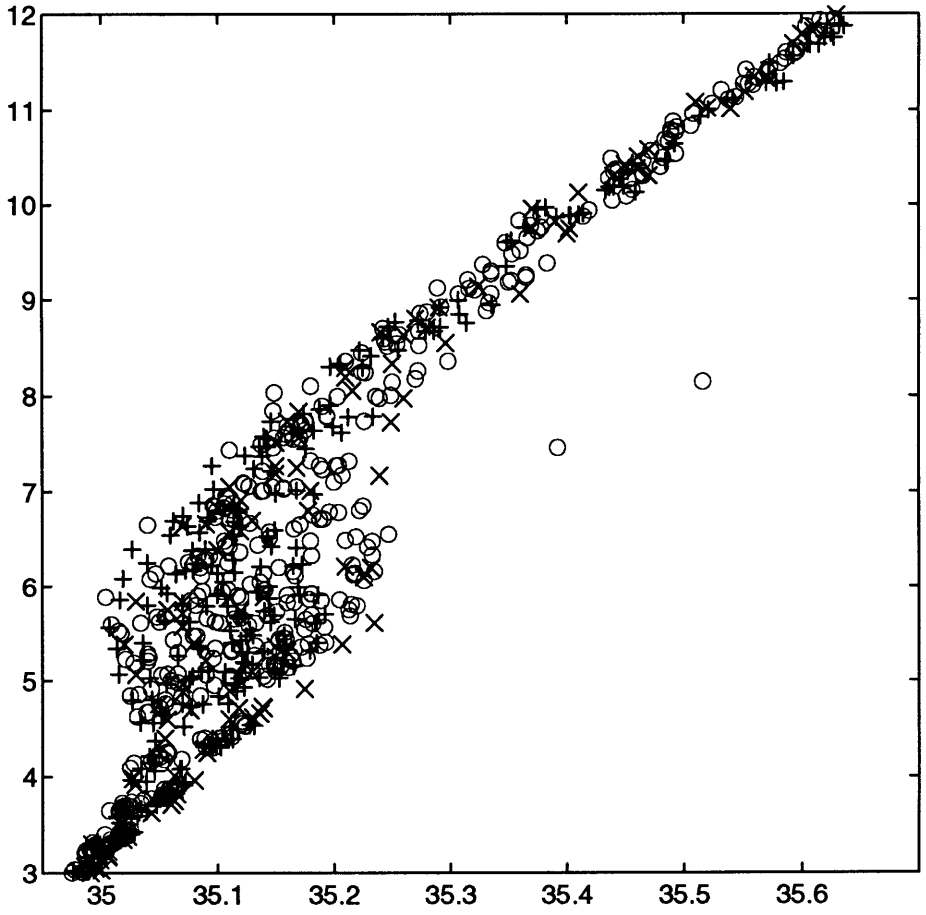

Figure 2.19: θ/S relationship for Upper North Atlantic Deep Water and Thermocline Water in the Canary Basin, data are from 1992(o), 1981(+) and 1957(x). Salinity data are in pss and temperature in °C.The two 1992 points with high salinity (larger than 35.3 pss) situated around 8 °C correspond to a Meddy detected in the area.

The two 1992 points with high salinity (larger than 35.3 pss) (figure 2.19) situated around 8 °C correspond to a Meddy detected in the area. The objective mapping has filtered out these anomalous temperature and salinity values. The Meddy only appears on the plots of raw temperature (Figure 1.2 A) and salinity (Figure 1.2 B) data.

2.5.3 Discussion

Thus, there are some indications of changes in the θ/S relationship with time. To illustration of the change in the deep water, we have plotted the θ/S relationship for AABW and LNADW in the North American Basin. Figure 2.20 presents the characteristics for these water masses on the three cruises and the linear regressions which were computed to represent them. In the deep water, the tendency is to become warmer or fresher with time, while above 3°C the tendency over time is to be colder or saltier. In the North American Basin around 1.9 °C, the water tends to be fresher by -0.001 pss/decade, while in the Canary Basin, in the LNADW, this tendency is slightly greater with a rate of change of -0.002 pss/decade.

In the Lower Thermocline Water, the mean salinity has increased over time in the North American Basin, larger in the last decade than previously. In the Canary Basin, there is an oscillatory behavior is with values going from higher in 1958 to lower in 1981 and higher again in 1992.

The accuracy of the measurements, especially in the 1957 data, is a limiting factor. However, the large numbers of θ/S samples allowed the uncertainly to be reduced at to ± 0.001 pss. Our results are significant within this error. Tendencies, especially in deep water, are steady over time, since uncertainty during 1992-1981 is quite a bit lower than in the previous period. The steadiness of the tendency gives more credibility to the results obtained for the period 1981-1957.

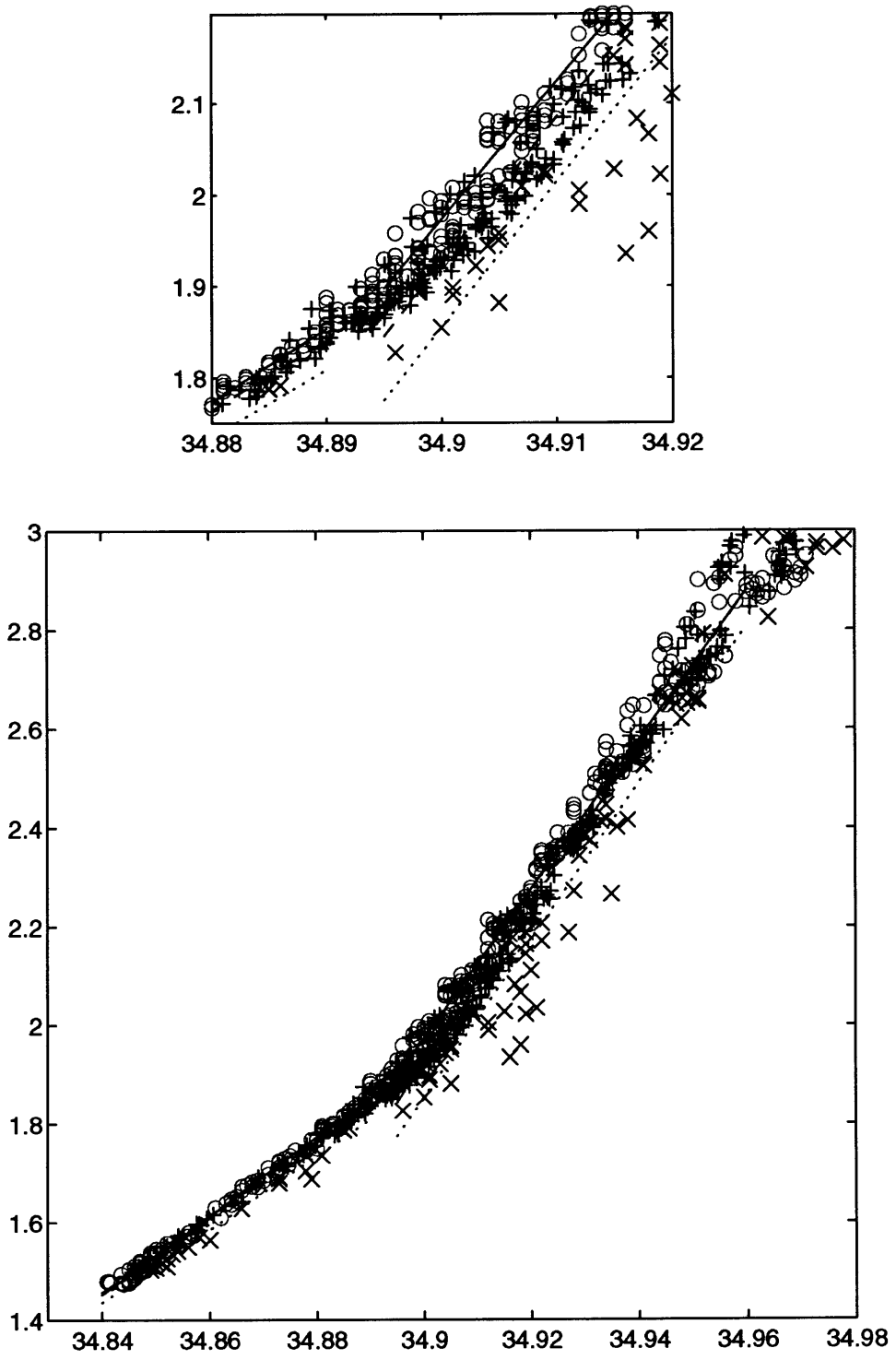

Figure 2.20: θ/S relationship for LNADW and AABW at 24.5 in the North American Basin, data are from 1992(o), 1981(+) and 1957(x). Salinity data are in pss and potential temperature in °C. Linear regressions for the 3 cruises in both LNADW and AABW are plotted, 1992 (solid), 1981 (dashed) and 1957 (dotted). The upper plot zooms in on the region between 1.75 and 2.2°C and 34.88 and 34.92 pss.

Other known problems when salinity comparisons are performed deal with the calibration of the water samples. Mantyla (1980) confirmed that systematic errors have occurred from using different batches of Standard Sea Water (SSW) at sea. Mantyla (1986) gave a series of adjustments that may reconcile the differences. Prior to SSW batch P91 (March 1980), SSW was certified for chlorinity only. The chlorinity-conductivity relationship was not the same for all the batches. During 1957, the batch of SSW used was number 26, (Figure 4, Mantyla 1986). The old chlorinity standardized data overestimate the new conductivity derived salinity by 0.001 pss. However, this variation is within our computed uncertainty.

Differences found in water masses and in θ/S characteristics, even in deep water are apparently larger than the differences associated with the batch water chlorinity/conductivity differences.

Chapter 3

Comparison over time of Ocean Heat Transport

3.1 Introduction

The poleward transport of heat is a major factor in the maintenance of climate. A surplus of solar energy is absorbed in the tropics and then exported to higher latitudes to balance a net energy loss in regions of low solar input. The conduction of heat by the solid earth is negligible, implying that the oceans and the atmosphere are responsible for most or nearly all the transport. The relative importance of sea and air in transporting heat depends upon the latitude. Vonder Haar and Oort (1973) found that, in the region of maximum net northward energy transport by the ocean-atmosphere system (30-35°N), the ocean carries 47% of the required energy. At 20°N, the peak ocean flux accounts for 74%. Newell *et al.,* (1974), Oort and Vonder Haar (1976), Carissimo*et al.,* (1985) and Hsiung *et al.,* (1989) updated those values. Our section at 24.5 °N is located where the ocean likely transports more of the solar energy than does the atmosphere towards the pole to maintain the global heat balance.

Combining the Pacific heat transport with the established value of Atlantic heat transport across 24°N, Bryden *et al.*, (1991) give a total ocean heat transport of 2.0 x 10^{15}W, larger than the atmospheric heat transport of 1.7 x 10^{15}W.

The purpose of the present study is to compare the heat transport at 24.5 °N in the Atlantic, estimated from data taken on three cruises in 1992, 1981 and 1957 and to determine whether or not there is some trend in long-term variation.

There are several methods for calculating ocean heat transport, depending on the data sources: (1) bulk formulas, requiring calculations of air-sea heat exchange, (2) subtracting the atmospheric transport from the total transport required by the radiation balance at the top of the atmosphere measured by satellite, (3) direct estimates of the ocean currents and their temperatures.

The first type estimates the heat exchange at the air-sea interface. The horizontal divergence of heat in a water column is given approximately by the exchange of heat across the air-sea interface. This quantity is obtained through a set of empirical equations from measurements of air temperature, water temperature, wind speed, dew point, barometric pressure and cloudiness. Hastenrath (1980) gave a heat flux of $\sim 1.55 \times 10^{15}$ W crossing latitude of 24 °N in the Atlantic. Bryden and Hall (1980) using air-sea exchanges computed by Bunker (1976), found a poleward flux of 1.11×10^{15} W.

The second method computes the difference between the heat budget of the earth obtained from satellite radiometer data and the atmospheric heat flux measured by radiosonde. Vonder Haar and Oort (1973), Oort and Vonder Haar (1976), Newell *et al.,* (1974), Oort and Vonder Haar (1976), Carissimo *et al.,* (1985) and Hsiung *et al.,* (1989) made those calculations.

The third method is based directly on oceanographic data. The more problematic point is the determination of the reference level velocities for geostrophic calculations. Bryan (1962) used wind stress values to calculate Sverdrup transport. Bryden and Hall (1980) and Hall and Bryden (1982) require that the ocean interior transport balance the Gulf Stream transport through the Straits of Florida. Roemmich

(1980), Wunsch (1980) and Roemmich and Wunsch (1985) used the inverse method of estimating reference level velocities (Wunsch, 1978). In the inverse method, water masses, or layers, in which the transport out the area between two sections must to be equal to the transport into the area, are defined. Measurements within the water column can also be used to identify the mechanisms that are responsible for this transport.

Hall and Bryden (1982) estimated the heat flux at 24 °N in the 1957 IGY section to be 1.2 x 10^{15} W. The same result was obtained by Roemmich (1980) using inverse calculations. Roemmich and Wunsch (1985) compared the 1957 data with the 1981 section and found the heat transport to be indistinguishable from computations of air-sea heat exchange. They attributed the steadiness of the heat transport to the invariance of the zonally averaged meridional circulation.

From Bottomley *et al.* (1990), the North Atlantic Sea Surface Temperature (SST) was higher than the average (max 0.2 °C) for a long period from the late 1930's to the middle 1960's. Then a short cooling period occurred until the beginning of the 1980's. The rest of the 1980's and the beginning of the 1990's were also warmer than average. The first cruise (1957) took place during the first warm period. During 1981 SST, was colder in the northern part but around the mean value at 25°N., and 1992 can be considered a warmer year with an annual mean 0.2°C warmer than the average 1951-1981 (Newell per. com.). Our goal is to determine whether this mean surface temperature correspond to any measurable change in the ocean heat transport.

3.2 Components of Atlantic Heat Transport at 24.5°N

The heat flux due to ocean currents across any latitude is well approximated by

$$T = \int\int \rho \, C_p \theta V dz \, dx \tag{3.1}$$

where the integration is over depth and longitude and V is the north-south component of the absolute velocity of the water across the latitude circle in question, in this case 24.5 °N. The variables ρ, C_p and θ are the density, the specific heat capacity and the potential temperature respectively. The mass of the system must be conserved. As we consider the North Atlantic essentially a closed basin north of 24.5°N, the meridional heat transport in the North Atlantic alone can be calculated by integrating (3.1) only in that ocean (Hall and Bryden, 1982).

Northward heat transport by ocean currents is the result of water flowing northward at one temperature and returning southward at a lower temperature. Temperature fluxes are considered to be the product of the estimated mass transport and a calculated averaged temperature. This temperature, called velocity weighted average temperature, is calculated dividing volume transport into temperature flux:

$$\theta_v = \frac{\int_W^E \int_0^{H(x)} \theta V dx dz}{\int_W^E \int_0^{H(x)} V dx dz} \tag{3.2}$$

Following the method of Hall and Bryden (1982), transport at 24.5 °N is separated into the Gulf Stream transport through the Florida Straits and the mid-ocean transport in the section between Africa and America. In this mid-ocean section, transport is separated into geostrophic and Ekman transport components.

Since conservation of mass is required, northward transport by the Gulf Stream flowing through the Straits of Florida and Ekman transport in the surface layer must balanced by the southward geostrophic transport in the interior of the section.

We shall consider each component separately; Florida Straits, Ekman layer flow and Mid-ocean geostrophic flow.

3.2.1 Florida Straits flow

During the 1981 and 1992 cruises, sections across the Florida Straits were made at 26 °N. However, to consider a mean flow across the Florida Straits section, we will use long term values rather than the cruise data. Larsen (1992) estimates the mean voltage-derived transport for the Florida Current at 27 °N to be 32.3 ±3.2 x 10^6 m^3s^{-1}, and the velocity weighted temperature to be 19.1 ±0.6 °C.

Using more than two years of PEGASUS ocean current measurements at 27 °N. Leaman *et al.* (1987) found a similar average northward volume flux for the Florida Current of 31.7 ± 3.0 x 10^6 m^3 s^{-1}. They also gave a transport of 27.3 x 10^6 m^3 s^{-1} between Key West and La Havana (but this value is less accurate because of meandering effects).

According to Finlen (1966) (from Schmitz *et al.* 1992), approximately 2 x 10^6 m^3 s^{-1} on average joins the Florida Current in the Straits of Florida through the Providence Channels located at roughly 26 °N, which is effectively north of the 24.5°N section. Subtracting this amount to the values given previously we obtain the northward transport of the Florida Current across 24.5°N to be 30 x 10^6 m^3 s^{-1}. The velocity-weighted average temperature is 19.1 °C. This value is consistent with the value given by Niiler and Richardson (1973).

3.2.2 Ekman layer flow

The zonally integrated meridional Ekman volume transport is computed by:

$$\int (\tau^x / f\rho) dx \tag{3.3}$$

where τ^x is the eastward wind stress, ρ is the density and f is the Coriolis parameter.

Böning *et al.*, (1991) compare the Hellerman-Rosenstein (1983) climatology with the Isemer and Hasse (1987) which represent a version of the Bunker Atlas for the North Atlantic (Bunker 1976). At 24.5 °N the zonally averaged annual mean eastern wind stress changes from about -0.5 dyn cm^{-2} (Hellerman-Rosenstein) to about -0.6 dyn cm^{-2} (Isemer and Hasse, 1987). Uncertainty in wind stress estimate are large. Changes in wind stress may have occurred in recent periods but there are not adequate data to support quantitative estimates. The Northward Ekman transport at 24 °N was estimated by Roemmich and Wunsch (1985) to be 6 ± 2 x10^6 m^3 s^{-1} from the wind stress tabulations of Hellerman and Rosenstein (1983). Changes in the last decade will be assumed smaller than the uncertainty of 2 Sv given by Roemmich and Wunsch (1985). The temperature transport was determined by Hall and Bryden (1982) by

$$\int (\tau^x / f\rho)\theta C_p dx \tag{3.4}$$

where the potential temperature θ was obtained by averaging the surface values with the 50 meters temperature values. Dividing the volume transport into the temperature flux, they obtained a velocity-weighted average temperature of 26.0°C for the Ekman flow in the mid-ocean section. Sea surface temperature may vary by ± 0.3°C over the three sections.

3.2.3 Mid-ocean geostrophic flow

The North Atlantic is essentially a closed basin, the northward Florida Current and wind driven transport across 24.5°N must be compensated by a southward flow across the section from the Bahamas to Africa, which is in geostrophic balance. From the hydrographic data, we can compute the geostrophic flow through the section. While there has not been time to carry out a full analysis of the geostrophic velocities for the Hespérides 1992 section completed only 9 months ago, we will present some

estimates of the mid ocean meridional circulation using end stations at the eastern and western edges of the 1992 section and compare them with similar calculations for the 1981 and 1957 sections.

3.3 Comparison on heat flux

Once we have determined the three components of the temperature transport, the heat flux across this latitude of the Mid-Atlantic can be written by

$$T_{NA} = \int\int_{FS} \rho C_P \theta V_{FS} dz dx + \int\int_{MO} \rho C_P \theta V_{Ekman} dz dx + \int\int_{MO} \rho C_P \theta V_{geostrophic} dz dx \quad (3.5)$$

where NA denotes North Atlantic, FS denotes Florida Straits and MO denotes our mid-ocean 24.5 °N section.

A mass conservation argument requires that the 30 x 10^6 m^3 s^{-1} of northward transport in the Florida Current and the 6 x 10^6 m^3 s^{-1} of northward Ekman transport be compensated by the 36 x 10^6 m^3 s^{-1} of southward transport within the mid-ocean section.

Our objective is to compare the heat flux estimates made from the 1957, 1981 and 1992 sections. We are going to calculate a general profile of geostrophic velocities and obtain a barotropic velocity by the mass balance shown previously. Then we will compute the heat transport and compare the three different cruises. We will do the simplest calculation of heat flux by using the mean meridional flow from a single pair of station. This pair consists of the westernmost station of each section, at the western boundary and a representative eastern station, both deeper than 4000 m. The chosen stations were stations 99 and 13 for the 1992 cruise, 236 and 162 for the 1981 cruise and stations 3623 and 3595 for the 1957 cruise. The North Atlantic at

those latitude is separated by the Mid-Atlantic Ridge. In our simple model we will assume that there is not net mass transport below 4000 m and that the contributions to the heat flux from the flow below 4000 m are negligible. Also we will assume that there is no pressure gradient across the Mid-Atlantic Ridge where it protrudes above 4000 m. While these assumptions are not really valid, we are trying to do a simple comparison of heat transport for the three sections, treating each in a similar manner.

For the geostrophic calculations we need an initial reference level. The general southward flow of AABW and AAIW below and above the North Atlantic Deep Water respectively, suggest two possible reference levels, one at about 4000 m and the other at roughly 1000 m (Speer and McCartney, 1991). Roemmich (1980) used both 1000 and 4000 m as initial reference levels for his heat flux calculations. Roemmich and Wunsch (1985) obtained a northward flow as intermediate waters above a zero-crossing at about 1300 m. We have chosen an initial reference level of 1100 m depth for geostrophic velocity calculations between the pair of end-stations. Initially we calculated the geostrophic velocity profiles for 1992, 1981 and 1957 cruises assuming a zero velocity at 1100 m. For each of the standard depths (as mentioned in table 1.1), we have calculated the area. The total vertical area across the section from surface to 4000 m is 237.3 x 10^6 m^2. Integrating in the vertical, we obtain the geostrophic transport through those upper part of the section. Mid-ocean geostrophic transport referenced 1100 m is -36.9 x 10^6 m^3 s^{-1}, for 1992, -31.7 x 10^6 m^3 s^{-1} for 1981, and -41.0 x 10^6 m^3 s^{-1} for 1957 cruises.

Within our assumption for mass conservation, we compensate exactly for the combined northward Gulf Stream and Ekman transport, a total transport of -36 x 10^6 $m^3 s^{-1}$ is required in the the Mid-ocean. The addition of a uniform southward -0.004 cm s^{-1} velocity to the geostrophic velocity profile for the 1992 data resulted exactly in a southward mid ocean geostrophic transport of -36 x 10^6 m^3/s. This velocity was 0.018 cm s^{-1} for the 1981 cruise and -0.021 cm s^{-1} for the 1957 cruise. Figure 3.1

presents the zonal absolute velocity profiles for the three cruises down to 4000 m such that each profile yields a southward transport of -36 Sv.

A comparison of these velocity profiles for the different cruises shows velocities which are similar in a large scale structure. There is a slight reduction in the strength of the thermocline southward flow during 1992 and a slight increase in strength of the southward flow in the UNADW. Between 700 and 1000 m, the northward flow appears larger during 1992 and 1957 than in 1981.

For heat flux computations, we need the average potential temperature in each standard depth for each cruise (Table 3.1) Using equation (3.2), extending the integration from surface to 4000 m, we have obtained the velocity-weighted average temperature for the three cruises (Table 3.2).

We follow the analysis that Bryden *et al.* (1991) have done for the transpacific 24 °N section. Combining the Ekman layer, Florida current, and mid-ocean geostrophic components, we can compare the net heat transport across the section. The northward, wind-driven transport of 6 x 10^6 m^3s^{-1} at an average temperature of 26 °C and the northward Florida Straits transport of 30 x 10^6 m^3s^{-1} at 19.1 °C are balanced by the southward mid-ocean return transport of 36 x 10^6 m^3s^{-1} at an average temperature of 10.14, 10.84, and 10.47 °C for the 1992, 1981, and 1957 cruises, respectively.

The heat flux can be written as

$$T_{NA} = (FS_T\, t_{FS} + EK_T\, t_{EK} + MO_T\, t_{MO})\, \rho\, C_P \tag{3.6}$$

where FS_T stands for transport in the Florida Straits and t_{FS} is the weighted-velocity averaged temperature for this transport, and analogous terms are used for Ekman and geostrophic Mid-ocean transport.

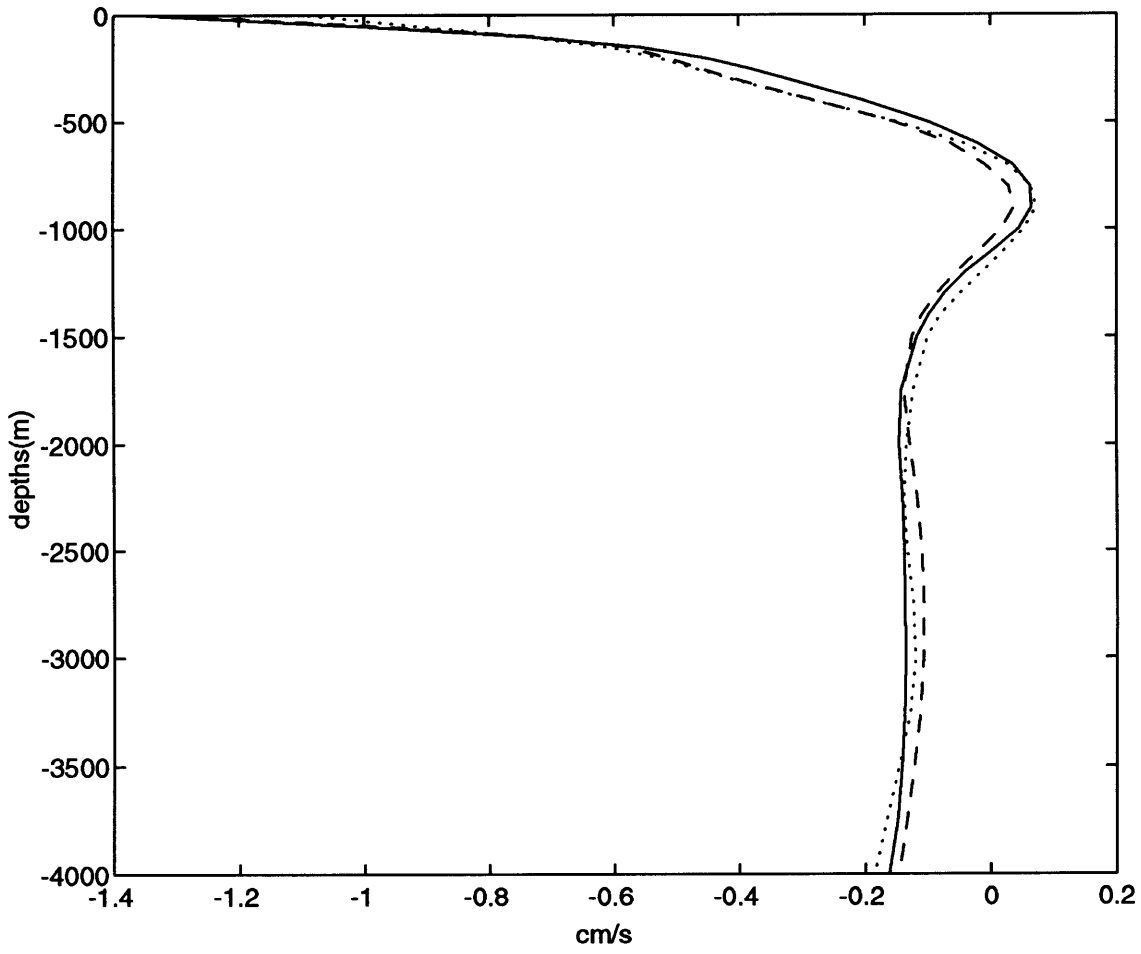

Figure 3.1: Zonal velocities calculated from surface to 4000 m for 1992 (solid), 1981 (dashed) and 1957 (dotted).

depth (m.)	θ_{1992} °C	θ_{1981} °C	θ_{1957} °C
0	26.35	26.55	26.47
50	24.10	24.68	25.62
100	21.93	21.67	22.05
150	20.37	19.94	20.17
200	18.76	18.42	18.65
250	17.72	17.38	17.71
300	16.93	16.65	16.88
400	15.40	15.34	15.53
500	13.78	13.85	13.93
600	12.20	12.27	12.20
700	10.60	10.62	10.47
800	9.01	9.01	8.82
900	7.72	7.70	7.50
1000	6.83	6.74	6.55
1100	6.24	6.16	5.96
1200	5.78	5.73	5.51
1300	5.41	5.38	5.16
1400	5.08	5.05	4.86
1500	4.77	4.76	4.60
1750	4.15	4.16	4.03
2000	3.66	3.66	3.57
2250	3.26	3.26	3.20
2500	2.96	2.96	2.94
2750	2.72	2.72	2.72
3000	2.52	2.53	2.53
3250	2.36	2.37	2.37
3500	2.22	2.23	2.24
3750	2.11	2.12	2.14
4000	2.03	2.03	2.05

Table 3.1: Average potential temperature calculated from surface to 4000 m at 24.5°N at standard depths for each of the cruises, 1992, 1981 and 1957

year	θ_v(°C)
1992	10.14
1981	10.84
1957	10.47

Table 3.2: Velocity-weighted average temperature (°C) calculated at 24.5°N for each of the cruises, 1992, 1981 and 1957

year	Component heat flux	Transport (x $10^6 m^3 s^{-1}$)	Temp differences (°C) with Mid-ocean	Northward heat transport(10^{15}W)
1992	Ekman layer	6	26.0 - 10.14 = 15.86	0.39
	Florida Straits	30	19.1 - 10.14 = 8.96	1.10
				Net = 1.49 x 10^{15}W
1981	Ekman layer	6	26.0 - 10.84 = 15.16	0.37
	Florida Straits	30	19.1 - 10.84 = 8.26	1.02
				Net = 1.39 x 10^{15}W
1957	Ekman layer	6	26.0 - 10.47 = 15.53	0.38
	Florida Straits	30	19.1 - 10.47 = 8.63	1.06
				Net = 1.44 x 10^{15}W

Table 3.3: Components of the heat fluxes, transport, difference of temperature, northward heat transport and net heat transport across 24.5°N for 1957, 1981 and 1992.

Because the Mid-ocean transport above 4000 m compensates the other transport, $MO_T = -FS_T - EK_T$, the equation (3.6) can then be written as

$$T_{NA} = \{ FS_T (t_{FS} - t_{MO}) + EK_T (t_{EK} - t_{MO}) \} \rho C_P \qquad (3.7)$$

Table 3.3 shows the values for the terms of equation (3.7). Transport by Florida Straits and Ekman layer, differences of temperature with Mid-ocean section and the total net transport for each cruise.

3.4 Discussion

The object of these simple calculations is to compare the mid-ocean velocity profiles and resulting flow estimates across 24 °N for our three cruises by this simple calculation of heat fluxes. A more realistic calculation would include the deep water flow below 4000 m depth, and the contribution from the shallow eastern boundary current, particularly the coastal current which is inshore from the first deep station near Africa and the contributions from flows along the Mid-Atlantic Ridge.

Below 4000 m, Hall and Bryden (1982) found southward transport by the North Atlantic Deep Water (-9.5 Sv between 3500 and 4500 m), and northward transport at the bottom by the Antarctic Bottom Water (6.8 Sv). We assume both of them are compensated below 4000 m for the three cruises. We could have included 2 Sv of northward transport, but our uncertainty is larger than that value.

Changes in Ekman transport is another factor to consider for a more complete calculation, both components wind stress and sea surface temperature could have some contribution to the changes in the heat transport.

The values obtained for the net heat transport for each of the three cruises in these conditions are the same within the range of the errors we have in the calculations. This value is 1.44 x 10^{15}W with a statistical deviation of $\pm$0.05 x 10^{15}W. The northward heat transports for the 1957 and 1981 24°N sections were estimated by Roemmich and Wunsch (1985) to be 1.1 and 1.2 PW using a variety of inverse model calculations. We expect that a full analysis of the 1992 Hesp'eridesérides section will also yield a northward heat transport of about 1.2 PW. Thus the assumptions that we have make in making this simple calculation of the ocean heat transport lead to overestimating the heat transport by about 0.2 PW. We are mostly interested, however, in possible time changes in the heat transport.

The results leads us to the conclusion that there is no significant difference over time between the heat flux estimated from the three surveys performed in 1957, 1981 and 1992 at 24.5°N . There has been no measurable tendency in heat transport over the last 35 years.

The structure continues to be defined as a southward flow in the thermocline above about 600 m, a core of northward flow (perhaps of Antarctic intermediate water) between 700 and 1100 m, and a generally southward flow from 1200 to 4000 m depths.

We find no changes in the large scale vertical distribution, although there are some changes in the magnitudes of the flows. The fact that between 700 and 1000 m northward flow seems to be larger during 1992 and 1957 than in 1981 could be related to the changes in salinity detected around those depths in the Canary Basin. The mean salinity was reduced by 0.017 pss between 1957 and 1981 and increased by 0.028 pss from 1981 to 1992. This is the depth range of the AAIW which is relatively fresh. Stronger northward flow of AAIW in 1981 may have led to the lower salinities observed in 1981.

Conclusions

In this thesis we have used hydrographic data to examine the changes in oceanographic conditions at 24.5 °N in the subtropical North Atlantic. The most significant finding is that there is a long time scale warming in an ocean-wide band from 1000 m to 3000 m over the entire 35-years period from 1957 to 1992.

In the second chapter, the choice of a data interpolation scheme was presented. We compared spline interpolation and objective mapping. There is a high degree of similarity between cubic spline smoothing with a gaussian filter and objective mapping methods. The results of the two methods, are within the expected error in all regions except the boundaries. Cubic spline is simpler to use, but the advantage of calculating expected errors made objective mapping the most suitable method of interpolation for this analysis.

A general warming was found over the upper 3000 m of the North Atlantic at 24.5°N, over the entire 35-year period. There is warming in the layer from surface down to 400 m, cooling between 400 and 500 m, and a significant warming between 600 and 2750 m. Significant cooling is found in water deeper than 3000 m in both the North American and the Canary Basins. The 1992 section was 0.1 $\pm$0.09 °C warmer than the 1957 section above 3000 m depth, with a tendency of 0.03 °C /decade. This tendency characterized both periods, 1981-1957 and 1992-1981. There is high variability over time over most of the upper 1000 m. Below 1000 m, a significant warming of 0.1$\pm$0.02 °C has been observed. The rate of warming between 1000 and

3000 m is 0.028±0.007°C/decade, a far more significant value but similar to that found from 100 m to 3000 m.

Below 3000 m depth, the temperature decreases are statistically significant. The cooling rate is -0.008±0.005 °C/decade in the North American Basin and in the Canary Basin is -0.004±0.001°C/decade. This cooling has not been regular. Strong cooling occurred in the Canary Basin for the 1981-1957 period and in the North American Basin for 1992-1981. Changes in salinity at 24.5 °N are around 0.003 pss/decade above 3000 m and -0.002 pss/decade below 3000 m in the North American Basin and -0.001 pss/decade in the Canary Basin. There is a general cooling and freshening in the western boundary below 2000 m. Differences are greater than -0.05 °C and - 0.01 pss for most of the area west of 70 °W. The eastern boundary was also subject to cooling and freshening but in a lesser amount.

In Chapter Two we also discussed the relationship between changes in temperature and the associated changes in water mass volume. The cooling detected between 400 and 500 m occurs between the Upper and Mid-thermocline. Below this region, water is warmer in the lower thermocline and UNADW layers. In deep water we found cooling of the LNADW in both basins.

A warming at a constant pressure is equivalent to a deepening of isotherms. Cooling produces uplifting of isotherms. The nonuniform change of the depth of isotherms results in a change in the volume of water masses, as can be seen in Table 2.9. Over the 35 years in question the thermocline and deep water have increased in volume and the volume of NADW has decreased in both basins. Thus, it appears that the NADW is affected by both warming in its upper part and cooling in its deeper part.

Expansion in the North American Basin occurs in the transition zone between AABW and LNADW, at a rate of 9 km^2/year. This rate is nearly constant over the

total period studied. In the Canary Basin, the expansion is larger and has mostly taken place in the last 11 years. Contraction occurs in the NADW. In the North American Basin, the contraction of LNADW decreases from a rate of -13 km^2/year in 1957-1981 to a rate of -9 km^2/year in the period 1981-1992. In the Canary Basin most of the reduction occurred in the first period. In the UNADW contraction occurred in both periods but was larger from 1981 to 1992. Thermocline water has expanded. In the lower thermocline, the expansion occurred in the first period and in the mid-thermocline during the last period.

Before discussing what these changes mean for the North Atlantic general circulation, let us first reiterate some of our conclusions concerning the θ/S relationship. There are some indications that the θ/S relationship at 24.5 °N has changed over time. Below a potential temperature of 3°C, the tendency is for water to become warmer or fresher, while above 3 °C the water appears to become colder or saltier. In the lower thermocline water, mean salinity has increased with time in the North American Basin, more so in the last decade than previously. In the Canary Basin, an oscillatory behavior was evident with a reduction in the mean salinity from 1957-1981 and an increase from 1981-1992. Increases in salinity in the lower thermocline layer during the last decade were of the order of 0.025 pss in both basins.

There are a number of possible explanations for these temperature and salinity changes. NADW is affected by warming in the upper portion by the mid and lower thermocline water and cooling in the deeper portion perhaps by cooling and reduction of the transport of the deep western boundary current. The lower thermocline water, in the tropical North Atlantic region, is dominated by the South Atlantic Water (Wright and Worthington, 1970). Farther north in the eastern North Atlantic this water mass gives way to the saline Mediterranean water. Worthington (1976) placed the limit between this two water masses at 35.0 pss. At 6 °C (Figure 23 of his paper),

the boundary is situated at 24.5 °N in the central part of the section but around 20°N in the eastern basin and around 22°N in the western basin.

We found indications of water fresher than 35.0 pss, (at 1000 m depth), in the 1992 cruise near 50°W (Figure 1.3). These low salinity spots also appear in the 1981 cruise (Roemmich and Wunsch, (1985), Figure 2 c), and in the 1957 cruise (Fuglister, 1960; Plate 71) but to a greater extent (i.e. between 45 and 65 °W). In this area the longitudinal gradient of salinity is of the order of 0.1 pss per 4°or 400 km, (from Figure 23 Worthington, 1976). The temperature gradient is around 1 °C for the same meridional distance. Meridional motion of the front between the two water masses, of the order of 2 degrees in latitude, could cause an increase in temperature and salinity of the same order as the differences we have found at 1000 m. This lifting might have occurred with more intensity from 1957 to 1981 in the central part of the North Atlantic and during the last period over the eastern and western sides of the basin.

In a calculation of the geostrophic transport between pairs of stations referenced to 1100 db for the three cruises (not included in the thesis), I found a persistent reduction on the northward transport between 800 and 1000 m depth for the two periods. This reduction of transport of AAIW is consistent with the idea of southward motion of the front of influence of AAIW.

Roemmich and Wunsch (1984) in the 36°N section found that negative differences in temperature tend to compensate the positive ones so that the total average temperature was unchanged from 1959 to 1981. They found a thicker layer of negative temperature differences between 100 and 700 m, and warming below. It is possible that since they found no net warming, the warming which we find only affects the subtropical North Atlantic. North of this area the cooling in the upper layers compensates for the warming below.

According to Brewer *et al.* (1983), changes in the Denmark Strait overflow of ventilated waters from convective basins to the north caused widespread freshening of the deep Subpolar water during the 1960's and 1970's. At 24.5 °N, cooling and freshening in the deep western boundary occurred during the first period (1957-1981); and after 1981, the cooling and freshening in the western boundary has been reduced but the effect has expanded all around the western basin. The Canary Basin has been cooling and freshening but in a lesser amount than the North American Basin.

Lazier (1980) found a decreased production of LSW in the 1970's. Later he reports (Lazier, 1988) that by the mid-1980's conditions in these waters had returned to those of the early 1960's. This water flows southward at about 1500 m depth in the western boundary, and a reduction in the source strength would presumably produce a lesser amount of LSW and therefore a decreased influence on the UNADW. The MOW (warmer and saltier than the LSW) could also influence the UNADW and it leads to increases in temperature and salinity.

Rohling and Bryden (1992), in a study of the variation in characteristics of the Mediterranean Intermediate Water (MIW) and Western Mediterranean Deep water (WMDW) in the western Mediterranean, find an increase in temperature and salinity with time. The Mediterranean Overflow Water would have an increase in temperature and salinity. The fact that the changes at 24.5 °N do not show a zonal gradient does not lend evidence to such hypothesis.

Finally, using a simple heat transport calculation, we find that there is no significant difference between the heat fluxes estimated from the three surveys performed in 1957, 1981, and 1992 at 24.5°N .

Precise calculations of heat flux still needs to be done, as well as a comparison of the fluxes of heat, salt, oxygen and nutrients with whose carried out by Rintoul and Wunsch (1990).

The rate of temperature change, between 100 and 3000 m, observed over the period 1957 to 1981 by Roemmich and Wunsch (1984) has remained steady in the last decade. This trend in the subtropical North Atlantic is a very important climatic issue.

Comparing sections of hydrographic data is the best way to find temperature and salinity trends over time, but these sections are available only at selected times separated by long time intervals. Other measurement systems must be used between hydrographic samples. To examine the structure of the climate variability long time series hydrographic stations like the Bermuda are very useful. A project to create a sampling station over time has been proposed by R. Molina (Instituto Español de Oceanografía, Centro Costero de Santa Cruz de Tenerife) off the Canary Islands. Time series in the Eastern North Atlantic would be very helpful for understanding the circulation of this area and its influence in the rest of the North Atlantic.

REFERENCES

Ahlberg A. J., E.N. Nilson and J. L. Walsh (1967) *The theory of splines and their applications.* New York Academic Press, 1967. 284 pp.

Barber, C.R. 1969. The International Practical Temperature Scale of 1968. *Meteorologia* **5**,(2):35-44

Bevington, P. R., and D. K. Robinson (1992) *Data reduction and error analysis for the physical sciences.* McGraw-Hill, Inc. 328 pp.

Böning C. W., R. Döscher and H. J. Isemer (1991) Monthly Mean Wind Stress and Sverdrup Transport in the North Atlantic: A comparison of the Hellerman-Rosenstein and Isemer-Hesse Climatologies *J. Phys. Oceanogr.***21**, 221-235.

Bottomley, M., C.K. Folland, J. Hsiung, R.E. Newell and D.E. Parker (1990) *Global Ocean Surface temperature atlas 'Gosta'.* Bracknell (U.K.) The Met. Office, Massachusetts Institute of technology. 313 pp.

Bretherton F. P., R. E. Davis and C. B. Fandry (1976) A technique for objective analysis and design of oceanographic experiments applied to MODE-73.*Deep Sea Res.***23**, 559-582.

Brewer P.G., W.S. Broecker, W.J. Jenkings, P.B. Rhines, C.G. Rooth, J.H. Swift, T. Takahashi and R.T. Willians. (1983). A climatic freshening of the deep Atlantic north of 50°N over the past 20 years, *Science* **222** 1237

Bryan K. (1962) Measurements of meridional heat transport by ocean currents. *J. Geophys. Res.*, **67**, 3403-3414.

Bryan K. (1982) Poleward heat transport by the ocean: observations and model. *Ann. Rev. Earth Planet. Sci.*, **10**, 15-38.

Bryden H. L. and M. M. Hall (1980) Heat Transport by Currents Across 25°N Latitude in the Atlantic Ocean. *Science*, **207**, 884-886.

Bryden, H. L., D.H. Roemmich and J.A. Church (1991) Heat transport across 24°N in the Pacific. *Deep Sea Res.*. **38** (3) 297-324

Brown, N. L. (1984) A precision CTD microprofiler. IEEE Conference on Engineering in the Ocean Environment, **2**, 270-278

Bunker A.F. (1976) Computations of Surface Energy Flux and Annual Air-Sea Interaction Cycles of the North Atlantic Ocean. *Monthly Weather Review*, **104**, (9) 1122-1140.

Carissimo, B.C., H. Oort and T.H. Vonder Haar (1985) Estimates of the meridional energy transports in the atmosphere and ocean *J. Phys. Oceanogr.***15** 82:91.

Edmond J. M. and G. C. Anderson (1971) On the structure of the North Atlantic Deep Water. *Deep Sea Res.***18** 127-133.

Finlen, J. R., (1966) Transport investigations in the northwest Providence Channel, Sc M. thesis, 110 pp., Univ. of Miami, Coral Gables, Fla.

Fofonoff, N.F. and H. Bryden (1975) Specific gravity and density of seawater at atmospheric pressure. *J. Geophys. Res.***33**, Supplement, pp. 69-82.

Fuglister, F.C (1960) Atlantic Ocean Atlas of temperature and salinity profiles and data from the International Geophysical Year of 1957-1958. *Woods Hole Oceanographic Institution Atlas Series* 1, 209 pp.

Fukumori I, F. Martel and C. Wunsch (1991) The Hydrography of the North Atlantic in the early 80s. An Atlas. *Progress in Oceanography*, **27** 1-110.

Fukumori I and C. Wunsch (1991) Efficient representation of the North Atlantic hydrographic and chemical distributions. *Progress in Oceanography*, **27** 111-195.

Gunn, J. T. and D. R. Watts (1982) On the currents and water masses north of the Antilles/Bahamas arc. *J. Mar. Res.***40** 1-18

Hall M. M, and H. L. Bryden (1982) Direct estimates and mechanisms of ocean heat transport. *Deep Sea Res.***29** (3), 339-359.

Hastenrath S. (1980) Heat Budget of Tropical Ocean and Atmosphere. *J. Phys. Oceanogr.***10**, 159-170.

Hellerman S. and M. Rosenstein (1983) Normal Monthly Wind Stress Over the World Ocean with Error Estimates. *J. Phys. Oceanogr.***13** 1093-1104.

Hsiung, J and T. Houghtby (1989). The annual cycle of oceanic heat storage in the world ocean. *Quart. J. Roy. Meteor. Soc.* **115** 1-28

Isemer H.-J. and L. Hasse (1987) The Bunker climate atlas of the North Atlantic Ocean Vol.2 *Air-Sea Interactions*, Springer-Verlag, 256pp.

Joyce, T. M. (1993) The long-term hydrographic record at Bermuda *Nature* (submitted).

Larsen J. C. (1992) Transport and heat flux of the Florida Current at 27°N derived from cross-stream voltages and profiling data: theory and observations. *Phil. Trans. R. Soc. Lond.* A **338**, 169-236.

Lazier, J. R. N. (1980) Oceanographic Conditions at Ocean Weather Ship Bravo, 1964-1974 *Atmosphere-Ocean* **18** (3), 227-238.

Lazier, J. (1988). Temperature and salinity changes in the deep Labrador Sea, 1962-1986, *Deep Sea Res.***35** 1247

Leaman K. D., R. L. Moliniari and P. S. Vertes (1987) Structure and Variability of the Florida Current at 27°N:April 1982 - July 1984. *J. Phys. Oceanogr.***17**, 565-583.

Levitus, S. (1989a) Interpentadal variability of Temperature and Salinity at Intermediate Depths of the North Atlantic Ocean, 1970-1974 Versus 1955-1959. *J. Geophys. Res.***94** (C5) 6091-6131.

Levitus, S. (1989b) Interpentadal variability of Temperature and Salinity in the Deep North Atlantic, 1970-1974 Versus 1955-1959. *J. Geophys. Res.***94** (C11) 16125-16131.

Liebelt, P.B. (1967) em An introduction to Optimal Estimation, Addison-Wesley, Reading, Mass., 273 pp.

Mamayev O., H. Dooley, B. Millard and K. Taira (1991) Processing of oceanographic station data. Joint panel on Oceanographic Tables and Standards (JPOTS) **UNESCO** 138pp

Mantyla, A. W., (1980). Electrical conductivity comparisons of Standard Seawater batches P29 to P84 *Deep Sea Res.***27A** 837-846

Mantyla, A. W., (1987). Standard Seawater Comparisons Updated. *J. Phys. Oceanogr.***17** (4), 543-548

Mantyla, A. W. and J. L. Reid (1983) Abyssal characteristics of the World Ocean waters. *Deep Sea Res.***30** 805-833

McCartney, M. S. and L. D. Talley (1982) The Subpolar mode water of the North Atlantic Ocean. *J. Phys. Oceanogr.*, **12**, 1169-1188.

Millard R. C., Jr (1982) CTD calibration and data processing techniques at WHOI using the 1978 practical scale. Marine Technology Society Conference paper.

Millard R. C., W. B. Owens and N. P. Fofonoff (1990) On the calculation of the Brunt-Väisäla frequency. *Deep Sea Res.***37**, (1), 167-181.

Millard R. C., G. Bond and J. Toole (1993) Implementation of a Titanium Strain Gauge Pressure Transducer for CTD Applications. *Deep Sea Res.*(in press.)

Millard R. C. and K. Yang (1993) CTD Calibration and Processing Methods used at Woods Hole Oceanographic Institution. Woods Hole Oceanographic Technical report (in press.)

Newell, R.E., J.W. Kindson, D.G. Vincent and G.J. Boer (1974). *The General Circulation of the Tropical Atmosphere and Interaction with Extratropical latitudes*, Vol 2, M.I.T. press p. 68

Niiler P. P. and W. S. Richardson (1973) Seasonal Variability of the Florida Current *J. Mar. Res.***31**, (3), 144-167.

Oort A. and T. H. Vonder Haar (1976) On the Observed Annual Cycle in the Ocean-Atmosphere Heat Balance Over the Northern Hemisphere. *J. Phys. Oceanogr.***6**, (6), 781-800.

Pickart, R. S. (1992) Water mass components of the North Atlantic deep western boundary current. *Deep Sea Res.***39** (9), 1553-1572.

Reid J. L. and R. J. Lynn (1971) On the influence of the Norwegian- Greenland and Weddell seas upon the bottom waters of the Indian and Pacific oceans. *Deep Sea Res.***18**, 1063-1088.

Rintoul S. R. and C. Wunsch (1990) Mass, heat, oxygen and nutrients fluxes and budgets in the North Atlantic Ocean. *Deep Sea Res.***20** 1-23. Roemmich D., (1980) Estimation of meridional heat flux in the North Atlantic by inverse methods *J. Phys. Oceanogr.***10**, 1972-1983.

Roemmich D., (1983) Optimal Estimation of Hydrographic Station Data and Derived Fields. *J. Phys. Oceanogr.***13**, 1544-1549.

Roemmich D. and C. Wunsch (1984) Apparent changes in the climatic state of the deep North Atlantic Ocean. *Nature*, **307**, (5950), 447-450.

Roemmich D., and C. Wunsch (1985) Two transatlantic sections: Meridional circulation and heat flux in the subtropical North Atlantic Ocean. *Deep Sea Res.*, **32**, 619-664.

Rohling, E.J. and H.L. Bryden (1992) Man-induced salinity and temperature increases in Western Mediterranean Deep Water. *J. Geophys. Res.*, **97**, 11191:11198.

Saunders, P.M. (1981) Practical conversion of pressure to depth. *J. Phys. Oceanogr.*, **11** (4), 573:574.

Schmitz W. J. and W.S. Richardson (1991). On the transport of the Florida Current. *Deep Sea Res.*,**15** 679-693

Schmitz W. J., J. D. Thompson and J. R. Luyten (1992) The Sverdrup Circulation for the Atlantic along 24°N. *J. Geophys. Res.***97**, (C5), 7251-7256.

Schmitz, W.J. and M.S. McCartney (1993) On the North Atlantic Circulation. *Reviews of Geophysics* **31**, (1), 29-49.

Speer K. G. and M. S. McCartney (1991) Tracing Lower North Atlantic Deep Water Across the Equator *J. Geophys. Res.***96** 20, 443-20,448

Thompson, W. J., (1984) *Computing in Applied Science*, Willey, New York.

Tsuchiya, M., L. D. Talley and M. S. McCartney (1992) An easter Atlantic section from Iceland southward across the equator. *Deep Sea Res.***39**, 1885-1917.

Vonder Haar, T. H. and A. H. Oort (1973) New Estimate of Annual Poleward Energy Transport by Northern Hemisphere Oceans. *J. Phys. Oceanogr.***2**, 169-172.

Warren B. (1981) Deep circulation of the world ocean. In *Evolution of physical oceanography* MIT press. 6-41

Weiss, R.F., J.L. Bullister, R.H. Gammon and M.J. Warner (1985). Atmospheric chlorofluoromethanes in the deep equatorial Atlantic. *Nature* **314** (6012), 608-610.

Whitehead J. A. and L. V. Worthington (1982) The flux and mixing rates of Antarctic bottom water within the North Atlantic. *J. Geophys. Res.***87** 7903-7924.

Worthington, L. V., (1976) In the North Atlantic Circulation. *The John Hopkins Oceanogr. Stud.*, **6**, 110 pp.

Worthington, L. V. and W. R. Wright (1970) North Atlantic Ocean atlas of potential temperature, salinity in the deep water including temperature, salinity and oxygen profiles from Erika Dan cruises of 1962. *The Woods Hole Oceanographic Institution Atlas Series*, **2**, 24 pp, 58 plates.

Wright W.R. and L. V. Worthington (1970) The water masses of the North Atlantic Ocean, a volumetric census of temperature and salinity, *Serial Atlas of the Marine Environment*, Folio **19**, American Geographical Society 8pp., 7 plates

Wunsch, C. (1978) The North Atlantic General Circulation West of 50°W Determined by Inverse Methods. *Reviews of Geophysics and space physics* **16**, (4) 583:620.

Wunsch, C. (1980) Meridional heat flux of the North Atlantic Ocean *Proceeding of the National Academy of Science*, **77**, 5043-5047.

Wunsch, C. (1985) Can a Tracer Field Be Inverted for Velocity?. *J. Phys. Oceanogr.*, **15**, 1521-1531.

Wunsch, C. (1989) Tracer inverse problems. *Oceanic Circulation Models: Combining Data and Dynamics* 1-77pp. D.L.T. Anderson and J. Willebrand (eds.), Kluwer Academic Publishers.

Wüst G. (1933) Schichtung und Zirku-lation des Atlantischen Ozeans. Das Bodenwasser und die Gliederung der Atlantischen Tiefsee. In: *Wissenschaftliche Ergibnisse der Deutschen Atlantischen Expedition auf dem Forschungsund Vermessungsschiff "Meteor" 1925-1927* **6** (1), 106 pp. (Bottom Water and the Distribution of the Deep Water of the Atlantic, M. Slessers, translator, B. E. Olson, ed., 1967, U. S. Naval Oceanographic Office, Washington, D.C., 145 pp.)

Wüst G. (1935) Schichtung und Zirkulation des Atlantischen Ozeans. Die Stratosphare. In: *Wissenschaftliche Ergibnisse der Deutschen Atlantischen Expedition auf dem Forschungsund Vermessungsschiff "Meteor" 1925-1927* **6** (2), 180 pp. (The Stratosphere of the Atlantic Ocean, W.J. EMERY, editor, 1978. Amerind, New Delhi, 112 pp.)